DEVELOPMENT OF NANOPARTICLE MEDIATED DRUG DELIVERY SYSTEM FOR ANTICANCER BIOACTIVE COMPOUNDS

Thesis Submitted

in Partial Fulfillment of the Requirment for the

Degree of

DOCTOR OF PHILOSOPHY

Submitted by:

Ritu

2K19/PHDBT/13

Under the supervision of

Supervisor	**Co-supervisor**
Dr. Asmita Das	**Dr. Prakash Chandra**
Associate Professor	**Assistant Professor**
Department of Biotechnology	**Department of Biotechnology**
Delhi Technological University	**Delhi Technological University**

To the
Department of Biotechnology
DELHI TECHNOLOGICAL UNIVERSITY
(Formerly Delhi College of Engineering)
Shahbad Daulatpur, Main Bawana Road, Delhi-110042
July, 2024

Dedicated

to

My

Parents

DELHI TECHNOLOGICAL UNIVERSITY
(Formerly Delhi College of Engineering)
Shahbad Daulatpur, Main Bawana Road, Delhi-110042

CANDIDATE'S DECLARATION

I, Ritu, 2K19/PHD/BT/13, hereby certify that the work which is being presented in the thesis entitled **"Development of Nanoparticle mediated Drug Delivery System for Anticancer Bioactive Compounds"** in partial fulfillment of the requirements for the award of the Degree of **Doctor of Philosophy**, submitted in the Department of Biotechnology, Delhi Technological University is an authentic record of my own work carried out during the period from 19th July 2019 to 31st July 2024 under the supervision of Dr. Asmita Das and Co Supervision Dr. Prakash Chandra, Department of Biotechnology, Delhi Technological University.

The matter presented in the thesis has not been submitted by me for the award of any other.

Place: Delhi
Date: 17 December, 2024

Candidate's Signature
Ritu (2K19/PHDBT/13)

This is to certify that the student has incorporated all the corrections suggested by the examiners in the thesis and statement made by the candidate is correct to the best of our knowledge.

Signature of Supervisor(s)
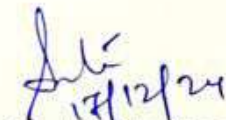
Signature of External Examiner

DELHI TECHNOLOGICAL UNIVERSITY
(Formerly Delhi College of Engineering)
Shahbad Daulatpur, Main Bawana Road, Delhi-110042

CERTIFICATE

Certified that Ritu (2K19/PHDBT/13) has carried out their search work presented inthis thesis entitled **"Development of Nanoparticle mediated drug delivery system for anticancer bioactive compounds"** for the award of Doctor of Philosophy from Department of Biotechnology, Delhi Technological University, Delhi, under our supervision. The thesis embodies results of original work, and studies are carried out by the student herself and the contents of the thesis do not form the basis for the award of any other degree to the candidate or to anybody else from this or any other University/Institution.University/Institution.
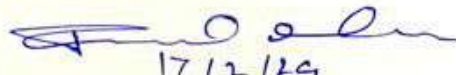
Place: Delhi

Date: 17 Dec, 2024

Dr. Asmita Das
Associate Professor
Department of Biotechnology
Delhi Technological University
(Supervisor)

Dr. Prakash Chandra
Assistant Professor
Department of Biotechnology
Delhi Technological University
(Co-Supervisor)

Prof. Yasha Hasija
HoD
Department of Biotechnology
Delhi Technological University

ABSTRACT

Colorectal cancer remains a significant global health challenge, particularly affecting individuals aged 50 and older. Primary prevention strategies, including healthy lifestyle choices, risk avoidance, and early detection through regular screening, are crucial in reducing its incidence and impact. Early detection methods such as stool-based tests and colonoscopies, along with treatments tailored to the cancer stage, play a pivotal role in managing the disease. While current treatments like surgery, chemotherapy, radiotherapy, targeted therapy, and immunotherapy are effective, they often come with substantial side effects. The effectiveness of FDA-approved anticancer drugs in treating colorectal cancer is limited, and they often come with significant side effects.

Our research delves into the alterations in gene expression induced by chemotherapeutic agents and explores the potential of various natural compounds to counteract these disruptions. We aim to mitigate the dysregulation in gene expression provoked by chemotherapy administration by strategically using natural compounds. By elucidating these mechanisms, we seek to enhance the efficacy of cancer treatment while minimizing adverse effects on gene expression. The current research performs expression profiling of gene alterations in colorectal cancer and the effects of chemotherapy with an irinotecan based on datasets GSE62322 and GSE72484. Parsing differentially expressed genes in colorectal cancer versus normal tissue and in samples after chemotherapy versus not-treated ones helped explain irinotecan's effect on gene expression and its relation to serious side effects. Our findings demonstrate that many genes altered by chemotherapy are involved in crucial cancer progression pathways and are thus associated with adverse effects, such as anemia, bone marrow depression, nausea, fatigue, diarrhea, neutropenia, and cholinergic syndrome.

We intended to identify specific molecular targets that could be associated with the side effects of FDA-approved drugs. In this respect, such unintended adverse reactions could be expected when these drugs interact with their targets. While considering substitutes for traditional chemotherapy, we focused on the potential use of natural

compounds, especially EGCG, as potent agents against cancer with minimized side effects. Our study in molecular dynamics revealed a promising interaction of EGCG against human TOPO I, showing its potential to act as an inhibitor of the tumor as irinotecan does and evade AChE that causes cholinergic syndrome. While EGCG is a naturally occurring substance, it can potentially produce dose-dependent toxicity in normal human cells. To address this issue, we have developed drug delivery through nanoparticle-mediated mechanisms. Because calcium carbonate nanoparticles (CCN) have been shown in the literature to have the following properties: abundant, less harmful to cells, safe, biocompatible, pH-responsive, and gradually biodegradable, we synthesized CCN using the chemical precipitation method.

Calcium carbonate nanoparticles ($CaCO_3$) would be ideal for targeted drug delivery to cancer cells during therapy because they are stable in neutral and basic pH conditions but dissolve in an acidic environment.

Because cancerous cells have a low pH, they cause $CaCO_3$ to dissolve and release encapsulated medications, such as EGCG. The drug releases very little at a neutral pH, similar to healthy tissues' pH, but a lot more when the pH is acidic (pH 4-6). By maintaining therapeutic levels, this controlled release minimizes potential risks associated with EGCG overdose, including nephrotoxicity and myelosuppression. Furthermore, it was observed that the drug-loaded $CaCO_3$ nanoparticles showed decreased cell viability based on the results of the MTT assay. Flow cytometry analysis revealed significantly higher incidents of both the early and late apoptosis stages than the drug administered alone. The results thus indicate that the $CaCO_3$ nanoparticle delivery system has improved the therapeutic efficacy of the drug while potentially reducing its cytotoxic side effects.

In conclusion, our discovery opens up prospective pathways for customized medicine and improved patient care in the field of cancer treatment by offering insights into the molecular reactions responsible for the side effects of FDA-approved drugs. The findings of the study might act as a basis for further investigation and treatment advancements in the field of oncology. In conclusion, different cancers have high death rates and varied biology and molecular characteristics. We can learn more about the pathogenic mechanisms behind colorectal cancer by employing bioinformatics techniques and undertaking thorough investigations of gene expression, biological

processes, and pathways. This information offers insightful information for further investigation of treatment plans, including combinatorial therapies. Continued research can lead to innovative cancer treatments inspired by nature, transforming the therapeutic landscape for better outcomes.

In summary, our findings provide significant insight into the molecular mechanisms underlying irinotecan-mediated side effects and thereby offer a new dimension in cancer therapy through the rational use of natural compounds and nanoparticle-mediated drug delivery. This nanoparticle-mediated delivery system showed promise for safe and efficient targeted cancer therapy. Future research should elucidate the mechanisms of selective toxicity and conduct in vivo testing to evaluate the pharmacokinetics, biodistribution, and therapeutic efficacy of EGCG-loaded CCNPs using animal models. Additionally, exploring this nanocarrier system for other therapeutic agents could broaden its application within nanomedicine. Expanding studies to include various natural compounds could identify new candidates with superior efficacy and minimal side effects. Our study underscores the potential of integrating bioinformatics, molecular biology, and nanotechnology to develop novel, targeted cancer treatments, enhancing patient care and overcoming limitations of conventional therapies. We shall strive to unravel these mechanisms with the idea of developing better cancer treatment strategies with reduced adverse effects, thus leading to the ultimate goal of personalized medicine and improved patient care in oncology. Further research in this line could lead to nature-inspiring and innovative cancer therapies that will transform treatment landscapes and be more effective for patients with colorectal cancer and beyond.

ACKNOWLEDGEMENT

I am delighted to express my profound gratitude and appreciation towards numerous individuals who have provided unwavering support and assistance throughout my Ph.D. study and research journey. First and foremost, I extend my heartfelt thanks to **Prof. Prateek Sharma, Vice Chancellor, DTU, Delhi**, and **Prof. Jai Prakash Saini, Former Vice Chancellor, DTU,** for generously providing me with exceptional facilities and infrastructure that have been pivotal in facilitating my research work.

I am immensely grateful to my supervisor, **Dr. Asmita Das,** and Co-supervisor **Dr. Prakash Chandra** for their invaluable guidance, motivation, and extensive knowledge. Their tireless support and unwavering patience have been instrumental in my research journey, and I am grateful for their exceptional mentorship. I could not have asked for a better advisor to lead me through my Ph.D. study.

Furthermore, I would like to acknowledge and extend my sincere thanks to **Prof. Yasha Hasija** (Head and DRC Chairperson), Department of Biotechnology, and **Prof. Pravir Kumar**(Former Head & DRC Chairman), Department of Biotechnology, DTU, Delhi, for their valuable insights and suggestions, which have been remarkable in enhancing the quality of my research work.

I would also like to express my sincere gratitude to the members of the DRC and SRC, including **Prof. Jai Gopal Sharma, Dr. Navneeta Bharadvaja, Dr. Smita Rastogi**, and **Dr. Kriti Bhandari,** Department of Biotechnology, DTU, Delhi, for their continuous support, encouragement, and constructive feedback throughout my research.

In addition, I am immensely grateful to the technical staff, particularly Mr. Chhail Bihari Singh, Mr. Jitender Singh, Mr. Lalit, and all the staff members of the Department of Biotechnology, who have provided me with constant assistance whenever I required their support.

Ritu

2K19/PHD/BT/13

TABLE OF CONTENTS

LIST OF TABLES

LIST OF FIGURES

conversion of acetylcholine (ACh) substrate to choline. This inhibition of AChE by Irinotecan can lead to an accumulation of ACh, resulting in a condition known as cholinergic syndrome. Cholinergic syndrome is characterized by a range of symptoms, diaphoresis, including abdominal cramping, diarrhoea, and excessive salivation, sweating, and flushing of the skin. On the other hand Epigallocatechin gallate (EGCG), derived from Phyllanthus emblica, exhibits minimal binding affinity towards acetylcholinesterase. Consequently, it is unlikely to effectively inhibit the enzyme and is thereby associated with a low probability of causing any side effects typically attributed to AChE inhibition.

Abbreviation

CRC- Colorectal cancer

AChE - acetylcholinesterase

EGCG- epigallocatechin gallate

CIN - Chromosome Instability

MSI-H - microsatellite instability

MMR - mismatch repair

HNPCC - Hereditary Non-Polyposis CRC

FIT - fecal immunochemical test

ICIs - immune checkpoint inhibitors

DC - dendritic cells

MDSC - myeloid-derived suppressor cells

MHCI - MHC class I

NK cell - natural killer cells

NKT cell - natural killer T cells

PD-L1 - programmed cell death 1 ligand 1

TAM - tumor-associated macrophages

Cytotoxic T cells, and

Treg cell - regulatory T cells

APCs - antigen-presenting cells

CTLA-4 - Cytotoxic T-Lymphocyte Associated Antigen 4

PD-1 - Programmed Death Receptor 1

NSCLC - non-small cell lung cancer

ES-SCLC - extensive-stage small cell lung cancer

HRS - Hodgkin Reed-Sternberg

ACT - Adoptive cell transfer therapy

5-FU - 5-fluorouracil

VEGF - Vascular Endothelial Growth Factor

TP - Thymidine Phosphorylase

PPIs - protein-protein interactions

DMSO - dimethyl sulfoxide

DEGs - differentially expressed genes

COAD - colorectal Adenocarcinoma

GEPIA - Gene Expression Profiling Interactive Analysis

TOPO I - Topoisomerase I

SSBs - single-strand breaks

DSBs - DNA double-strand breaks

PLIP - Protein-Ligand Interaction Profiler

MD - molecular dynamics

RMSD - root mean square deviation

RMSF - root mean square fluctuation

MMGBSA - Molecular Mechanics Generalized Born Surface Area

MMPBSA - Molecular Mechanics/Poisson-Boltzmann Surface Area

BBB- Blood Brain Barrier

PAINS - Pan Assay interference compounds

TPSA- Topological Polar Surface Area

CCN - calcium carbonate nanoparticles

MTT - 3-(4,5-dimethyl-2-thiazolyl)-2,5-diphenyl-2-H-tetrazolium bromide

PI - propidium iodide

CHAPTER I

Introduction

CHAPTER 1: INTRODUCTION

1.1.OVERVIEW

Colorectal cancer (CRC) stands as a significant global health concern, ranking as the third most prevalent malignancy and the second leading cause of cancer-related deaths[1]. According to the American Cancer Society, 2018, CRC affects about 1.8 million people globally[2]. It is the third most common cancer after lung and breast cancers. Alarming statistics indicate that in 2020 alone, approximately 1.9 million new cases of CRC were reported worldwide, accompanied by a staggering 0.9 million fatalities[3, 4]. Notably, the burden of CRC is more pronounced in highly developed nations, although its incidence is steadily rising in middle- and low-income countries due to the influence of Westernization[5]. While modern treatments like surgical resection, radiotherapy, and chemotherapy have made substantial strides, a pressing need remains for more sophisticated prognostic tools and innovative treatment approaches[6]. The intricate interplay between genetic and epigenetic factors significantly contributes to the initiation and advancement of colon cancer[7]. These abnormalities can disrupt the normal gene regulation in crucial cellular processes like cell growth, division, and programmed cell death. Consequently, uncontrolled cell proliferation occurs, leading to the formation of tumors[8]. In the realm of CRC treatment, surgery remains a primary approach. At the same time, first-line chemotherapeutic agents like 5-fluorouracil, irinotecan, and oxaliplatin are commonly employed as stand-alone treatments or as part of post-surgical regimens [9]. There might be systemic side effects from the treatment that include fatigue, headache, pain, musculoskeletal symptoms, increased risk of bleeding and bruising, changes in cognitive function, and bone loss, hair loss, making patients go through a lot of discomfort and hence diminishing their quality of life (Fig.1.1). These side effects are mostly seen after chemotherapy sessions. However, different effects and their intensity vary from person to person. The basis of drugs involved, dosage, and individual response are major contributory factors. High doses of chemotherapy drugs can be toxic to the bone marrow and may suppress it. Bone marrow suppression is one of the significant toxicities that decreases the production of red blood cells, white blood cells, and platelets. This

may cause delay, dose reduction, or even interruption in the chemotherapy regimen being followed by a patient, affecting treatment effectiveness [10].
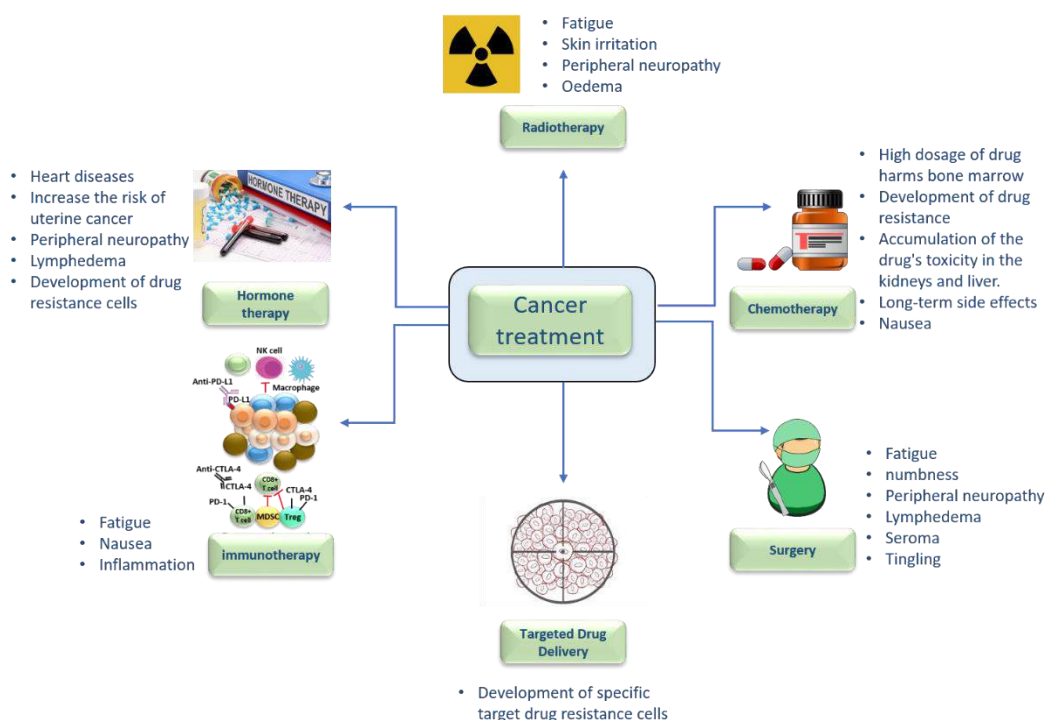
Figure 1. 1 Overview of Cancer Therapies and Their Side Effects. The figure depicts some of the cancer therapies: chemotherapy, immunotherapy, hormone, radiotherapy, surgery, and targeted drug delivery; their common side effects include nausea, fatigue, pain, and organ-specific problems.

The development of chemoresistant cancer cells forces oncologists to increase drug dosages for patients, which then accumulate in the kidneys, liver, heart, and lungs. This increased level of toxicity not only worsens the side effects of the chemotherapy but also decreases its general effectiveness, leading to failures in treatment[11]. Lastly, such massive use of chemotherapy leads to suppression of the immune system and the appearance of neutropenia—the severe decrease in white blood cells, mainly neutrophils, responsible for fighting infections in human organisms. Thus, patients become more susceptible to bacterial superinfections[12].

An alternative approach needs to be adopted for the treatment of cancer that would avoid adverse side effects caused by the presently available chemotherapy drugs. The alternative treatment must utilize a mechanism that would act specifically to kill cancer cells and thus exhibit anticancer activity without eliciting the side effects due to binding with non-intended molecular targets. Natural compounds offer an excellent

alternative to conventional drugs with lower inherent toxicity[13]. Many natural compounds have been found to suppress tumor growth in colorectal cancer by arresting the cell cycle in a specific phase of proliferation or inducing apoptosis in the cancer cells[14]. A modern approach to cancer treatment is generally termed combination therapy, where one or more substances are combined, including conventional chemotherapeutic agents with natural or multiple natural agents simultaneously. This approach, practically in many applications, achieves greater efficacy than the sum of the separate effects of agents, leading to higher drug concentrations or amplifying the applied combined impact of the agents[15]. Additionally, some natural products elicit cytotoxic effects on tumor cells.

Combination therapy has also targeted several signaling pathways by using several mechanisms to reduce the development of resistance against the antitumor drug. This approach reduces the patient's burden by replacing part of the conventional chemotherapeutic dose with a natural substance with a defined effect[16]. Most natural compounds are generally well-tolerated by patients and have not been found to cause toxic effects even when administered at high doses. The most studied plant-derived compounds for improving the effectiveness of conventional chemotherapeutic drugs in colorectal cancer are curcumin (diferuloylmethane), resveratrol (3,4',5-trihydroxystilbene), and (-)-Epigallocatechin gallate (EGCG). Besides, these compounds are particularly noticed to block or reverse the acquired drug resistance.

Further, for the enhanced therapeutic efficacy of these natural compounds, a sophisticated delivery system in the form of nanoparticles should be considered. The basis of nanotechnology in drug delivery is to provide a controlled drug release mechanism, improved bioavailability, and targeting of tumor sites. Thus, a steady exposure of tumor cells to the natural compounds is obtained by a sustained release mechanism for maximum therapeutic efficacy.

Nanoparticles can also be incorporated as a vehicle for delivering such phytochemicals, increasing the potency of the natural compounds at the site of cancer. Nanoparticles engineered with natural compounds can enhance phyto-bio availability and make them available at target sites, concentrate on the desired amount in the tumor area, and minimize exposure to healthy tissues. This targeted approach improves the treatment's therapeutic impact and reduces systemic toxicity and side effects. Such

compounds will be utilized to develop an effective, risk-reduced cancer treatment and advanced delivery systems like nanoparticles. This new strategy genre addresses conventional chemotherapy's failures and gives a more precise and patient-friendly approach to cancer therapy.

Chapter II

Literature review

CHAPTER 2: LITERATURE REVIEW

2.1. Etiology of cancer

The majority of colorectal malignancies (CRC) are thought to arise from precursor lesions called colorectal adenomas, according to a widely recognized paradigm[17]. The term "adenoma-to-carcinoma sequence" refers to the phenomenon. According to this model, the natural history of CRC proceeds along a specific course. When the first mutations arise, the normal colon and rectum epithelium changes into colorectal adenoma[18].

 Adenomas then develop into advanced adenomas after that. After significant genetic alterations, progressed adenoma becomes colorectal cancer[19]. According to the American Joint Committee on Cancer (AJCC), colorectal cancer advances through stages, from stage I to stage IV, if it is not discovered and treated[20]. The serrated pathway is one of the various colorectal carcinogenesis pathways that have been identified. This route is poorly understood and may account for up to 30% of colorectal malignancies[21]

2.1.1. The Adenoma-Carcinoma Pathway

The development of malignant adenomas in the colon's mucosal lining is the cause of colorectal cancer. The majority of CRC cases (70–80%) are caused by this mechanism, which primarily follows the adenoma-carcinoma pattern[22]. This process, which is sometimes referred to as the Chromosome Instability (CIN) pathway, is caused by a sequence of genetic changes that eventually proceed from adenomas to cancer[23]. Mutations in the adenomatous polyposis coli (APC) gene, which controls cell division and proliferation, are usually the first step in the process[24]. The malignant conversion of adenomas into carcinomas is further encouraged by subsequent mutations, such as those in the TP53 tumor suppressor gene and the KRAS oncogene(Fig. 2.1). Remarkably, the left colon and rectum are where this route is most commonly seen[25].

2.1.2. The Serrated Adenoma Pathway

About 10–30% of cases of colorectal cancer have the serrated adenoma route, which is more frequently located in the right colon[26]. A characteristic molecular characteristic of cancers arising from this route is high-level microsatellite instability (MSI-H)[27]. Mutations in DNA mismatch repair (MMR) genes, including MLH1, MSH2, and MSH6, cause this instability and decrease MMR function[28]. As a result, tumors bearing the MSI-H mutation have a tendency to accumulate genetic changes that aid in the tumors' development into malignancies(Fig.2.1). Remarkably, MSI-H tumors are linked to Lynch syndrome, a genetic disorder marked by an elevated risk of many malignancies in addition to sporadic colorectal cancer[29]. The effectiveness of screening colonoscopies in avoiding right-sided colon cancer may be impacted by the difficulty in detecting sessile serrated adenomas, a precursor lesion in this route[30, 31].

2.1.3. Genetic Colorectal Cancer

Although most CRC occurrences are incidental, about 5% of cases are genetically related[32]. One such genetic condition is called Familial Adenomatous Polyposis (FAP), which is characterized by the development of numerous colonic adenomatous polyps, frequently starting at an early age[33]. If surgery is not performed to remove the colon and rectum, individuals with FAP have a nearly 100% lifetime risk of getting CRC. A small percentage (3-5%) of all instances of CRC are caused by Lynch syndrome, commonly referred to as Hereditary Non-Polyposis CRC (HNPCC)[34]. Germ-line mutations, mostly in the MLH1 and MSH2 genes, which encode proteins essential for DNA repair, cause this disease[35]. In addition to colorectal cancer, Lynch syndrome leads to gastric, ovarian, endometrial, and small bowel cancers. Early detection and prevention efforts rely heavily on the identification and treatment of these inherited illnesses[36].
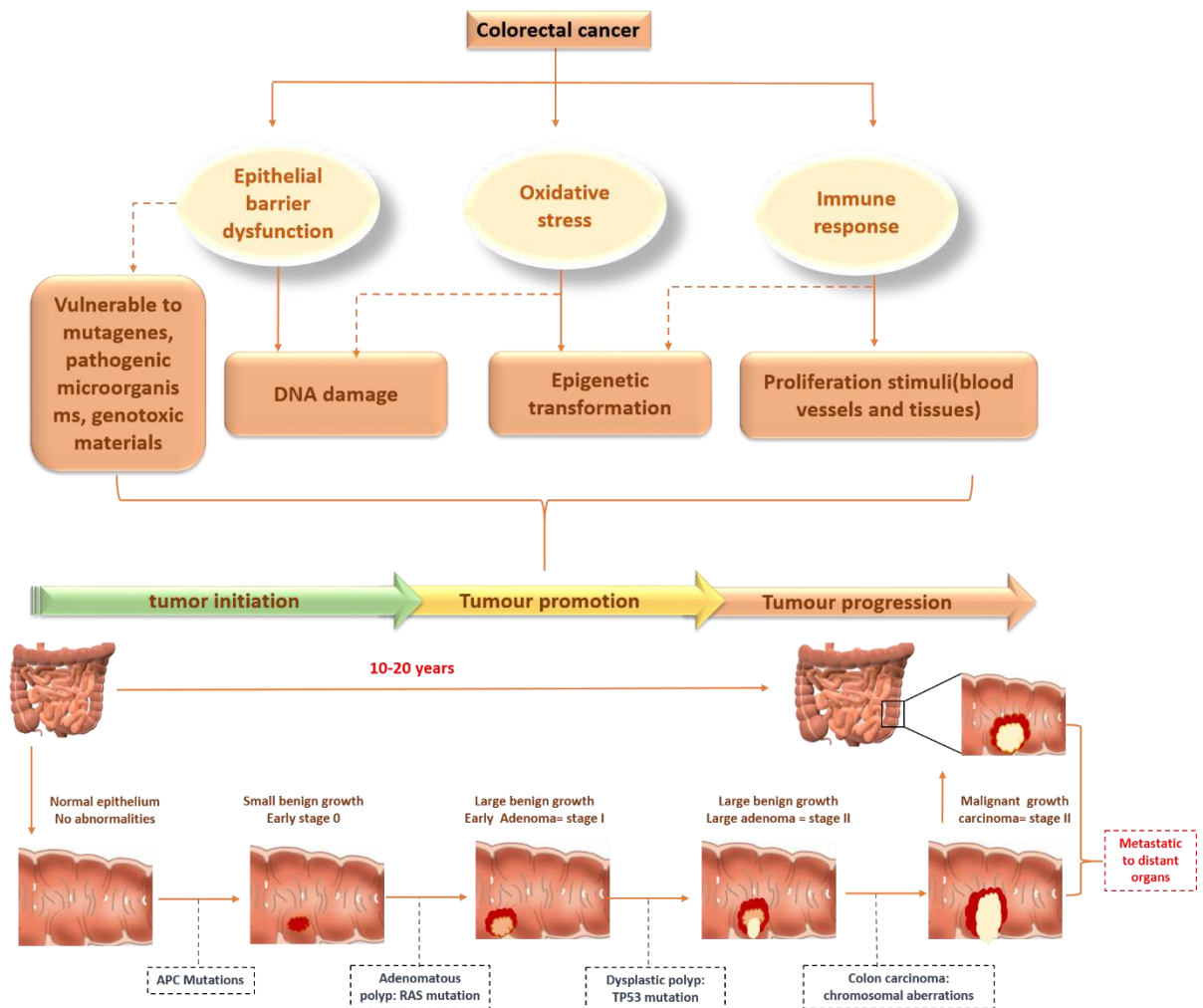
Figure 2.1 Mechanisms of development and progression of CRC from stage 0 to metastatic phase.This figure illustrates the multistep process in colorectal cancer development, from normal epithelial cells to adenocarcinoma and finally metastatic carcinoma. All events occurring at each step are depicted, which range from genetic mutations to environmental influences and behavioral lifestyles. Progression from stage 0 carcinoma in situ through stages I-III of local and regional spread to stage IV distant metastasis is described with its morphologic and molecular alterations in each phase.

2.2. Screening

Advanced stages of CRC, particularly stages III and IV, are closely linked to increased mortality rates, underscoring the critical importance of early detection[37]. It's estimated that approximately 25% of individuals aged 50-79 years in Western countries harbor colorectal polyps. While not all polyps progress to cancer, if they do, the process typically spans over 10-15 years[38]. The primary goal of CRC screening programs is to identify and remove polyps and detect CRC before symptoms manifest.

There are two main screening strategies available first is Fecal Occult Blood Testing and endoscopics strategies.

2.2.1. Fecal Occult Blood Testing (FOBT)

FOBT is the most widely used screening test for CRC. The technique detects hidden blood in stool, indicating possible CRC. This is a non-invasive, inexpensive, easy to use, and at-home test. As bleeding from CRC is intermittent, FOBTs are repeated annually or biennially to increase sensitivity. There are two main types: guaiac-based FOBT and fecal immunochemical test.

i.   Guaiac Fecal Occult Blood Test (gFOBT)

The gFOBT detects hidden blood in stool through a chemical reaction using the pseudo-peroxidase activity of hemoglobin. The test is carried out by applying a stool sample onto guaiac paper and it turns blue on contact with hemoglobin due to an oxidative reaction. The most common CRC screening test method used is gFOBT due to its simplicity, wide availability, and very low cost. however, dietary and gastrointestinal factors can affect results. This test has low sensitivity for CRC of 25%-38% and for advanced adenomas of 16%-31%[39].

ii.   Fecal Immunochemical Test (FIT)

The fecal immunochemical test uses monoclonal or polyclonal antibodies that recognize and bind to intact globin of human hemoglobin and thereby offer higher specificity for colorectal bleeding. It has higher sensitivity for CRC and advanced adenomas than gFOBT, though with slightly lower specificity[40]. FIT can either be qualitative or quantitative, the latter providing automated reading and adjustable thresholds. Compliance is higher with FIT compared to gFOBT. The majority of Western nations have implemented CRC screening programs, with the most prevalent method being the FIT administered annually to biennial individuals aged 50-74 years[41]. A positive FIT result prompts further evaluation through colonoscopy. For

example, in the Stockholm-Gotland Region, CRC screening targeting individuals aged 60-69 commenced in 2008. During the inaugural year, 64% of the targeted population participated in the screening. Of those with a positive test result, 88% underwent subsequent colonoscopy procedures[42, 43].

2.2.2. Flexible Sigmoidoscopy (FS)

Flexible sigmoidoscopy represents an endoscopic screening method for colorectal cancer. It visualizes directly the rectum, sigmoid, and part of the descending colon. Its usage is restricted only to the left side of the colon while permitting examination by direct vision of the colon, tissue sampling, and removal of polyps[44]. FS allows for the direct investigation of the distal colon, biopsy, and polyp removal. RCTs (Random control trials) showed that FS decreased CRC mortality by 22%-31% and incidence by 18%-23%. However, proximal lesions can be missed, particularly in women. FS also entailed variable adherence rates of 14%-81%, but it detected more adenomas than stool tests[45].

2.2.3. Colonoscopy

A colonoscopy assesses the whole colon and allows biopsy and polyp removal in one sitting. It has the advantage of longer screening intervals—typically every 10 years after a normal examination. In addition, for lesions, colonoscopy can evaluate characteristics of the lesions, like adenomas versus hyperplastic polyps, and precancerous or early malignant changes[46]. This is an extremely sensitive and specific tool; however, it lacks RCTs associating its usage with decreased CRC mortality. Observational studies associate its use with a 67%-77% reduction in CRC incidence and a 31%-65% reduction in mortality. However, this is an invasive, expensive procedure requiring rigorous bowel preparation[47].

i. Virtual Colonoscopy

Virtual colonoscopy includes CT colonography and MR colonography. The former, CTC, is a test with good accuracy for CRC and large adenomas, but it uses radiation.

The latter, MRC, although with good results, is still hampered by higher costs and more complex logistics[48]. Positive findings by both techniques need to be followed up with endoscopy, and neither of these modalities has been shown to lower CRC incidence or mortality.

ii.   Colon Capsule Endoscopy(CCE)

Colon capsule endoscopy of the small bowel rapidly emerged as a first-line imaging modality for patients with obscure gastrointestinal bleeding; CCE had an early phase of skepticism. This was due to high procedural costs, an extensive bowel cleansing undertaken to achieve only reasonable adenoma detection rates, and a limitation of not being able to take biopsies [49]. In 2006, the first generation of colon capsule endoscopy, CCE-1, PillCam Colon; Given Imaging Inc., Yoqneam, Israel, now Covidien/Medtronic, a less invasive and wireless technique for the visualization of the large bowel, was introduced[50]. By 2009, a second generation of colon capsule endoscopy was developed, called CCE-2, which significantly improved the viewing angle and adjusted the frame rate for a panoramic view. Since then, indications have been evaluated and established for several CCE purposes[51].

2.3. Therapeutic Approaches

2.3.1. Local Approaches - Radiation Therapy:

In the treatment of rectal cancer, neoadjuvant therapy—a combination of chemotherapy and radiotherapy—has successfully decreased tumor burden at intermediate and advanced stages, with the goal of lowering the risk of local recurrence and enhancing overall survival[52]. Though it doesn't considerably improve overall survival, preoperative radiation therapy seems to be more successful in lowering local recurrence than postoperative therapy[53]. There are two types of radiotherapies: short-course and long-course. The long-course has a higher rate of acute toxicity and similar late adverse effects[54]. Precisely targeting tumors with little exposure to healthy tissue, novel delivery techniques such as intensity-modulated radiotherapy

(IMRT) present encouraging benefits for patients with rectal cancer[55, 56]. Potential benefits of IMRT include accelerated surgery, aided healing following surgery, and enhanced tolerance to adjuvant chemotherapy. Although radiation treatments are beneficial for stage II and III colorectal cancer (CRC), they carry a risk of long-term harm to important organs[57]. The large-scale implementation of IMRT has been quite challenging due to the high cost and complexity involved, with sophisticated equipment and comprehensive QA (quality assurance) systems required, along with a multi-disciplinary team.

2.3.2. Immunotherapy as an option for cancer treatment

In 2018, the Nobel Prize in Medicine or Physiology recognized the ground breaking impact of checkpoint blockade therapy in cancer treatment[58]. As part of their immune response, tumors have developed mechanisms to produce an immunosuppressive microenvironment, which hampers the immune system's ability to remove cancer cells effectively(Table 2.1)[59]. Several processes contribute to this immunosuppression, as described below [60]. Firstly, there is a significant increase in CD25+ regulatory T cells (Tregs): Tregs, a distinct subgroup of T cells, play a critical role in preventing exaggerated immune responses and upholding immune tolerance. Tregs accumulate in the TME, suppressing the activity of effector T cells and other immune cells. Tregs employ diverse strategies to exert their suppressive function. One of their mechanisms involves the secretion of immunosuppressive cytokines such as interleukin-10 (IL-10) and transforming growth factor-beta (TGF-β). Additionally, Tregs can establish inhibitory interactions through direct cell-to-cell contact [61, 62]. Reduced diffusion of cancer-specific CD4+ and CD8+ effector T cells: Cancer cells are likely to be killed by CD4+ helper T cells as well as CD8+ cytotoxic T cells(Fig. 2.3). Infiltration of these effector T cells into tumors can, however, be limited by the TME [63] By removing regulatory barriers that separate immune cells like T-cells from malignant cells, this strategy unleashes the immune system's potential to identify and combat cancer cells[64]. Development of Anti-CTLA-4 and anti-PD-1/PD-L1 therapies have revolutionized the field of cancer immunotherapy by targeting key immune checkpoint molecules and enhancing anti-tumor immune responses[65]. There have been numerous attempts to develop monoclonal antibodies that specifically target co-inhibitory transmembrane receptors (PD-1). PD-L1 and PD-L2 ligands are present

in a small subset of NK cells, dendritic cells, and antigen-stimulated B and T lymphocytes[66]. PD-1 inhibits adaptive immunity during sustained antigen exposure in multiple cancers. CTLA-4, an additional immune checkpoint that has been used for the survival of metastatic melanoma, helps in decreasing the T-cell response[67]. Ipilimumab, an approved anti-CTLA-4 therapy, blocks the CTLA-4 receptor on T cells, allowing the immune system to decipher and combat tumor cells [68]. Notably, the use of checkpoint inhibitors, such as pembrolizumab and nivolumab, has been approved for a variety of cancers with high genomic instability[69]. However, it is a major breakthrough in cancer treatment that they are able to use the immune system's capacity against cancer along with several challenges [70]. The treatment of highly mutated tumors in CRC that are mismatch-repair-deficient (dMMR) or have high levels of microsatellite instability (MSI-H)—referred to as dMMR–MSI-H tumors—with immune checkpoint therapy was approved by the FDA in 2017. The tumors that are mismatch-repair-proficient (pMMR), microsatellite-stable (MSS), or have low levels of microsatellite instability (MSI-L) are referred to as pMMR–MSI-L tumors, and they do not respond well to the existing immune checkpoint inhibitors (ICIs). Although these medications are good at increasing T-cell activity against cancer, they can also trigger autoimmune reactions as a result of T-cell activation, which can lead to related side effects(Fig.2.2)[71]. A very important role that antibodies play in targeted cancer therapy is in the recognition and binding of epitopes formed on the surface antigens of malignant cells to inhibit their growth and spread. These treatments often lead to the development of some side effects like infusion reactions, fatigue, nausea, diarrhea, skin reactions, infections, hematologic toxicities, and damage to organs such as kidneys, hearts, livers, and lungs(Table. 2.2). For example, the monoclonal antibody bevacizumab (Avastin), when taken in conjunction with chemotherapy, prevents new blood vessels from supplying tumors, therefore decreasing the growth of malignancies[117](Table. 2.2). However, it has a significant risk of intestinal perforation in addition to vascular adverse effects including hypertension and infrequent instances of stroke or heart attack[118]. Immune resistance mechanisms in these tumors have been proposed to include low tumour mutation burden and absence of immune cell infiltration.
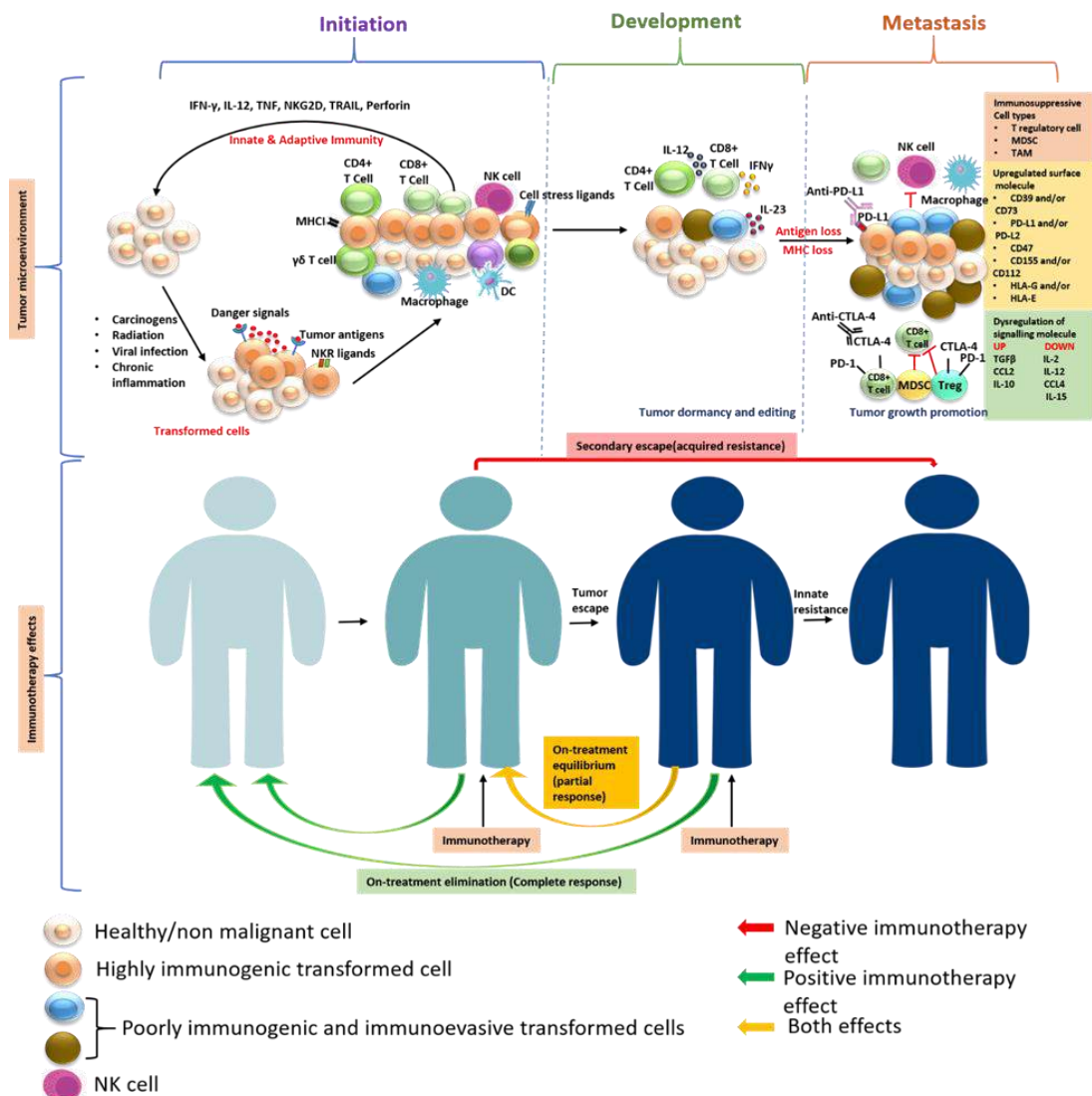
Figure 2.2. Tumor microenvironment and Response to Cancer Immunotherapy. This figure elucidates the intricate phases of cancer—initiation, development, and metastasis. In the development phase, the innate and adaptive immune systems collaborate to seek out and obliterate transformed cells that have eluded natural tumor-suppression mechanisms, halting tumor growth before clinical detection. Tumors move on to the development stage, which is characterized by restricted growth and adaptive immune sculpting of tumor immunogenicity, if the metastatic phase fails. The metastasis phase follows, where tumors, through activation of immunosuppressive and immunoevasive pathways, surge unhindered into clinical visibility. Immunotherapy's effectiveness lies in its ability to rekindle antitumor immune responses; its success is marked by a complete response when tumors revert to the initiation phase, or a partial response when they are pushed into on-treatment development phase. Acquired resistance may emerge if immunotherapy fails to fully conquer tumor-induced immune suppression, permitting the outgrowth of immune-resistant tumor clones. Key immune players include dendritic cells (DC), myeloid-derived suppressor cells (MDSC), MHC class I (MHCI), natural killer cells (NK cell), natural killer T cells (NKT cell), programmed cell death 1 ligand 1 (PD-L1), tumor-associated macrophages (TAM), Cytotoxic T cells, and regulatory T cells (Treg cell).

Table 2.1. The specific name or trade name of the antibody and their Mechanism of Action: The primary mode of action or mechanism by which the antibody functions in cancer treatment, such as blocking signaling pathways, targeting immune checkpoints, delivering payloads, etc.

Classes of immunomodulatory antibodies	Mechanism of Action	Examples of Drugs
Monoclonal antibodies	Target tumor-associated antigens to induce an immune response	Trastuzumab, Rituximab, Cetuximab, Brentuximab vedotin, Daratumumab, Mogamulizumab, Atezolizumab
Checkpoint inhibitors	Block immune checkpoint pathways to unleash T cells	Ipilimumab, nivolumab, pembrolizumab, atezolizumab, durvalumab, and relatlimab are among the approved antibodies targeting CTLA-4, PD-1, PD-L1, and LAG-3 for various therapeutic purposes.
Bispecific T-cell engagers	Link T cells and cancer cells to induce T cell-mediated lysis	Blinatumomab, Catumaxomab, Mosunetuzumab
Antibody-drug conjugates	Deliver cytotoxic drugs selectively to cancer cells	Ado-trastuzumab emtansine (T-DM1), Brentuximab vedotin (Adcetris), Trastuzumab deruxtecan (Enhertu), Sacituzumab govitecan (Trodelvy)
Immunomodulatory cytokines	Activate T cells and NK cells to kill cancer cells	Interleukin-2 (IL-2), Interferon-alpha (IFN-alpha), Interleukin-12 (IL-12), Interleukin-15 (IL-15), and Interleukin-21 (IL-21) are examples of immunomodulatory molecules that have been studied for their potential therapeutic applications in various diseases.
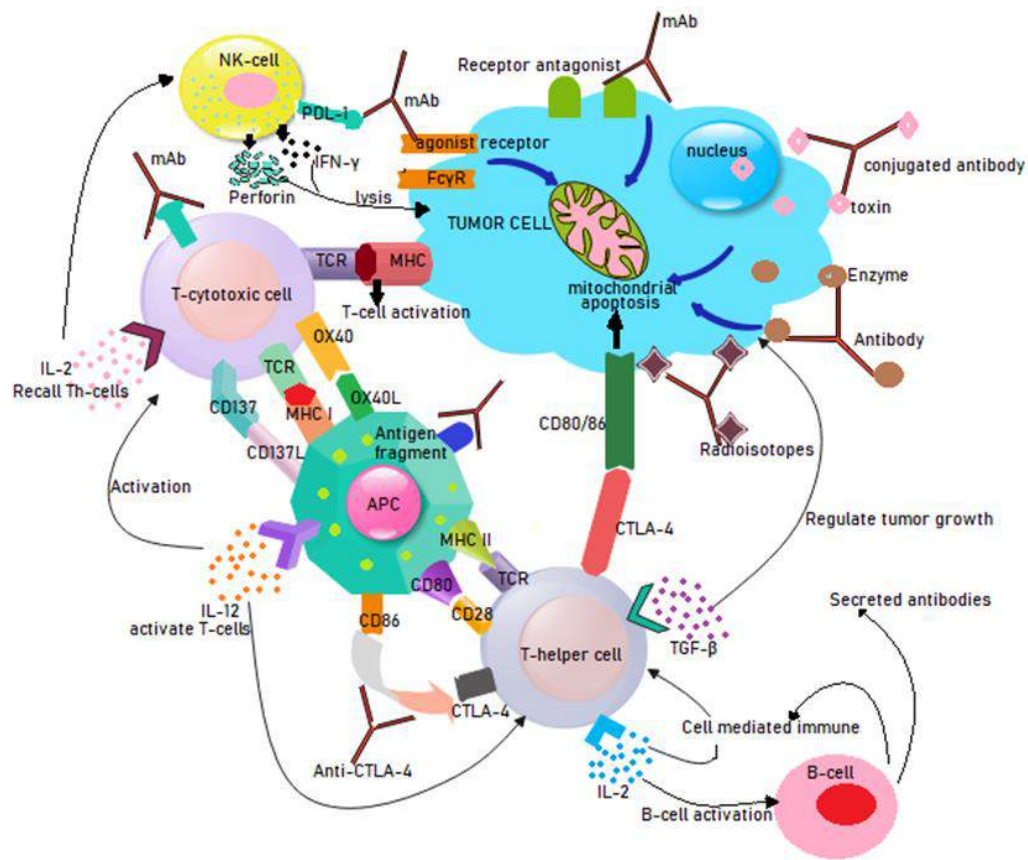
Figure 2.3. Monoclonal antibody therapeutics, T-cell interaction with APC and tumor cell. The rejections of tumor cells are mediated by several types of leukocytes and monoclonal antibodies which act on their surface glycoproteins and help in initiating optimal immune responses by APCs (antigen-presenting cells), B-cell, and T-cells. Different Immunostimulatory mAbs upon binding to their specific receptor either promote lymphocyte/immune activation (agonist) or promote activation of dendritic cells (APC) that contribute to immune evasion. Many antibodies conjugated with different molecules like toxins, enzymes, and radioisotopes directly activate mitochondrial apoptosis and result in the direct killing of malignant cells. The interaction between APC and T cells can initiate the secretion of interleukin-12, Transforming Growth Factor β, and interleukin-2 and which activates and recalls of Th1-type immune response against cancer, the distinction of unsophisticated T-cells into effector cells, and inhibition of normal stromal, hematopoietic and epithelial cell growth respectively.

Table 2.2 Immune checkpoint inhibitors (ICIs) as Immune Boosters:

Name of antibodies and their combinations	Targets	Type	FDA Approval	Type of cancer and targeting cells	Common side effects	References
Alemtuzumab	**Anti-CD52**	**Humanized monoclonal antibody**	**2001**	In B-cell chronic lymphocytic leukemia, Alemtuzumab targets CD52, a cell surface antigen expressed on these immune cells. By binding to CD52, Alemtuzumab induces depletion of B-CLL lymphocytes, leading to reduced tumor burden.	Depletion of B-CLL lymphocytes, potentially leading to reduced immune function, infusion reactions, increased risk of infections.	[72]
			2014	**Multiple Sclerosis (MS)**		[73][74]
Atezolizumab	**PD-L1**	**Humanized Fc-engineered**	**2016**	Targets macrophages, activated T-cells, keratinocytes, and dendritic cells in Urothelial carcinoma, NSCL.	Fatigue, nausea, diarrhea, decreased appetite, skin rash, immune-related adverse events.	[75][76]
Chemotherapy (cisplatin + gemcitabine			**2016**	The addition of atezolizumab to cisplatin and gemcitabine regimens has demonstrated the potential to enhance overall survival and progression-free survival in patients diagnosed with advanced or metastatic urothelial carcinoma and non-small cell lung cancer.		[77]
Bevacizumab + chemotherapy (carboplatin + paclitaxel)			**N/A**	The treatment regimen combines the targeting of tumor vasculature with the augmentation of the anti-tumor immune response. Encouraging findings from clinical studies have shown positive outcomes when atezolizumab is added to bevacizumab and chemotherapy, particularly in advanced ovarian cancer and non-squamous non-small cell lung cancer.		[78]
Chemotherapy (carboplatin + paclitaxel)			**N/A**	The combination therapy of atezolizumab with carboplatin and nab-paclitaxel has demonstrated substantial advancements in both progression-free survival and overall survival, surpassing the outcomes achieved with chemotherapy alone. This establishes the effectiveness of this combination as a viable first-line treatment option for patients with metastatic non-squamous non-small cell lung cancer (NSCLC).		[79]
Chemotherapy (etoposide + carboplatin)						
daratumumab			**N/A**	The inclusion of atezolizumab alongside chemotherapy has shown significant improvements in both overall survival and progression-free survival among patients		[80]

Varlilumab (agonist anti-CD27 mAb)			**N/A**	diagnosed with extensive-stage small cell lung cancer (ES-SCLC).		[81]
Durvalumab			**2019/20**	Daratumumab has demonstrated immune-modulating effects, including enhancing T-cell responses and NK cell-mediated cytotoxicity. By combining it with atezolizumab, which blocks the PD-L1/PD-1 immune checkpoint pathway, the aim is to further enhance the anti-tumor immune response	Infusion reactions, fatigue, nausea, respiratory infections, neutropenia.	[82]
Anti-OX40 mAb (MOXR0916)			**2019/20**	Preclinical studies and early-phase clinical trials have explored the synergistic effects of these two agents in activating the immune system and enhancing anti-tumor responses. The rationale behind combining varlilumab and atezolizumab is to target different immune checkpoints simultaneously, promoting a more robust and sustained immune response against cancer cells. Durvalumab and atezolizumab are immune checkpoint inhibitors that effectively target the PD-L1/PD-1 pathway, thereby augmenting the immune response against tumors. Restoring antitumor surveillance through T-cell activation In patients previously treated with platinum-based chemotherapy in advanced NSCLC, it did not improve efficacy compared to atezolizumab monotherapy.	Fatigue, cough, dyspnea, rash, diarrhea, decreased appetite, pruritus.	[83] [84]
Avelumab	**PD-L1**	**Fully human**	**N/A**	Targets macrophages, DCs, activated T-cells, and keratinocytes, in refractory ovarian cancer. Further studies are warranted to confirm these findings and explore their long-term benefits.	Infusion reactions, fatigue, nausea, diarrhea, decreased appetite, rash, peripheral edema, musculoskeletal pain, Immune-mediated pneumonitis, hepatitis, colitis, endocrinopathies, severe infusion reactions, hepatotoxicity, thrombocytopenia	[85] [86]
			2017	Merkel Cell Carcinoma		[87]
			2018	PD-L1 PD-L1 inhibitor Locally and advanced urothelial carcinoma		
Utomilumab (an anti-CD137mAb)			**N/A**	Suppress signaling through the immune checkpoint. One antibody releases the inhibitory effects of the immune checkpoint (Nivolumab) and another antibody directly activates the adaptive immunity.		[88, 89]
Blinatumomab	**Anti-CD3/CD19**	**Bispecific antibody**	**N/A**	Targets B-cells, follicular DCs in B-cell precursor acute lymphoblastic leukemia.	fatigue, nausea, diarrhea, decreased appetite, rash, peripheral edema,	[90]

					musculoskeletal pain,	
Brentuximab vedotin	**Anti-CD30**	**Chimeric IgG1, ADC with MMAE payload**	**N/A**	Targets Hodgkin Reed-Sternberg (HRS) cell in classical Hodgkin lymphomas	Fatigue, nausea, vomiting, diarrhea	[91]
Camrelizumab **Gemcitabine + cisplatin**	**PD-1**	**Humanized IgG4 antibody**	**N/A**	Osteosarcoma, Nasopharyngeal carcinoma	Infusion reactions, fatigue, nausea, back pain, fever, cough, upper respiratory tract infection.	[92]
Cantuzumab mertansine	**CanAg (a glycoform of MUC1)**	**Humanized IgG1 with DM1 payload**	**N/A**	Activated T-cell, B-cell, and epithelial cell in colorectal cancer	Diarrhea, nausea, mulculoskeletal pain	[93]
Cemiplimab	**PD-1**	**Fully human IgG4**	**2018**	Cutaneous squamous-cell carcinoma	Respiratory infection, diarrhea, nausea	[94][95]
Daratumumab **Durvalumab**	**CD38**	**Humanized IgG1**	**N/A** **N/A**	Multiple myeloma Multiple myeloma Decreased regulatory T-cell frequency and LAG3+ T-cell proportion and CD8+ T-cell expression of TIM-3, without affecting T- or NK-cell frequencies	Infusion reactions, fatigue, nausea, back pain, fever, cough, upper respiratory tract infection.	[96] [97]
Durvalumab **Chemotherapy (cisplatin + gemcitabine)**	**PD-L1 and PD-1** **PD-L1**	**Engineered human**	**2019** **2017**	Durvalumab prevents the interaction between PD-L1 and its receptor PD-1 on T cells, effectively inhibiting the PD-1/PD-L1 immune checkpoint pathway. The immune system's restrictions are lifted by this blockage, enabling T cells to identify and target cancer cells for attack. By restoring anti-tumor immune responses, Durvalumab offers a promising approach for the treatment of urothelial carcinoma, NSCLC Urothelial carcinoma	fatigue, nausea, diarrhea, decreased appetite, rash, peripheral edema, musculoskeletal pain,	[98] [99]
Gemtuzumab Ozogamicin	**CD-33**	**Humanized IgG4, ADC with calicheamicin payload**	**N/A**	Targets Monocytes, granulocytes, and myeloblasts cells in Acute myeloid leukemia	fatigue, nausea, diarrhea, decreased appetite,Infusion reactions, back pain, fever, cough, upper respiratory tract infection. rash, peripheral edema, musculoskeletal pain,	[100]
Imalumab (BAX69) + Panitumumab		**MIF– mediated emission of cytokines (IL-1β, TNFα)**	**N/A**	Hampering the proliferation of MIF overexpressing malignant cells	fatigue, nausea, diarrhea, decreased appetite, rash, peripheral edema,	[101]

					musculoskeletal pain,	
Ipilimumab	**CTLA-4**	**Recombinant fully human antibody IgG1**	**N/A** **2011**	Melanoma, kidney tumor CD80/CD86 interact with CTLA-4 to induce T-cell activation and block the interaction of CTLA-4 with its ligands Metastatic melanoma	fatigue, nausea, diarrhea, decreased appetite, rash, peripheral edema, musculoskeletal pain,	[102, 103] [104, 105]
Nivolumab **Cabiralizumab** **Anti-CD40 mAb**	**PD-1**	**Fully human IgG4**	**N/A** **N/A** **N/A** **2015**	Melanoma, NSCLC, renal cell carcinoma. Prevent conversion of adenosine-monophosphate to adenosine, It induces the activity of macrophages and down-regulates regulatory T cells Prevents osteoclast activation by blocking the inflammatory mediators secreted through macrophages. The basic aim behind the combination is to impede cancer-prompted immune suppression and the conscription of CSF1R-dependent tumor-associated macrophages. It can also enhance Tcell infiltration and induce adaptive immune responses the combination therapy of APX005M (sotigalimab) with chemotherapy, with or without nivolumab, showed promising efficacy in the treatment of metastatic pancreatic adenocarcinoma. The therapy was generally well-tolerated, with manageable side effects. PD-1 and CTLA-4, Blocking the T cell inhibitory pathway by obstructing ligand interaction with PD-L1/2 Metastatic, NSCLC, colorectal cancer, and squamous cell lung cancer,	fatigue, nausea, diarrhea, decreased appetite,Infusion reactions, back pain, fever, cough, upper respiratory tract infection. rash, peripheral edema, musculoskeletal pain,	[106] [107][108] [109] [110]
Obinutuzumab	**CD20**	**Humanized IgG1**	**N/A**	Pre-B-cell, resting B-cell, follicular DCs, circulatory T-lymphocytes in chronic lymphocytic leukemia.	peripheral edema, diarrhea, bonemarrowsupression	[111]
Ofatumumab	**CD20**	**Humanized IgG1**	**N/A**	Targets Pre-B-cell, resting B-cell, follicular DCs, circulatory T-lymphocytes in chronic lymphocytic leukemia	peripheral edema, fatigue, muscles pain, heart deseases	[112]
Pembrolizumab **BRAF inhibitor + MEK**	**PD-1 or PD-L1/L2**	**Human Antibody IgG4**	**2016** **2014**	Its binding hinders the antineoplastic responses by preventing PD-1 from engaging its ligands head and neck cancer, NSCLC Melanoma	fatigue, nausea, diarrhea, decreased appetite,Infusion reactions, back pain, fever, cough, upper respiratory tract infection. rash,	[113] [114, 115]

inhibitor; Ipilimumab					musculoskeletal pain,	
Chemotherapy (carboplatin + pemetrexed); Chemotherapy			2015	Non-Small Cell Lung Cancer		[116]
Tremelimumab	CTLA-4	Humanized IgG2	N/A	Targets T-cell activated B-cells in melanoma, solid tumors		[117]

2.3.3. T-Cell Boosting Therapies:

I. *Adoptive Cell Transfer Therapy:* Adoptive cell transfer therapy (ACT) involves using either autologous or allogeneic cells to enhance immune function[118]. Tumor-infiltrating lymphocytes (TILs), chimeric antigen receptor T (CAR-T) cells, and T cell receptor (TCR) modified T cells are utilized in ACT[119]. While TILs have shown potential in identifying multiple targets in cancer cells, CAR-T cells are designed to target specific antigens like carcinoembryonic antigens (CEA) in CRC. However, challenges such as producing tumor-specific T cells for each patient and the risk of graft-versus-host disease in allogeneic transplants need to be addressed[120, 121].

II. *Vaccines:* Cancer vaccines aim to elicit an immune response against tumor-associated antigens, either through molecular-based, cell-based, or vector-based strategies[122]. While mRNA and DNA vaccines have shown impressive antitumor responses in CRC, cell-based vaccines utilizing dendritic cells and tumor cells have demonstrated potential efficacy, particularly in combination with chemotherapy and immunotherapy[123]. Vector-based vaccines, including live attenuated viruses, yeasts, and bacterial vectors, are emerging options for therapeutic vaccines against CRC, though clinical efficacy remains limited[124, 125].

III. *Role of Cytokines in CRC:* Cytokines play a crucial role in immune responses, with various cells secreting them to regulate immune function[126]. Cytokine-based therapies are complex, requiring a deep understanding of cytokine

biology to maximize antitumor activity while minimizing toxicity[127]. Clinical trials investigating cytokine-based therapies for CRC are ongoing, though preclinical studies are needed to assess potential toxicity. Cytokines have the potential to enhance natural killer (NK) cell and T lymphocyte function, promote lymphocyte infiltration into tumors, and persist in the tumor microenvironment, making them essential molecules in future CRC treatment strategies[128]. Many cytokines such as IL-1 and TNF-α are inherently toxic because of their marked proinflammatory activities[129].

2.3.4. Limitations and Challenges: Despite the promise of immunotherapy and T-cell boosting therapies, they come with long-term effects and limitations[130]. Monoclonal antibodies have a short half-life, limiting their efficacy, while sustained immune activation can lead to immune-related adverse effects (Fig. 2.4)[131]. Challenges such as solid tumor architecture hindering CAR-T cell infiltration and the technical and financial demands of personalized ACT need to be addressed[132]. Additionally, vaccination efficacy may be limited by immune rejection, and cytokine-based therapies may induce toxicity if not carefully regulated[133].
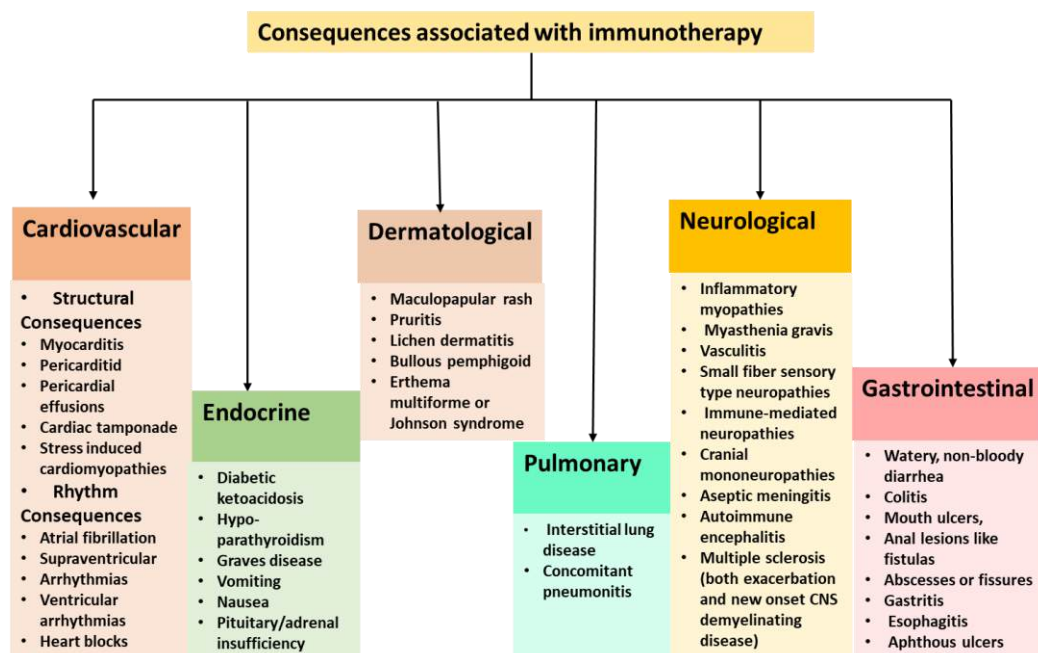
Figure 2.4. Figure illustrates a selection of immune-related adverse events (irAEs) associated with immune checkpoint blockade.

2.3.5. Systemic Approach - Chemotherapy:

A key component of treatment for colorectal cancer (CRC), chemotherapy slows the disease's progression and lengthens survival[134]. It is used in both the neoadjuvant and adjuvant stages of the disease. These results are largely attained with the use of approved cytotoxic medications like capecitabine, oxaliplatin, irinotecan, trifluridine-tipiracil, fluoropyrimidines, and 5-fluorouracil (5-FU)(Table. 2.3)[135]. As a common procedure in the adjuvant scenario, fluoropyrimidine-based chemotherapy is administered after surgery to effectively lower the risk of recurrence and increase overall survival rates[136]. But it's important to be aware of any possible negative effects these therapies may have.

Chemotherapy is essential in the treatment of cancer because it slows down or prevents the growth of cancerous cells, kills cancerous cells, or relieves cancer symptoms. On the other hand, chemotherapy presents several side effects on its patients: nausea, vomiting, hair loss, changes in bone marrow, and changes in mouth and skin health[137]. Other factors include changes in sexual function, fertility problems, and memory malfunctioning[138]. These are side effects which vary according to the type and location of the cancer, its stage, the general health of the patient, the kind of medication that is taken, and the dosage of the prescription.

Table 2.3 FDA approved drugs and their approval with their associated side effects

Targets	FDA-approved drug for colorectal cancer	FDA approval	Side effects	References
Antiangiogenic inhibitors **[Vascular Endothelial Growth Factor (VEGF)]**	**Adagrasib**	**2022**	Diarrhea, nausea, vomiting, fatigue, increased liver enzymes.	[139]
	Alymsys (Bevacizumab)	**2022**	Hypertension, bleeding, thromboembolic events, gastrointestinal perforation, wound healing complications.	[140]
	Avastin (Bevacizumab)	**2004**	Hypertension, bleeding, thromboembolic events, gastrointestinal perforation, wound healing complications.	[141]
	Bevacizumab	**2004**	Hypertension, bleeding, thromboembolic events,	[142]

			gastrointestinal perforation, wound healing complications.	
Topoisomerase inhibitor	**Camptosar (Irinotecan Hydrochloride)/ Irinotecan Hydrochloride**	**1996**	Diarrhea, neutropenia, nausea, vomiting, alopecia.	[143][144, 145]
Thymidine Phosphorylase (TP) inhibitors	**Xeloda** **Capecitabine**	**1998**	Diarrhea, hand-foot syndrome, nausea, vomiting, fatigue.	[146, 147]
	Lonsurf (Trifluridine and Tipiracil Hydrochloride)	**2015**	Myelosuppression,Fatigue, nausea, vomiting, decreased appetite	[148]
Epidermal Growth Factor Receptor (EGFR) inhibitors	**Cetuximab/Erbitux (Cetuximab)**	**2004**	Acneiform rash, infusion reactions, hypomagnesemia, fatigue, diarrhea.	[149]
	Cyramza (Ramucirumab)	**2014**	Hypertension, diarrhea, fatigue, decreased appetite, proteinuria.	[150, 151]
Topoisomerase inhibitor	**Eloxatin (Oxaliplatin)**	**2004**	Peripheral neuropathy, nausea, vomiting, diarrhea, myelosuppression.	[152]
Thymidine Phosphorylase (TP) inhibitors	**5-FU (Fluorouracil Injection)/ Fluorouracil Injection**	**1962**	Myelosuppression, mucositis, diarrhea, hand-foot syndrome, cardiotoxicity.	[152, 153]
	Fruquintinib/Fruzaqla (Fruquintinib)	**2023**	Hypertension, proteinuria, hand-foot syndrome, diarrhea, decreased appetite.	[154, 155]
	Ipilimumab	**2011**	Colitis, dermatitis, hepatitis, endocrinopathies, pneumonitis.	[156, 157]
	Keytruda (Pembrolizumab)	**2014**	Fatigue, pruritus, diarrhea, nausea, rash.	[158]
	Krazati (Adagrasib)		Allergic reactions, diarrhea, nausea, vomiting, mucositis.	[140]
	Leucovorin Calcium	**1982**	Neutropenia, anemia, thrombocytopenia, fatigue, nausea.	[159]
	Mvasi (Bevacizumab)	**2017**	Hypertension, bleeding, thromboembolic events, gastrointestinal perforation, wound healing complications.	[160, 161]
	Nivolumab/Opdivo (Nivolumab)	**2014**	Fatigue, rash, musculoskeletal pain, diarrhea, nausea.	[162–164]

	Oxaliplatin	2002	Peripheral neuropathy, nausea, vomiting, diarrhea, myelosuppression.	[165, 166]
Epidermal Growth Factor Receptor (EGFR) inhibitors	**Panitumumab**	2006	Dermatologic toxicity, hypomagnesemia, paronychia, fatigue, diarrhea.	[167, 168]
	Pembrolizumab	2014	Dermatologic toxicity, hypomagnesemia, paronychia, fatigue, diarrhea.	[169, 170]
Vascular Endothelial Growth Factor Receptor 2 (VEGFR2)	**Ramucirumab**	2014	Hypertension, diarrhea, fatigue, decreased appetite, proteinuria.	[171, 172]
	Regorafenib	2012	Hand-foot skin reaction, hypertension, fatigue, diarrhea, hepatotoxicity.	[173, 174]
Multiple Kinases, VEGFRR1-3, TIE2	**Stivarga (Regorafenib)**	2012	Hand-foot skin reaction, hypertension, fatigue, diarrhea, hepatotoxicity.	[175, 176]
Human Epidermal Growth Factor Receptor 2 (HER2) inhibitors	**Tucatinib**	2020	Diarrhea, nausea, fatigue, vomiting	[177, 178]
	Tukysa (Tucatinib)	2020	Diarrhea, nausea, fatigue, vomiting	[179]

2.4.   The urgency for an alternative approach in cancer therapy:

There is an urgent need for novel strategies like complementary and alternative medicine since efforts to improve the efficacy of cancer treatments have encountered significant obstacles in recent decades[180]. In this field, natural herbal remedies have attracted much interest from researchers and medical professionals because of their potential to prevent or improve the treatment of chronic illnesses, such as cancer[181]. As potential forms of complementary cancer treatments, several natural compounds alone or in combination shows promise. They are appealing because they can interact with various biological targets implicated in metastasis, medication resistance, and tumor growth [182]. Here are several reasons highlighting the need for natural compounds in cancer therapy.

I.   ***Diverse mechanism of action:*** Natural compounds have the potential to improve the effectiveness of current cancer treatments or reduce treatment resistance due to their multitargeting properties[183]. This is crucial as cancer cells can develop resistance to treatments targeting a single pathway.

II.   ***Epigenetic modulation:*** some natural compounds can modulate the epigenetic marks thereby influencing gene expression and potentially reversing abnormal cancer cell behavior [184].

III.   ***Reduced toxicity and side effects:*** The delicate balance between eradicating or killing tumor cells while protecting healthy ones is crucial to cancer treatment. A chemopreventive medication must show an acceptable safety profile and efficacy at low dosages to reduce serious side effects before it can be beneficial in human populations[185]. Natural dietary interventions, including eating more fruits and vegetables, are highly promising in chemopreventive research because of their proven ability to prevent and reduce cancer[186]. Recent studies have highlighted the significance of natural products as anticancer agents, offering low toxicity and durable effects, thereby enhancing the quality of life for patients[187]. These agents, derived from animals, plants, microorganisms, and marine organisms, constitute a significant portion (approximately 50%-60%) of chemotherapeutic agents[187–189]. Natural medicines have been shown to provide several benefits over conventional treatments, such as lower toxicity, lower costs, fewer side effects, and a well-established profile regarding carcinogenic potential.

IV.   ***Overcoming drug resistance***

         Multidrug resistance: Natural compounds can bypass or reverse the multidrug resistance mechanisms in cancer cells, forming a significant barrier to chemotherapy[190].

         Modulation of Drug Efflux: arious natural compounds have been reported as inhibitors against drug efflux pumps, including P-glycoprotein, raising the intracellular concentration of chemotherapeutic drugs[191].

V.   ***Immunomodulatory Effects***

         Boosting Immune Response: Natural products enhance an immune response to cancer cells within the body, elevating immunotherapy's efficacy[192].

Anti-Inflammatory: Chronic inflammation is a risk factor for cancers. Natural compounds may have anti-inflammatory aspects that reduce the chance of developing and progressing toward cancer[193].

VI. *Availability and Cost Effectiveness*

Natural Abundance: Many natural compounds are readily obtained from plants, marine organisms, microorganisms, etc., and are cost-effective reagents in drug design and discovery[194].

Traditional Medicine Integration: Many natural products have a very long history in traditional medicine that lays the basis for their safety profile and efficacy[195].

VII. *Chemical Diversity and Novelty*

Structural Diversity: The vast chemical space covered by natural products provides a rich source of novel structures that might be optimized for anticancer activity[196].

Identification of Lead Compounds: Natural products act as leads for drugs in development, therefore leading to the synthesis of analogues of enhanced potency and selectivity[194].

2.5. Natural compounds in cancer therapy

I. *Alkaloids:* Berberine, derived from various plants like Berberis vulgaris and Oregon grape, inhibits nuclear factor-kappa B and Wnt/β-catenin signaling pathways, exerting antiproliferative and antiapoptotic effects in cancer cells. It also modulates drug resistance mechanisms, making it promising for CRC treatment[197].

II. *Etoposide:* Etoposide is derived from the plant Mayapple and inhibits DNA topoisomerase II, blocking the replication of DNA with a consequent inability of the cell to divide[198].

III. *Vincristine and Vinblastine:* These amines are derived from the periwinkle plant, have the function of inhibiting microtubule formation, and are currently applied in practice to the therapy of many cancers, such as leukemia or lymphoma[199].

IV. ***Polysaccharides:*** Fucoidan, obtained from seaweed, has been found to suppress the toxicity of anticancer drugs in CRC, showing potential in combination therapy approaches[200].

V. ***Polyphenols:*** Curcumin, a well-known polyphenol, downregulates gene products involved in antiapoptosis, cell proliferation, invasion, and angiogenesis. It exhibits anticancer activities in various cancer cell lines and preclinical models, with phase I clinical trials demonstrating its safety and minimal side effects in CRC patients[201]. Gingerol, another potent polyphenol found in ginger, regulates multiple cell signaling pathways implicated in cancer initiation and progression[202]. In human colon cancer cell lines, gingerol reduces cell viability and induces cell cycle arrest, showing promise for CRC treatment.

VI. ***Terpenoids:*** Andrographolide, a terpenoid, activates proapoptotic signaling cascades and induces apoptosis in CRC cells, highlighting its potential as an anticancer agent[203].

VII. ***Polyunsaturated Fatty Acids***: Eicosapentaenoic acid (EPA) and docosahexaenoic acid (DHA), polyunsaturated fatty acids, have shown efficacy in treating various malignancies, including CRC. Their ability to target cancer cells holds promise for CRC therapy[204].

While conventional therapies such as surgery, radiation, and chemotherapy have advanced, they still fall short of ideal outcomes. Chemotherapy, in particular, is widely used but faces limitations such as poor water solubility, short elimination half-life, and toxicity[205]. Combination therapy has emerged as a strategy to address these limitations by simultaneously targeting multiple cellular or microenvironmental factors, leading to enhanced therapeutic benefits [206]. However, challenges such as differences in drug pharmacokinetics and biodistribution, low selectivity, and inherent biological complexity hinder its efficacy[207].

2.6.   Enhancing Therapeutic Efficacy with Nanoparticle-Mediated Drug Delivery Systems

Nanotechnology, propelled by the development of nanomaterial-based drug delivery systems, has played a crucial role in cancer prevention and treatment[208]. Drug-loaded nanoparticles, known as nanomedicines, hold promise in overcoming the limitations of conventional drugs by improving bioavailability, achieving targeted drug delivery, and reducing systemic side effects[209]. Some nanotechnology-based formulations, such as Doxil® and Abraxane®, have already received FDA approval[210].

Natural compounds have shown significant potential in cancer therapy due to their diverse mechanisms of action and reduced toxicity as discussed above. Their clinical application has been limited by various challenges, such as poor solubility, stability, bioavailability, and targeted delivery[211]. In relation, nanoparticle-mediated drug delivery systems have been found to become a very promising solution to these challenges in enhancing therapeutic efficacy against cancer through natural compounds[212]. Here are key reasons pinpointing the necessity of nanoparticle-mediated drug delivery systems for natural compounds in cancer therapy:

The field of nanoparticle-mediated drug delivery represents a promising frontier in overcoming the limitations of conventional medications. By utilizing a diverse array of materials and chemical strategies, drug delivery systems have been developed to enhance the therapeutic outcomes of various chemotherapeutic agents[213]. These systems achieve this by controlling the release rate of drugs, stabilizing them, and localizing their effects within the body. The rise of pharmaceutical nanotechnology has led to the development of nanoparticle-based drug delivery systems, including liposomes, polymeric nanoparticles, micelles, and dendrimers, which offer significant potential for improving human health[214].

The integration of nanomedicines with combination therapy offers even greater therapeutic potential by overcoming drug resistance and minimizing side effects[215]. Nanomedicines have been combined with conventional formulations to enhance therapeutic benefits, and novel nanomedicines for co- and dual-drug delivery have

been developed. Co-loading multiple therapeutic agents in a single nanocarrier can synchronize their pharmacokinetics and biodistribution, leading to synergistic anticancer effects[216]. Dual nanomedicines designed to target different cellular components or tumor microenvironment components can further improve therapeutic outcomes by reducing resistance and enhancing efficacy[217].

The present work focuses on the design, development, and evaluation of nanomedicine-based delivery of natural agents. Nanoparticles have been synthesized and characterized for their physicochemical properties. The efficacy of these nanoformulations has been evaluated in vitro using cancer cell lines, COLO320 DM-Human colorectal cell lines.

2.7.   RATIONALE OF THE STUDY

- ✓ Global cancer burden emphasizes the challenges in identifying effective therapeutic targets due to genetic variability across cancer types.
- ✓ The high incidence of chemotherapy-related toxicities, systemic side effects, and the development of chemoresistant cancer cells, highlights the urgent need for more effective and targeted, less harmful therapeutic options.
- ✓ The use of Natural Compounds are good alternatives due to their low toxicity, sustainability, potential anticancer properties and multi-targeting.
- ✓ Nanoparticle-mediated drug delivery systems (DDSs) can enhance the bioavailability of natural compounds, provide controlled and sustained drug release, and ensure targeted delivery to tumor sites, thereby maximizing therapeutic efficacy while minimizing systemic toxicity.

2.8. AIM AND OBJECTIVES

2.8.1. AIM

To conduct a computational analysis for identifying therapeutic targets, mitigate chemotherapeutic drug side effects using natural compounds, and synthesize nanoparticles for effective drug loading, with comprehensive response studies on toxicity and delivery efficiency.

2.8.2. OBJECTIVES

1. Screening of natural compounds for the anticancer properties and Computational analysis of therapeutic targets
2. Mitigation of side effects of chemotherapeutic drugs using Natural compounds
3. Synthesis and characterization of nanoparticles for drug loading, Response study for drug toxicity and drug delivery.

CHAPTER:III

Objective 1

> *Screening of natural compounds for the anticancer properties and Computational analysis of therapeutic targets*

CHAPTER III: OBJECTIVE 1

3.1. Rationale of the study

Colorectal cancer remains one of the leading causes of cancer-related mortality globally, despite the use of surgery, radiation, chemotherapy, targeted therapy, and other forms of treatments [218]. Nowadays, the objective has been to treat cancer as effectively as possible while reducing adverse effects. Irinotecan and 5-FU-based chemotherapy have been the conventional first-line treatment for mCRC, which was introduced some decades ago. Chemotherapeutic drugs can be harmful to normal cells because they attach to receptors that are not intended for them, which can cause unexpected side effects[137, 219]. As a result, the chemotherapeutic agent's selectivity for cancer cells compared to normal host cells has significant effects on the success rate of chemotherapy. Using the IntSide database (https://intside.irbbarcelona.org), a side effect analysis of FDA-approved chemotherapy drugs for colorectal cancer has been carried out. The most often prescribed medication for colorectal cancer has been included along with any adverse effects. The results showed that each treatment had unique side effects.

5-fluorouracil (5-FU): Depending on the dosage and individual variables, 5-fluorouracil (5-FU) frequently causes nausea and vomiting. When used with leucovorin, it can cause diarrhea, increased oral mucositis, and gastrointestinal tract ulcers. Even though severe myelosuppression is uncommon with typical dosages, it is nevertheless a major risk associated with chemotherapy[220, 221].

Irinotecan: Irinotecan induces two types of diarrhea: late-onset diarrhea brought on by oxidative stress-induced mucosal damage and early-onset diarrhea associated with cholinergic activity[222, 223].

Capecitabine (Xeloda): Known side effects of capecitabine include coronary vasospasm, cardiomyopathy, and other major artery damage. The most common

gastrointestinal hazard is diarrhea, and hand-foot syndrome may require dose withdrawal or reduction[224, 225].

Oxaliplatin: Adverse actions of oxaliplatin primarily include the gastrointestinal tract, peripheral nerves, and hematological system. It is mildly myelotoxic, causes peripheral neuropathy, and provokes nausea, vomiting, and diarrhea[226, 227].

Regorafenib: the most frequent adverse events are fatigue, hand-foot-skin responses, hoarseness, weight loss, nausea or vertigo, and hypertension. There are also more occurrences of weight loss and nausea or vertigo, but fewer of the other side effects[228, 229].

Trifluridine/tipiracil: the associated side effects include fatigue, nausea or vertigo, anemia, diarrhea, vomiting, leukopenia, neutropenia, weight loss or anorexia, and stomach discomfort. There were more cases of anemia and fatigue, but fewer reports of other adverse effects. The frequency of weight loss and anorexia was in line with previously published research[230, 231].

For example, cisplatin, oxaliplatin, and 5-fluorouracil (5-FU) are cytotoxic chemotherapy drugs that are frequently used in conjunction with irinotecan[232]. Furthermore, irinotecan-containing chemotherapy regimens are frequently combined with molecularly targeted medications such as aflibercept beta, bevacizumab, cetuximab, panitumumab, and ramucirumab. The combined effects of these molecularly targeted medications and chemotherapeutic medicines on cholinergic syndrome produced by irinotecan are still unknown, though. There is currently no comprehensive list of risks associated with irinotecan-related cholinergic syndrome[233, 234]. However, diarrhea, nausea, vomiting, hypotension (low blood pressure), hypersalivation (excessive saliva production), bradycardia (slow heart rate), abdominal cramps, acute diaphoresis (excessive sweating), and other symptoms often occur following irinotecan treatment. These symptoms are collectively referred to as cholinergic syndrome [235, 236].

To address this problem, we must first understand the gene expression levels in healthy versus non-healthy colorectal cancer samples and analyze the differences in their

expression patterns. Additionally, it is crucial to identify genes associated with irinotecan therapy by comparing the gene expression profiles of irinotecan-treated colorectal cancer samples with those that have not received the treatment.

According to recent studies, bioactive compounds produced from plants can increase therapeutic efficacy at lower doses, which lowers toxicity. Moreover, these substances have the ability to re-sensitize chemoresistant cells via a variety of molecular pathways, indicating a promising direction for cancer research. The potential of these substances to improve the effects of traditional chemotherapy medications on CRC has been thoroughly investigated. These include curcumin (diferuloylmethane), resveratrol (3,4',5-trihydroxystilbene), and (-)-Epigallocatechin gallate (EGCG). Blocking and reversing acquired drug resistance mechanisms is a specialty of these natural substances. Curcumin, resveratrol, and EGCG have been shown to be effective in re-sensitizing chemoresistant cells.

3.2. Methodology and materials required
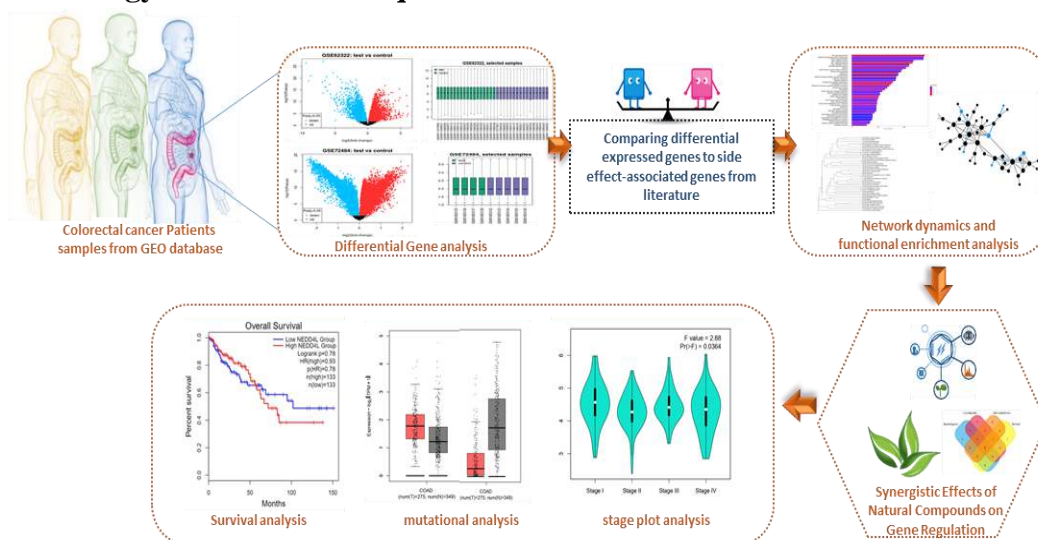
Figure 3. 1 Overview of Chapter Two methodology.

3.2.1. Data retrieval:

The datasets used in the study were obtained from the NCBI-GEO Database to analyse the differentially expressed genes in colorectal cancer versus normal samples. The GEO database contains a vast collection of valuable genomic studies, providing

processed and standardized information through various techniques. Two datasets were selected based on suitable numbers of samples and matching queries:

GSE62322: This dataset contains 114 samples, including 36 samples from normal women's colon samples 40 samples from primary colorectal cancer patients, and 38 samples from patients in which cancer metastasis to the liver (liver metastasis CRC samples).

GSE72484: The dataset comprises a total of 41 samples, including 9 from individuals with untreated CRC and 16 from those who received irinotecan treatment for CRC. This dataset is being examined to gain insights into alterations in gene expression resulting from irinotecan treatment and how these changes are linked to various side effects.

3.2.2. Differential gene expression analysis

To identify and analyze differentially expressed genes (DEGs) between colorectal cancer and control samples, we utilized the GEO2R tool available at http://www.ncbi.nlm.nih.gov/geo/geo2r/. This online tool makes it easier to compare microarray data and offers a list of genes with differential expression. We utilized the corrected and adjusted p-value (adj.P) to address the issue of false positive findings in our data analysis. The default option in GEO2R, the Benjamini and Hochberg false discovery rate approach, was used to produce the adj.P values, thus controlling for potential false positives. A lower adj.P value corresponds to a reduced false positive rate. Log FC values were employed to measure variations in gene expression, where positive values signified an increase in expression, and negative values indicated a decrease compared to the control group. Moreover, we considered a decrease in sample size during our analysis, categorizing genes with Log FC < 0 as down-regulated and those with Log FC > 0 as up-regulated.

The GSE62322 dataset was normalized before being put through a differential gene expression analysis with an adjusted (adj.) P-value 0.05 significant level, logFC values of 1 for upregulated genes, and -1 for downregulated genes. Similar to this, GEO2R was used to analyze the GSE72484 dataset, with a cut-off of adj. P-value 0.05, logFC value >0 for upregulated genes, and logFC value 0 for downregulated genes.

To identify shared differentially expressed genes, we compared the upregulated and downregulated genes in tumor samples with those in post-drug treatment CRC samples using Microsoft Excel. The DEG lists from datasets GSE62322 and GSE72484 were analyzed through conditional formatting, specifically, the "highlight cells rule" function, to identify and highlight duplicate values, thereby revealing the common set of differential genes.

3.2.3. Gene comparison with side-effects associated with genes

A comprehensive analysis was conducted on the gene dataset provided by the National Center for Biotechnology Information (NCBI) to identify genes associated with various side effects of FDA-approved drugs. Relevant genes related to side effects in the dataset were found upon close review, for comparison with the upregulated and downregulated genes previously collected from the two different datasets. The comparison study was thus carried out by manually cross-referencing the collected genes from the NCBI GENE dataset with a group of often-found differential genes so as to get a better understanding of specific genes associated with chemotherapeutic side effects. Use of Excel was made for this analysis. The goal of this strategy was to find any shared genes between the common differential genes and the side effect-associated genes.

3.2.4. Gene enrichment analysis

Using the ShinyGO 0.77 database, functional and route enrichment analysis was conducted. ShinyGO 0.77 offers thorough functional annotation tools to help in better understanding of biological roles of genes. It provides KEGG (Kyoto Encyclopedia of Genes and Genomes) pathway analysis and Gene Ontology (GO) analysis. To find enriched functional categories among the DEGs, GO enrichment analysis was carried out using the ShinyGO 0.77 database. The three primary components of the GO are molecular function, which refers to gene product activities at the molecular level, cellular component, which refers to gene product positions within cellular structures, and biological process, which refers to larger biological programs carried out by several molecular activities. P 0.05 was used as the significance threshold. These

include KEGG pathway diagrams that highlight your genes, hierarchical clustering trees and networks that summarize overlapping terms and pathways, protein-protein interaction networks, and plots illustrating gene characteristics.

3.2.5. Protein-protein interaction

The STRING database was used to assess functional protein interaction networks, specifically protein-protein interactions (PPIs). To analyze the PPI network, molecular complex detection was performed, focusing on modules that exhibited significant differences in gene expression ($|Log FC| > 2$ and $P < 0.05$). The PPI interactions were visualized using Cytoscape, a powerful software platform.

3.2.6. Exploring Natural Compounds with Extensive Gene Impact

This study mainly aimed at identifying the natural compounds that induced common DEGs and probably modulated various biological pathways and activities. The present study was conducted based on the GEO dataset GSE85871, which includes gene expression information for 102 different natural compounds. Each compound was assayed in two experiments, the results of which were compared with a blank group consisting only of DMSO. GEO2R, a program for comparing gene expression profiles, was used in the investigation to find DEGs for each natural compound in comparison to the control group (https://www.ncbi.nlm.nih.gov/geo/geo2r/). By contrasting the expression profiles of all substances in Microsoft Excel, common upregulated and downregulated genes were found. These naturally occurring compounds were screened for their potential to modulate these commonly expressed DEGs. The ranking of the compounds inducing the most significant changes in genes relative to standard DEGs was emphasized. First, the compound controlling the most substantial number of genes was selected. Then, subsequent compounds were picked for the capacity to change the expression of the most significant number of genes that hadn't been affected by the initial batch of compounds.

3.2.7. Analyzing the combination of natural compounds

After selecting the combination of natural compounds, the researchers mapped the genes overlapped by these compounds in a Venn diagram. After finding the shared genes, we submitted them for enrichment analysis through the ShinyGO tool for biological pathways and processes affected by the combination of compounds. We have conducted literature research to understand better the biological meaning of the chosen cocktail of natural compounds, covering all available information from PubMed, Google Scholar, SCOPUS, and other scientific databases. Such a literature review should have suggested which compounds regulate biological processes and pathways and thus completed the entire interpretation of the experimental results.

3.2.8. Natural Compound-Regulated Gene Survival and Mutation Analysis

The mutational frequencies within the identified candidate genes were thoroughly investigated using TCGA data accessed through the Gepia tool. Concurrently, survival analysis was performed to assess the impact of alterations in these genes on overall survival in colorectal cancer patients. Utilizing the TCGA dataset, the Kaplan-Meier estimator was employed for visualization, with statistical significance determined using the Logrank test P-value. Survival analyses, leveraging gene expression status, were conducted utilizing GEPIA2, with specific parameters set: Group Cutoff at Median and Cutoff-High and Cutoff-Low percentages, both at 50%. Additionally, survival maps were generated with a significance level set at 0.05 to represent the findings visually.

3.2.9. In silico and ADME and drug-likeness prediction

We utilized the SwissADME web tool for in silico ADME screening and drug-likeness evaluation of four natural compound that regulate the eight genes in combination. This platform, developed by the Swiss Institute of Bioinformatics, provided insights into four natural compounds targeting eight specific genes. Simple physicochemical properties such as molecular weight, refractivity, atom counts, and polar surface area were computed using PubChem. Drug-likeness was assessed against Lipinski, Ghose, Veber, Egan, and Muegge rules, with Abbot Bioavailability scores predicting oral

bioavailability. Lipophilicity and solubility were evaluated through Swiss ADME database.

3.3.Results

3.3.1. Analysis of Differential Gene Expression

Differential gene expression analysis was performed on the GSE62322 and GSE72484 datasets. In GSE62322, 953 genes were found to be upregulated in colorectal tumor samples compared to their respective normal samples, while 941 genes were downregulated. In the dataset GSE72484, a total of 528 genes exhibited upregulation in drug-treated samples from colorectal cancer (CRC) compared to non-treated samples(Fig.3.2). Additionally, 786 genes demonstrated downregulation in the same comparison. This analysis focused on identifying meaningful differences in gene expression and generating volcano plots for both datasets. In the plots, blue dots represent genes that do not exhibit significant differences between colorectal cancer patients and healthy individuals, indicated by $P \geq 0.05$ or $|\text{Log FC}| < 2$. Red dots, on the other hand, represent genes with significant differences ($P < 0.05$ and $|\text{Log FC}| > 2$). The genes represented by the red dots are considered candidate genes for further analysis, as they may have clinical significance. The results of this analysis are presented in Figure 3.3, showcasing the genes of interest and their differential expression patterns.

GENE EXPRESSION DATA

GEO Database

GSE62322 and GSE72484

Colorectal Tissue Sample Data
GSE62322

Drug treated Sample Data
GSE72484

- Primary Tumor samples: 40
  - Liver metastasis CRC Sample:38
    - Normal sample: 36

- CRC patients who underwent irinotecan treatment: 16
- Untreated CRC patients: 09

Differential Gene Expression
GEO2R
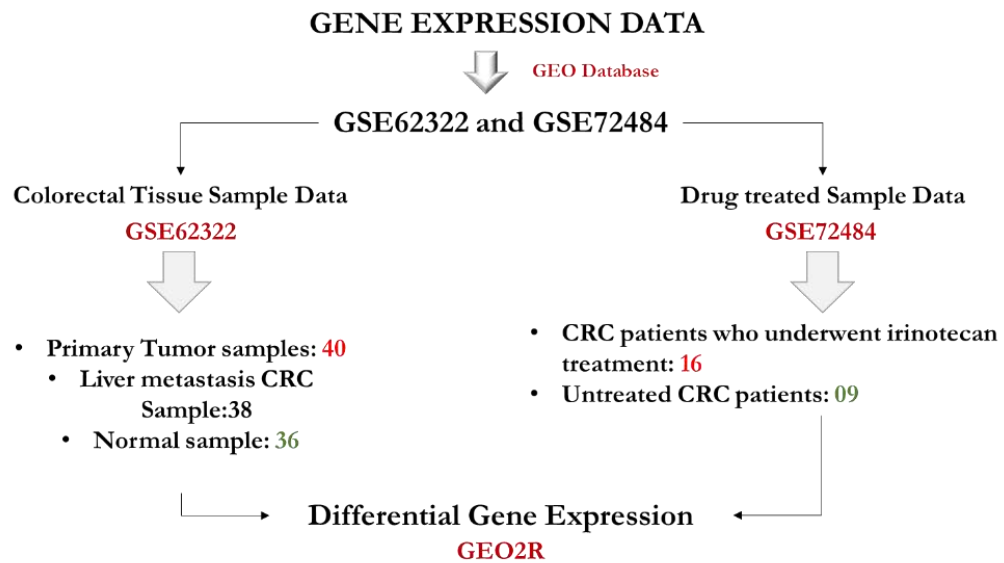
Figure 3. 2 figure illustrates the overall methodology used to analyze the gene expression data of colorectal cancer patient data and irinotecan-treated data.
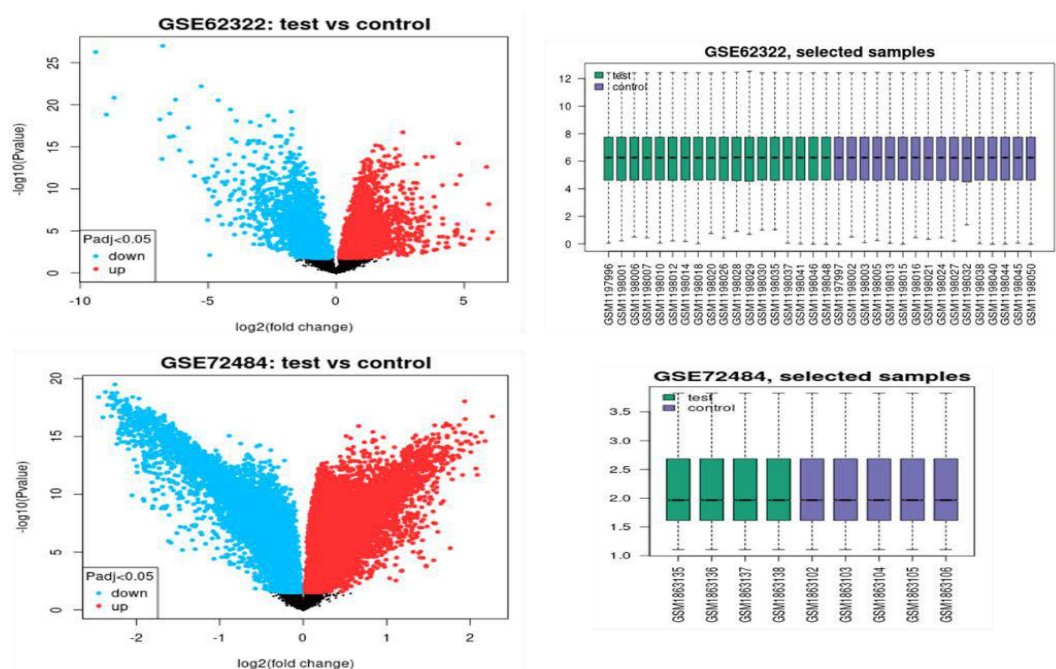
Figure 3. 3 Volcano Plots Depicting Differential Gene Expression. The plots show the results of gene expression analysis in colorectal tumor samples (GSE62322) and drug-treated colorectal cancer samples (GSE72484) compared to respective controls. Red dots represent genes with significant differences (P < 0.05, |Log FC| > 2), indicating potential clinical significance. Blue dots represent non-differentially expressed genes (P ≥ 0.05, |Log FC| < 2). Upregulated and downregulated gene counts are provided for each dataset, highlighting the molecular differences in colorectal cancer.

3.3.2. Common gene screening

By comparing the differentially expressed genes in CRC tumors and drug-treated samples, common DEGs were screened. Among the 953 upregulated DEGs in CRC tumors, 132 genes were found to be common with the 786 downregulated DEGs in drug-treated samples. These genes, upregulated in CRC tumor samples and downregulated in drug-treated samples, may be involved in the side effects of FDA-approved drugs. Similarly, out of the 941 downregulated DEGs in CRC tumors, 280 genes were common with the 528 upregulated DEGs in the drug-treated sample.

3.3.3. Identifying Genetic Culprits Behind CRC Therapy Side Effects

A comparison between multiple gene groups was done to find potential genetic influences connected to different side effects. These gene sets included 34 genes linked to abdominal pain, 117 genes linked to diarrhea, 26 genes linked to vomiting, 104 genes linked to fatigue, 60 genes linked to anemia, 55 genes linked to thrombocytopenia, nine genes linked to decreased appetite, 200 genes linked to neutropenia, 1252 genes linked to bone marrow depression, and 200 genes linked to neutropenia. This analysis aimed to find any genes that shared regulatory patterns with the groupings of upregulated and downregulated genes, as well as those linked to the aforementioned adverse effects. By looking at these overlapped genes, it was feasible to learn more about putative genetic pathways behind the incidence of these side effects. This thorough technique compared genes implicated in diverse side effects and looked for parallels to understand better the genetic mechanisms influencing side effects. By comparing gene expression data, we could pinpoint 46 common genes that were up and down-regulated(Table 3.1). Thirty four common genes among the elevated genes: THBS1, FGFR, WAS, B3GALT1, TRPM, KRT19, RAB27A, ABCB1, FAS, IL6R, ARRB1, PTGS1, NEDD4L, ROR1, SOCS2, DUSP1, DCN, TLR4, NR2F2, ADH1B, PDE4D, MYLK, SOCS3, PRKCB, GSN, CDKN2B, PTPN22, NT5E, SMAD1, KLF6, IGF1, AHNAK, GPR39, and MLXIP. Additionally, we found 12 common genes that were downregulated: ANGPT2, ETS2, PML, BRIP1, CD47, HMGB1, CYP3A5, HSPD1, PDPN, CDK1, GDF15, and FANCI(Table 3.1). The upregulated genes indicate increased activity and potential functional roles, while

the downregulated genes suggest decreased activity or regulation in the observed conditions.

3.3.4. Gene enrichment analysis

Functional enrichment analysis of DEGs revealed that the 46 discovered genes are implicated in critical functions across diverse biological processes, bringing novel insights into the molecular mechanisms underlying the side effects of FDA-approved medications. These include some key signaling channels among these activities, such as the P53 signal transduction system involved in controlling the cell cycle and preventing the development of tumors. It was further found that these DEGs affected the Fanconi anemia pathway, retinol metabolism, drug metabolism, and cytochrome P450 metabolism of xenobiotics(Fig. 3.4). They were also found to be associated with growth hormone synthesis, natural killer cell-mediated cytotoxicity, JAK-STAT, focal adhesion, and the mechanism for EGFR tyrosine kinase inhibitor resistance often developed by cancer cells. Other biological processes affected by these genes are the transport systems, protein metabolism, immunological response, and cell development and maintenance. Noticeably, these DEGs enriched the HIF-1, Rap1, and PI3K-Akt signaling pathways that play a central role in cell survival, proliferation, and angiogenesis(Fig.3.4) and (Fig.3.5). These results strongly suggest that these biological mechanisms and signal pathways are causally connected with the development of the aforementioned adverse effects and tumor progression (Fig.3.6).

Considering the implications of these findings, identifying drugs that can modulate the expression of these genes and restore their normal levels and function holds excellent potential for restoring normal biological processes. By targeting these genes, it may be possible to develop interventions to mitigate the aberrant activities associated with tumor progression.
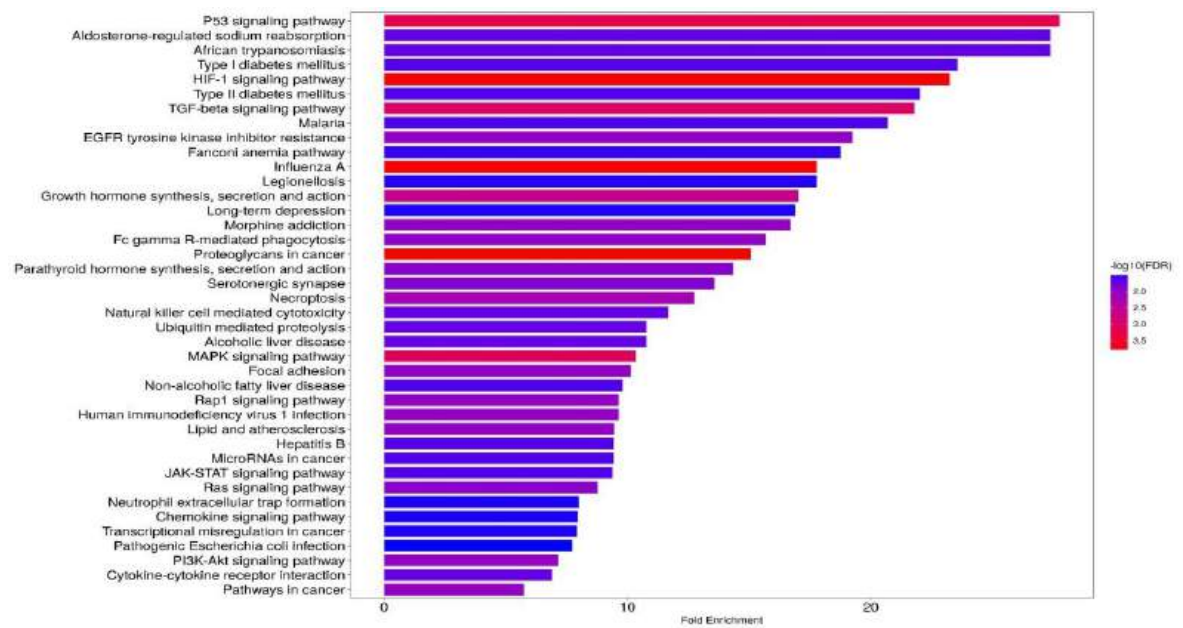
Figure 3. 4 Enrichment Analysis and hierarchical clustering trees of Differentially Expressed Genes (DEGs) in Colorectal Cancer. The figure shows the enriched biological processes and signaling pathways impacted by the 46 DEGs in drug-treated colorectal cancer samples (GSE72484). These genes are associated with key pathways, including P53 signaling, drug metabolism, EGFR tyrosine kinase inhibitor resistance, and cell survival pathways (HIF-1, Rap1, and PI3K-Akt). Targeting these DEGs may offer potential therapeutic strategies to counter tumor progression and improve treatment outcomes.
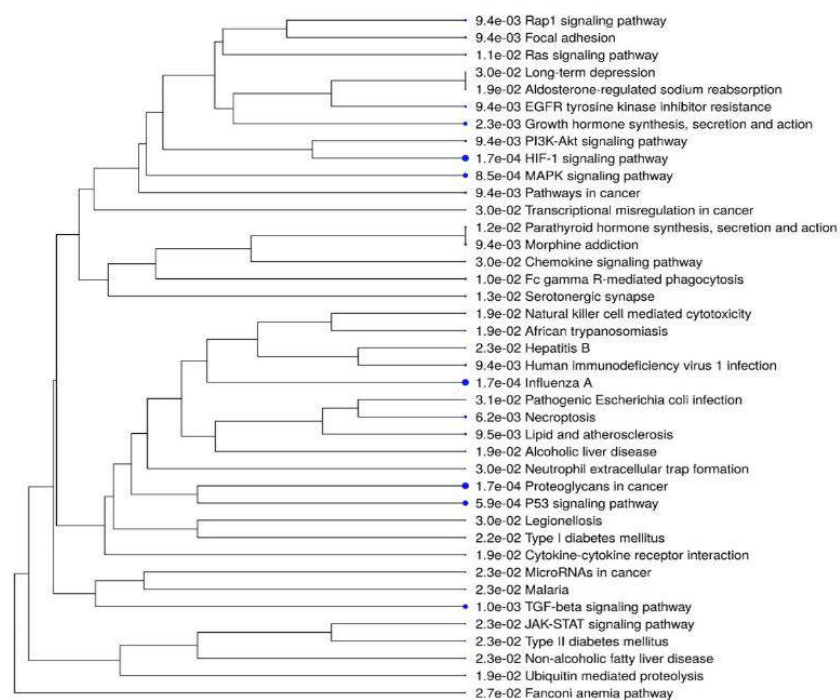
Figure 3. 5 Hierarchical diagram displaying gene interactions and links across multiple biological pathways. This picture illustrate a very entangled network of gene interactions, where nodes represent the single genes, while edges represent the interconnections between them. Nodes, colored and shaped differently, mark participation in different biological pathways. This image reflects how complicated the relationships and mechanisms of regulation between cellular processes are and how genes coordinate with and influence each other within the context of the larger environment of the biological systems.

The STRING database was used to analyze the PPI network, which revealed 46 Differentially Expressed Genes. These DEGs showed a close relationship within the network and were divided into three distinct groups using the Hidden Markov Model [237](Figure 3.7). Node degree analysis highlighted a strong association among BIRC5, MELK, CDC20, CCNA2, and EZH2, suggesting a clear positive correlation among these five gene clusters. Figure 3.7 displays the selected genes from these DEGs, emphasizing the major regulatory nodes. Furthermore, there was a significant association observed in other gene clusters such as ICAM1, IL6, CDH5, and PECAM1. Among these DEGs, EZH2 and IL6 were identified as intermediary hubs, playing important roles in the network.
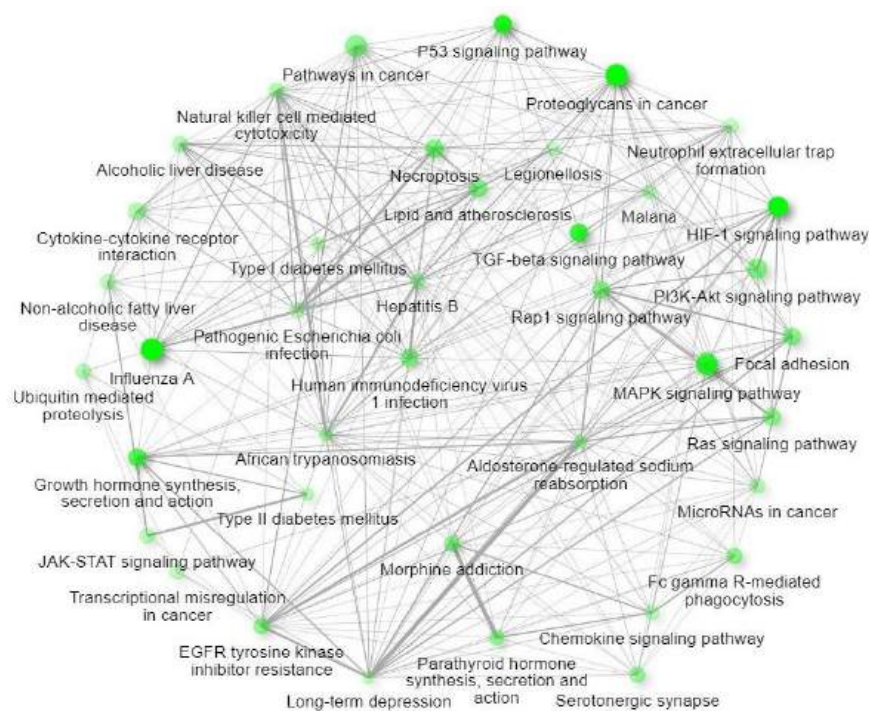
Figure 3. 6 Diagram of the interlinked biological pathways and related side effects implicated by FDA-approved drugs. Green dots represent common hubs linking differentially expressed genes that were identified in the study.
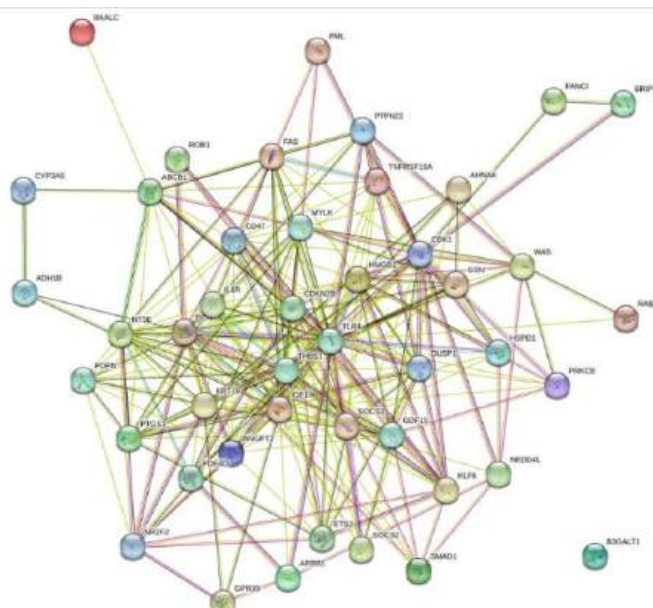
Figure 3. 7 Protein-Protein Interaction (PPI) Network of Differentially Expressed Genes (DEGs) in Drug-Treated Colorectal Cancer. The PPI network analysis using the STRING database identified 46 DEGs with close relationships.

3.3.5. Prioritizing Natural Compounds: Impact on Reversing DEG Expression

The GEO2R database was used to analyze detailed expression profiles for a sample containing 102 naturally occurring compounds with anticancer activity. These DEGs are those genes whose expression levels change upon exposure to each unique natural compound, as per a previously generated list of 46 common genes from two datasets in which 12 genes were downregulated, and 32 genes were upregulated. These lists were then compared with the DEGs from the 102 naturally occurring compounds. It was essential to find out which natural compounds had the most significant influence on reversing the expression of these widespread DEGs. Based on the findings, the natural substances were ranked according to how well they could reduce the expression of the most significant number of genes.

3.3.6. Synergistic Effects of Natural Compounds on Gene Regulation

The ability of a combination of natural substances to change the expression of a maximum number of genes among 46 frequent DEGs was carefully considered. Resibufogenin, the first compound tested, demonstrated modulation of 28 genes out of

the 46 DEGs. Other natural substances were examined for their ability to restore gene expression to address the remaining 18 genes. As a result, the genes curcullgoside, borneol, and β-ecdysterone, which regulated the remaining genes, were discovered. Out of the 46 prevalent DEGs, these four compounds were able to regulate 44 genes, effectively restoring gene expression to levels resembling those found in healthy matched tissues. Notably, the combination of natural compounds did not adequately activate two genes, FGFR and TRPM (Fig.3.8, 3.9).

Table 3.1. Common differentially expressed genes(46 in number) from two different datasets.

Upregulated genes	fc value	adjusted P value	Downregulated genes	fc value	adjusted P value
IL6R	-2.88041	1.65E-10	BRIP1	2.305483	4.08E-04
MLXIP	-1.117	0.00000788	GDF15	1.309853	2.81E-04
RAB27A	-1.0795	0.0000115	ANGPT2	2.407143	3.02E-04
SOCS3	-3.879	1.7570999	FANCI	2.135601	1.58E-05
WAS	-3.87944	1.0017901	HMGB1	0.67892	2.60E-04
TNFRSF10A	-3.91571	1.4540995	CYP3A5	0.938172	2.52E-04
MYLK	-3.92336	1.0737074	IGF1	1.099079	4.08E-04
PDE4D	-3.92742	1.0317549	PML	0.526942	2.60E-04
GPR39	-3.94142	1.0300514	CDK1	0.558689	2.59E-04
THBS1	-3.96528	1.0307419	HSPD1	0.70852	2.81E-04
KRT19	-3.98752	1.0206616	PDPN	0.673437	3.02E-04
PTGS1	-4.02027	1.0412291	CD47	0.611183	2.41E-04
ABCB1	-4.02674	1.0823671	ETS2	1.214165	2.25E-04
ADH1B	-4.05624	1.0677919			
BAALC	-4.0724	1.0320565			
IGF1	-4.14012	1.1995141			
B3GALT1	-4.16194	1.0087634			

TRPM	-4.1831	1.2646012			
KLF6	-4.18669	1.5390172			
TLR4	-4.22594	1.0825319			
FAS	-4.22904	1.0205674			
FGFR	-4.32038	1.0304485			
PTPN22	-4.38816	2.0021747			
DUSP1	-2.76418	0.0000137			
PRKCB	-1.46792	0.0000174			
CDKN2B	-1.52918	0.0000132			
GSN	-1.84632	0.0000156			
NT5E	-1.95191	0.0000167			
DCN	-1.57158	0.0000153			
ARRB1	-1.0622	0.0000172			
NEDD4L	-1.38851	0.0000178			
SMAD1	-2.27255	0.0000153			
ROR1	-1.06307	0.0000154			
NR2F2	-1.17045	0.0000199			
SOCS2	-1.77994	0.000016			
AHNAK	-1.15056	0.000016			

Table 3.2. Natural comounds and the number of genes regulated by them.

Natural Compound	Genes	Natural Compound	Genes	Natural Compound	Genes
Salidroside	**18**	**Phillyrin**	**19**	**Nitidine chloride**	**16**
Schisantherin A	**16**	**Resibufogenin**	**30**	**Bruceine**	**23**
Oxymatrine	**16**	**Alantolactone**	**14**	**Ginsenoside Rb3**	**23**
Silybin	**21**	**Ginkgolide B**	**14**	**Macrozamin**	**23**

Daidzin	22	Hyodeoxycholic acid	14	Tanshinone IIA	23
Scutellarein	23	Matrine	14	Bufalin	15
Gastrodin	19	Osthole	14	Cinnamic acid	15
Ginseooside Rd	24	stachydrine hydrochloride	14	Honokiol	15
Glycyrrhizic acid (2)	14	Ursodeoxycholic acid	14	Hyperoside	15
Schizandrin	16	ethyl caffeate	20	Puerarin	15
Astragaloside IV	21	Ferulic acid	20	Saikosaponin A	15
Benzoylaconitine	21	Isoalantolactone	20	Sanguinarine	15
Ginsenoside Rc	21	Tetrahydropalmatine	20	Sennoside A	15
Imperatorin	21	1bita-hydroxyalantolactone	22	Acteoside	17
L-scopolamine	21	Benzyl benzoate	22	Hesperidin	17
Saikosaponin D	21	Gallic acid	22	Hydroxysafflor yellow	17
Aconitin	18	Ginsenoside Rb1	22	Magnolol	17
Arenobufagin	18	Isoborneol	22	Resveratrol	17
Chlorogenic acid	18	Protocatechuic aldehyde	22	6-gingerol	24
Cinnamaldehyde	18	Salvianic acid A sodium	22	Andrographolide	24
Cinobufotain	18	Bacopaside l	23	Cholic acid	24
Deoxycholic acid	18	Benzoylhypaconitine	23	Ginsenoside Re	24
Gamabufatalin	18	bita-ecdysterone	25	Japonicone A	24
Uridonin	18	Chenodeoxycholic acid	23	Narciclasine	24
Anhydroicaritin	19	Ginsenoside Rb2	23	Notoginsenoside R1	24
Borneol	26	Muscone	23	Hypaconitine	12
Chelerythrine	19	Paeoniflorin	23	Liquiritin	12
Curcullgoside	26	Salvianolic acid B	23	Berberine hydrochloride	13

Dioscin	19	Telocinobufagin	23	Bufotaline	13
Emodin	19	Bilobalide	16	Ainsliadimer A	11
Gentiopicroside	19	Britanin	16	Geniposide	11
Ginsenoside Rg1	19	Cinobufogenin	16	Santonin	10
Lobetyolin	19	Ephedrine hydrochloride	16	Strychnine	10
Oleanic acid	19	Glycyrrhizic acid	16	Artemisinin	36
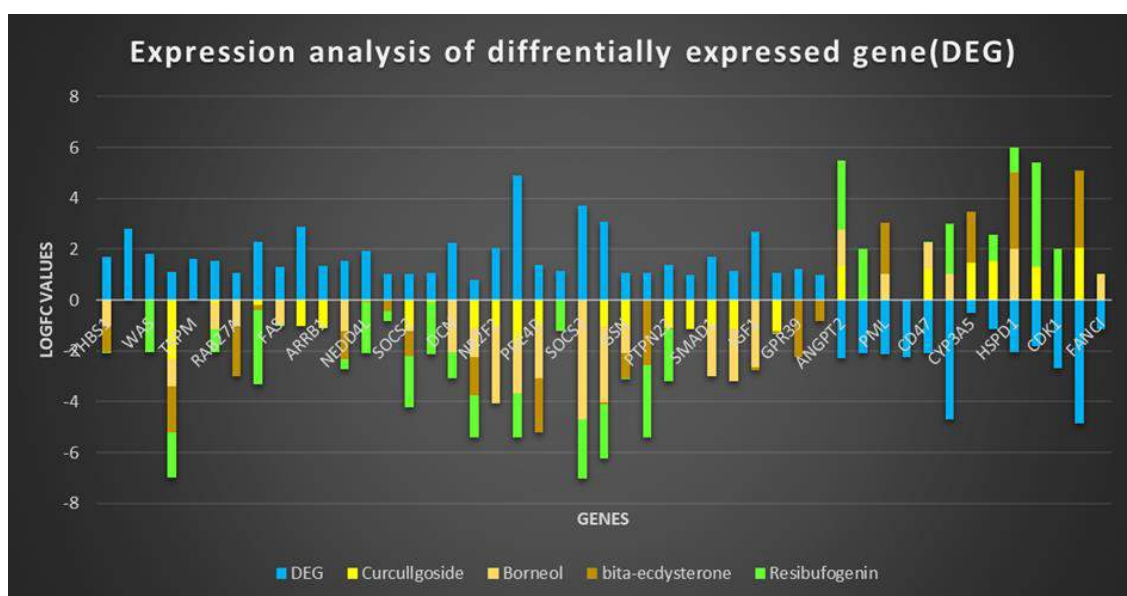
Figure 3. 8 Analysis of 34 Common Upregulated Genes and 12 Common Downregulated Genes in relation to the modulation/reversal of their expression by four natural compounds. (DEG - Differential gene expression)

Additional analysis compared the four natural compound individual impacts on the 46 DEGs. These 46 often targeted genes' involvement in crucial biological processes such as transport, immunological response, signal transduction, and nucleic acid metabolism control was revealed by enrichment analysis. These mechanisms significantly impact the immune system and the development of cancer. When these compounds were combined, it was found that numerous genes were more effectively regulated than when they were used separately(Table 3.2).. This implied the possibility

of synergistic effects, which could help minimize drug resistance and harmful side effects related to targeting single pathways.

On the other hand, different combinations of natural compounds targeted additional genes, with eight genes being regulated by all four compounds, ten genes by any three compounds, and 12 genes by any two compounds, according to the Venn diagram(Fig. 3.9). These additional genes included B3GALT1, NEDD4L, SOCS2, TLR4, PRKCB, GSN, ANGPT2 and CD47, which were controlled by all four compounds namely resibufogenin, curcullgoside, borneol, and β-ecdysterone. Only one of the four compounds impacted twenty-eight genes(Fig. 3.9 and Fig. 3.10). These genes also play a critical role in cancer progression and the manifestation of side effects from chemotherapy. As a result, the coordinated targeting of these genes offers hope for the successful treatment of colorectal cancer malignancies and decreases chemotherapy's side effects(Table 3.3).
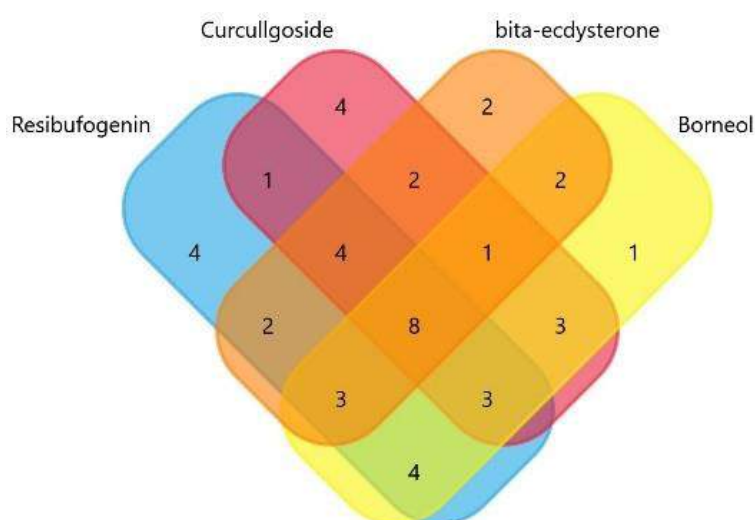
Figure 3. 9 Synergistic Modulation of Gene Expression in Colorectal Cancer by natural compounds. The Venn diagram shows the impact of combining natural substances on 46 Differentially Expressed Genes (DEGs) in drug-treated colorectal cancer. Resibufogenin modulated 28 genes, while curcullgoside, borneol, and β-ecdysterone regulated the remaining 18 genes. Together, these compounds restored gene expression in 44 DEGs, resembling healthy tissue levels. Combining the substances demonstrated synergistic effects, potentially minimizing side effects. Different combinations targeted additional genes, providing valuable insights for therapeutic strategies.
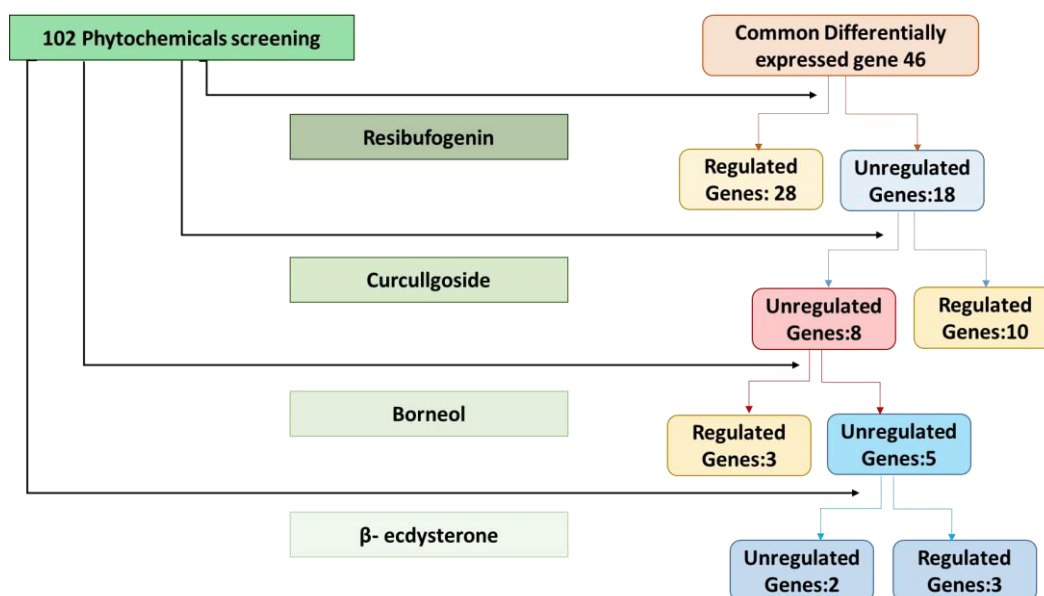
Figure 3. 10 The figure depicts the regulation of specific genes influenced by a subset of four natural compounds selected from a pool of 102 compounds.

3.3.7. Mutational and survival analysis of eight genes

The survival analyses on the TCGA-colorectal Adenocarcinoma (COAD) patient cohort were used to investigate the impact of B3GALT1, NEDD4L, SOCS2, TLR4, PRKCB, GSN, ANGPT2, and CD47 expression status on patient survival (Fig 3.11). Our findings revealed that in the COAD cohort, patients with high ANGPT2, PRKCB, NEDD4L, and CD47 expression experienced significantly worse disease-free survival (hazard ratio between 0.90 and 1.1). In contrast, high GSN and TLR4 expression showed no discernible effect on survival. Moreover, survival maps (Fig 3.12) uncovered cancer-type-specific effects of ANGPT2, PRKCB, NEDD4L, and CD47 expression levels on patient survival. These results indicate that in Colorectal cancer patients, reduced ANGPT2, PRKCB, GSN, TLR4, NEDD4L, and CD47 expression might lead to improved survival, potentially due to enhanced antigen presentation. However, it's important to note that these survival effects are not universally applicable across all cancer types. Given the considerable variability in immune infiltration, tumor mutational burden, and genomic profiles among different cancer types, it's expected that survival patterns will vary significantly based on cancer type.

Table 3.3. Commonly targeted genes and their roles in cancer progression as well as in the side effects

Gene	Role in Cancer Progression	Role in Chemotherapy Side Effects	References
B3GALT1	Implicated in tumor progression and metastasis	Potential influence on drug response or cellular mechanisms	[238]
NEDD4L	Regulates protein degradation; involved in cancer	May impact drug response or cellular pathways	[239, 240]
SOCS2	Negative regulation of cytokine signaling	Possible influence on treatment response or cellular processes	[241]
TLR4	Complex role in immune responses and cancer context	Variably affects immune responses and treatment outcomes	[242]
PRKCB	Role in cell proliferation, survival, and apoptosis	Potential impact on treatment response or cell processes	[243]
GSN	Impacts actin filament assembly; linked to cancers	Influence on cellular functions and possibly treatment	[244, 245]
CD47	Regulates cell death; implicated in immune evasion	Possible impact on immune response and treatment outcomes	[246, 247]
ANGPT2	Involved in angiogenesis; impacts tumor progression	Potential influence on vascularization and treatment effects	[248]
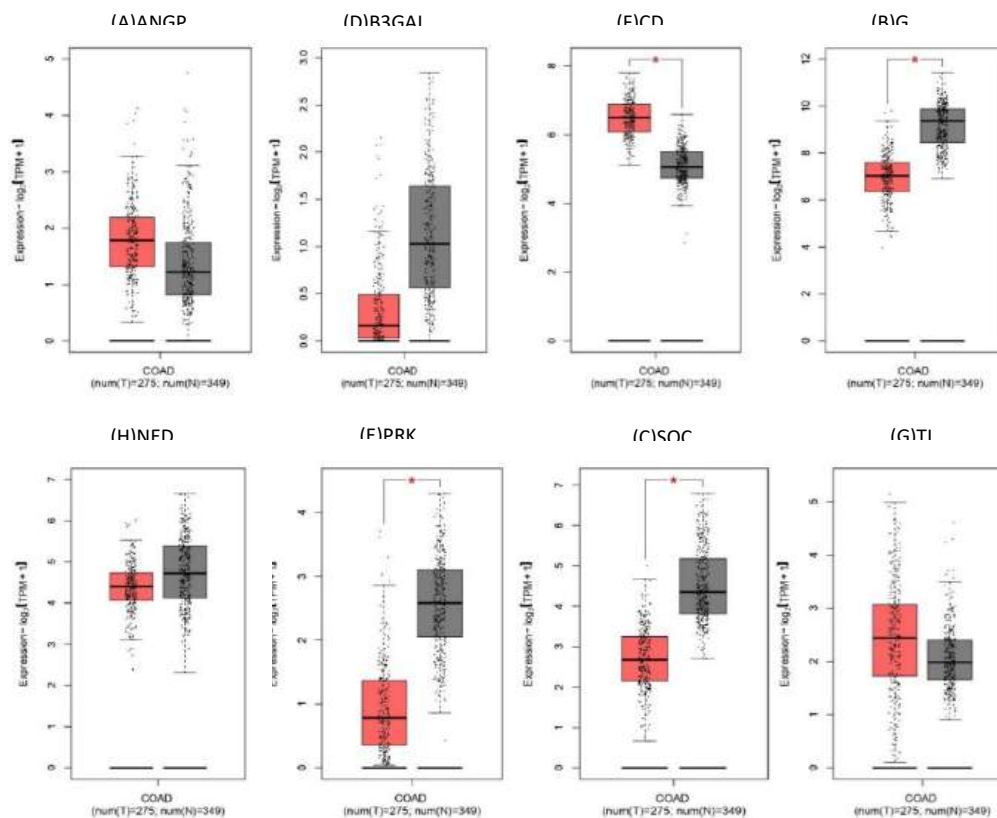
Figure 3. 11 Boxplots illustrating the expression profiles of B3GALT1, NEDD4L, SOCS2, TLR4, PRKCB, GSN, ANGPT2 and CD47 genes in Coloractal cancer, comparing tumor tissues (T, red box, n=275) to normal tissues (N, grey box, n=349) within the GEPIA database. Statistical significance (P<0.01) denoted by an asterisk (*) indicates differences in expression compared to normal tissues. (GEPIA stands for Gene Expression Profiling Interactive Analysis).
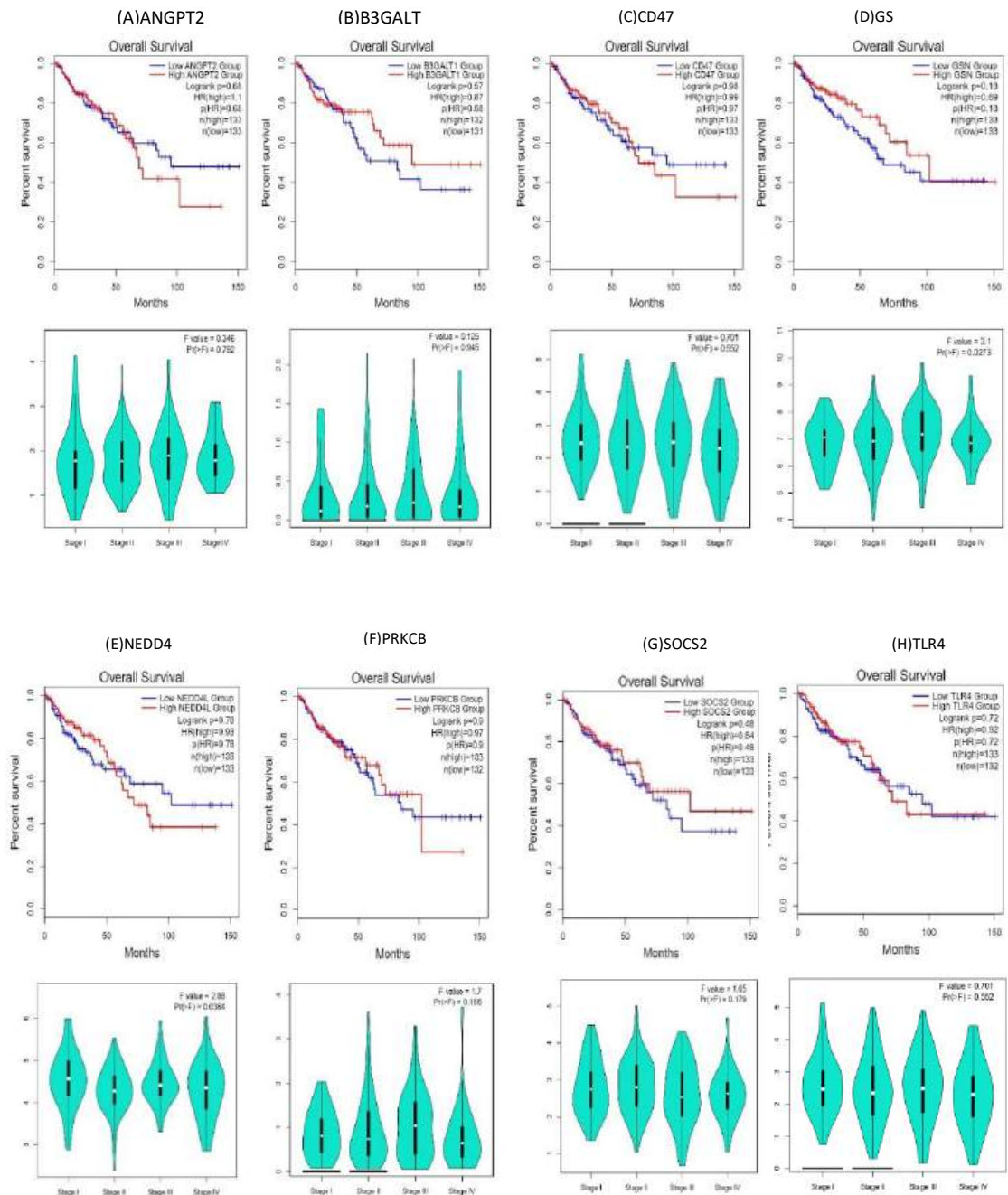
Figure 3. 12 Validation and survival analysis based on The Cancer Genome Atlas (TCGA) data conducted using the GEPIA platform (http://gepia.cancer-pku.cn/index.html), focusing on significant hub genes within the COAD cohort for overall survival analysis. Gene expression analysis of B3GALT1, NEDD4L, SOCS2, TLR4, PRKCB, GSN, ANGPT2 and CD47 across all stages (I–IV) of colorectal cancer (CRC). Conducting Kaplan-Meier overall survival analyses and predict stage plot on the top eight hub genes expressed in colorectal carcinoma patients using the GEPIA database.

ADME Analysis

All four designed compounds successfully cleared the drug-likeliness test, as demonstrated in Table 3.4. Additionally, they met the Lipinski rule of five criteria, a standard guideline in drug design. According to this rule, adherence to three out of the four criteria indicates compliance. Notably, all four developed compounds exhibited high gastrointestinal absorption rates. This breakthrough signifies significant progress in the quest for a cure for colorectal cancer(Fig 3.13).

(a)Resibufogenin   (b)Borneol   (c)Curcullgoside   (d)β-ecdysterone
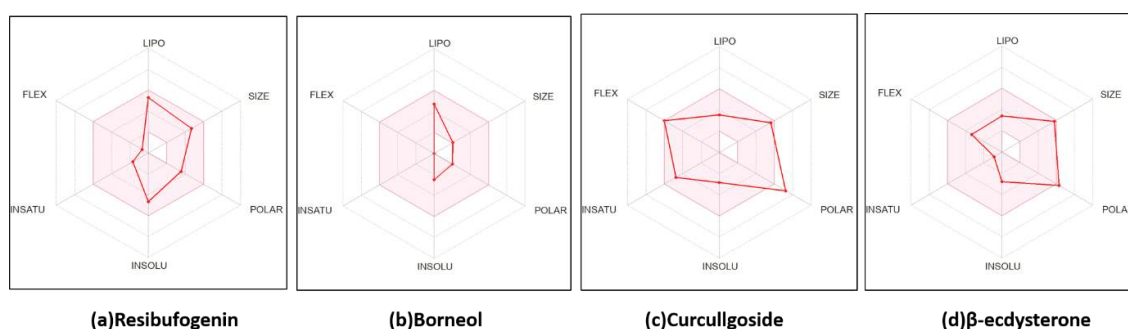
Figure 3. 13 The SwissADME bioavailability radar illustrates four bioactive drug-like molecules, where the pink segments highlight essential characteristics such as lipophilicity, molecular weight, solubility, and flexibility.

Table 3.4. Pharmacokinetic Assessments and Drug-likeness Calculations by SwissADME for Four Natural Compounds.

Parameters	Resibufogenin	Borneol	Curcullgoside	β-ecdysterone
BBB	Yes	Yes	No	No
Human intestinal absorption	High	High	Low	High
Log P	3.46	2.29	1.86	2.92
TPSA(Å)	62.97	20.23	164.37	138.45
Molecular weight(g/mol)	384.51	154.25	302.24	480.63
Class	Moderately Soluble	soluble	soluble	soluble
Log Kp(skin permeation)	-5.99 cm/s	-5.31	-8.65	-8.91
Lipinski	Yes	Yes	Yes	Yes
Ghose	Yes	No	Yes	No
Veber	Yes	Yes	No	No
PAINS	0 alert	0 alert	0 alert	0 alert
Bioavailability score	0.55	0.55	0.55	0.55

3.3.8. The Biological Network of Natural Compounds in CRC Regression

By locating their modes of action in the literature, the congruence analysis of the combination of chosen natural compounds was performed. This investigation sought to evaluate their ability to work in concert to target various pathways that interact to successfully promote tumor regression without producing unfavorable side effects.

i. ***Resibufogenin,*** a naturally occurring bufadienolide compound found in the skin and parotid venom glands of Bufo toads, has emerged as a potential candidate for cancer therapy due to its intriguing pharmacological properties[249]. Extensive research has explored its effects on various cancer types and their underlying molecular pathways. Resibufogenin has demonstrated its ability to inhibit cell proliferation by inducing cell cycle arrest, preventing rapid cancer cell growth and division[250–252]. One of the ingredients in the mixture, resibufogenin, stimulates autophagy by activating the PI3K/Akt/mTOR signaling pathway, which is a protein kinase B/mammalian target of rapamycin. Resibufogenin controls this mechanism, which results in caspase-dependent and mitochondria-mediated apoptotic cell death by reducing anti-apoptotic proteins and

increasing pro-apoptotic factors[253]. Resibufogenin reduces reactive oxygen species (ROS) by activating the Akt/ERK signaling pathway, which prevents tumor cell proliferation, migration, and invasion[254]. It also activates the IkB/NF-B pathway, which reduces the release of pro-inflammatory cytokines while increasing apoptosis via p53 and caspase signaling. Additionally, it has pro-apoptotic properties that cause cancer cells to undergo programmed cell death[255]. Resibufogenin prevents the creation of new blood vessels required for tumor growth and metastasis, another crucial anticancer strategy. It alters vital signaling pathways including PI3K/AKT and MAPK, which are frequently dysregulated in cancer, and it prevents cancer cell invasion and migration, hence reducing the likelihood of metastatic spread. By regulating apoptosis-related proteins, such as Bcl-2, Bax, and caspases, resibufogenin orchestrates the apoptotic process in cancer cells (Fig.3.14)[254]. Despite these encouraging results, additional preclinical and clinical research is necessary to determine the drug's safety and effectiveness in cancer treatment. Resibufogenin might aid in defending healthy tissues from harm brought on by chemotherapy drugs by lowering inflammation. According to some research, Resibufogenin may also preserve bone marrow, which is particularly vulnerable to damage from several chemotherapy treatments. It may lessen the severity and length of chemotherapy-induced myelosuppression, which results in low blood cell counts, by promoting bone marrow activity.

ii.   ***Borneol,*** a bicyclic organic compound commonly found in aromatic herbs like Blumea balsamifera and Dryobalanops aromatica, has been investigated for its potential anticancer properties through involvement in various cancer-related pathways[256]. The compound has shown chemopreventive attributes, likely stemming from its antioxidative capacity, which could modulate the Nrf2-ARE pathway and counteract harmful free radicals, thus mitigating DNA damage implicated in cancer initiation. Additionally, borneol exhibits antiproliferative capabilities by potentially downregulating the PI3K/AKT and MAPK pathways, hindering

cancer cell growth and division[257]. Moreover, in vitro investigations have revealed its ability to induce apoptosis in cancer cells by activating caspase cascades, which may involve the p53 pathway. This, in turn, promotes programmed cell death and diminishes tumor size[258]. [258]. Borneol also enhances drug delivery mechanisms could involve the modulation of ABC transporters, thereby increasing the intracellular accumulation of chemotherapeutic agents [259]. Additionally, its anti-inflammatory properties, likely linked to the inhibition of NF-κB signaling, might contribute to cancer prevention and treatment, given the association between chronic inflammation and cancer development(Fig.3.14) [260]. Despite these promising findings, most studies have been confined to cellular or animal models, with limited clinical trials in humans. Thus, the efficacy of borneol in cancer treatment necessitates further exploration, and any potential applications should be approached with caution, guided by evidence-based medical practices and under the supervision of qualified healthcare professionals.

In drug metabolism, borneol interacts with key Cytochrome P450 enzymes (CYP3A4, CYP2D6, and CYP1A2)[261]. Its role in neuroprotection is linked to BDNF, promoting neuronal survival and growth. In pain modulation, borneol interacts with OPRM1 (mu-opioid receptor) and TRPV1 (transient receptor potential vanilloid type 1 ion channel) genes, affecting pain perception[262, 263]. Borneol's cardiovascular effects, characterized by vasodilation and vascular function, are influenced by the NOS3 gene[264]. Borneol's impact on gastrointestinal integrity is associated with COX-1 and COX-2 genes, involved in prostaglandin production[265].

iii. *Curcullgoside* is a metabolite of Curcumin, a bioactive compound derived from turmeric, exerts its anticancer effects through modulation of several critical signaling pathways. By interfering with the nuclear factor-kappa B (NF-B) pathway, it reduces inflammatory reactions and impairs the growth and survival of cancer cells[266]. Curcumin hinders the growth of cancer cells by blocking the phosphatidylinositol 3-kinase (PI3K)/protein kinase

B (AKT) pathway. This increases apoptosis. Curcumin also affects the Mitogen-Activated Protein Kinase (MAPK) pathway, altering cell cycle progression and death[267]. Its downregulation of Cyclooxygenase-2 (COX-2) expression contributes to its anti-inflammatory and anticancer properties. Moreover, curcumin inhibits angiogenesis by targeting vascular endothelial growth factor (VEGF) expression and impairs new blood vessel formation crucial for tumor growth. Lastly, curcumin induces apoptosis through the modulation of Bcl-2 family proteins and caspases, providing an additional mechanism to combat cancer cells[268].

Additionally, it reduced the levels of a number of pro-inflammatory cytokines in the serum, including TNF-, IL-1, IL-6, IL-10, IL-12, and IL-17A[269]. Curculigoside dramatically reduced cell proliferation in a concentration- and time-dependent manner in in vitro experiments employing fibroblast-like synoviocytes (MH7A cells) obtained from patients with rheumatoid arthritis. In terms of mechanism, curculigoside increased cytosolic NF-κB p65 and IB while downregulating the levels of JAK1, JAK3, and STAT3(Fig.3.14). These results imply that the regulation of the JAK/STAT/NF-κB signaling pathway by curculigoside may be the cause of the compound's anti-arthritic actions[270, 271].

iv. ***β-ecdysterone***, a plant sterol similar to estrogen, shows promising potential as a bone regeneration regulator. It also enhanced alkaline phosphatase activity and calcium nodule formation, indicating improved bone regeneration capacity[272]. Mechanistically, β-ecdysterone activated the BMP-2/Smad/Runx2/Osterix signaling pathway, as confirmed by DNA sequencing. By suppressing VEGF-induced regulation of the Akt/mTOR signaling pathways, β-ecdysterone prevents VEGF-induced migration, tube formation, and proliferation as well as cell proliferation[272, 273]. Through the inhibition of IKK1/IKK2, which regulates tumor cell proliferation and angiogenesis, β-ecdysterone suppresses NF-kB. Through the downregulation of cMyc and HIF1 through upstream effectors like mTOR, it demonstrates an anti-inflammatory response that prevents angiogenesis and cell proliferation(Fig.3.14)[274].

By targeting multiple pathways and processes, the combination of these natural compounds demonstrates a highly potent multifaceted antitumor and immunomodulatory role, contributing to the regression of colorectal cancer. The biological network formed by these compounds offers a promising approach for combating CRC tumors effectively(Fig.3.14).
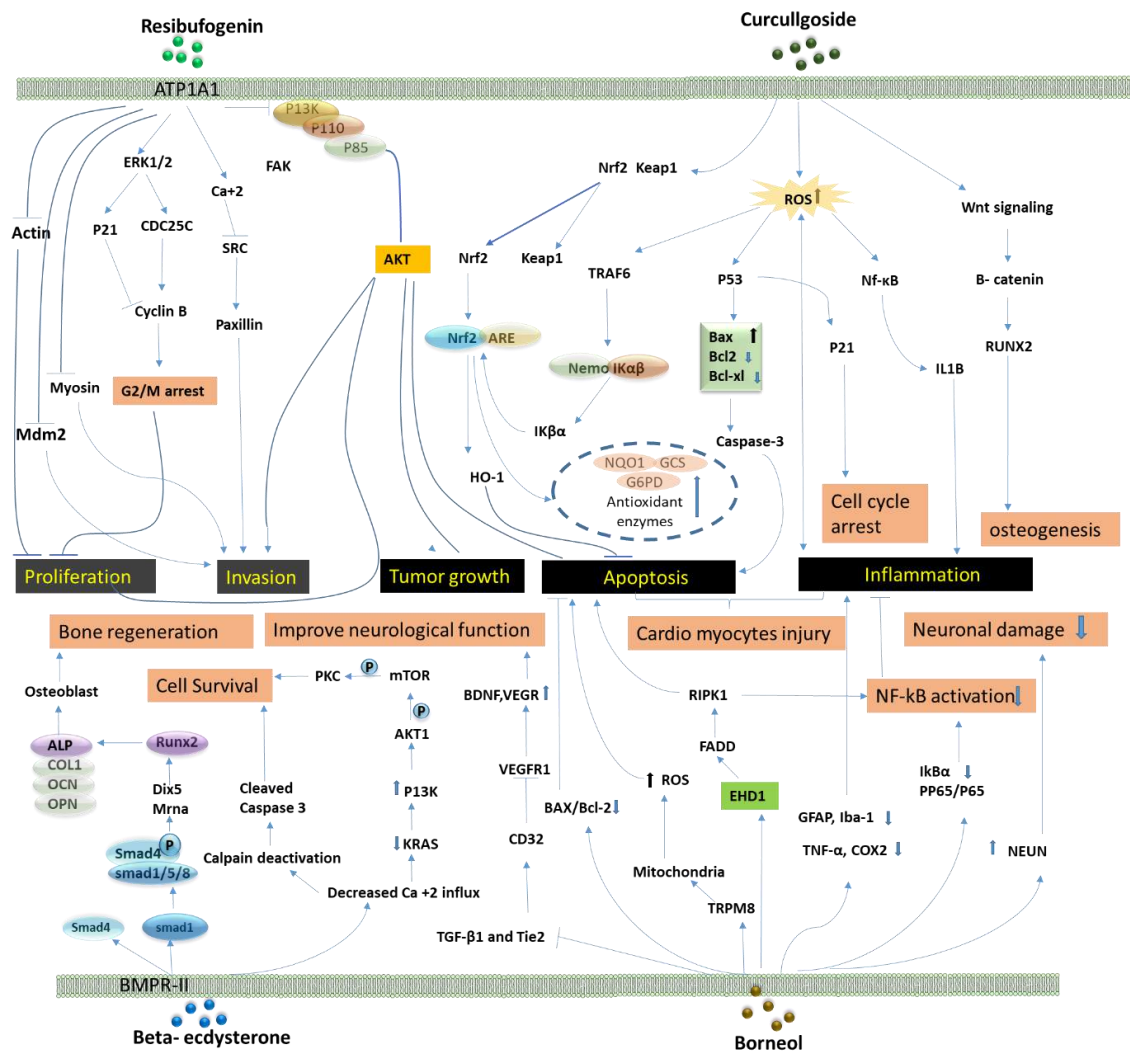
Figure 3. 14 the figure illustrates the proposed mechanisms of action of a combination of selected natural compounds in colorectal cancer regression. The compounds—Resibufogenin, Borneol, Curcullgoside, and β-ecdysterone—work synergistically to target various pathways involved in colorectal cancer progression. The combination of these compounds offers a multifaceted approach to induce tumor regression in colorectal cancer therapy while minimizing side effects.

Table 3.5 Irinotecan-Mediated Side Effects and Associated Genes.

Side effects	Gene involved in side-effects	Common genes after drug treatment
Anemia	GATA1,AGT,BRIP1, LPIN2, MAOB, REN, SOD2, RPS7, EGFR, ABCC2, TNFSF10, PARP1, FANCI, RPL35A, CASP9, RPS14, EPB41, PARP1, BRCA1, SOD2, BRIP1, RPS7, CYP3A4, RPS14, FANCI, PARP1, MAOB, LPIN2, EPB41, NFKBIA, ABCB1, AGT, RPL35A, GATA1, PARP1,CASP8, CYP3A7	**ABCB1, BRIP1, FANCI,**
Thrombocytopenia	TNFRSF10A, VERFA ,WAS, GATA1, CYCS, ETV6, TNFSF10, ABCC2, THBS1, CYP3A4, MGMT, CYP2B6, GASP3, CYP3A5, CASP9, ABCG2, CASP8, ABCB1, CYP2B6, SUMO1, CDC42	**TNFRSF10A,WAS, THBS1, CYP3A5, ABCB1**
Decrease apetite	CASP8, CASP3, CYP3A7, ABCC2, CYP3A4, POLE2, ABCB1, CYP3A5ABCG2	**ABCB1, CYP3A5**
Neutropenia	CYP3A5, TNFRSF10A, CYP3A7, UGT1A6, VPS45, CASP8, ABCB1, ABCG2, CASP3, WAS, TP53, UGT1A1, RELA, CASP9, CDC42, GATA1, PDE4D, AGR2, VPS45, SCARA5, PTPN5, ADAMTS18, MLXIP, UGT1A, BAALC, KRT19, ANGPT2, GATA1, TNFSF10, CASP8, CYP3A5, ERCC1, PTX3, SOCS3, BRCA1, TLR4, NPPB, HLA-DQB1, ABCC2, TREM1, DPYD, TNF, IL10, UGT1A1, CXCL8, TP53, ABCB1, IL6, TGFB1, MTHFR, CRP, SCARA5, PTPN5, ADAMTS18.	**CYP3A5, TNFRSF10A, ABCB1, WAS, PDE4D, MLXIP, BAALC, KRT19, ANGPT2, SOCS3, TLR4,**
Diarrhea	ABCG2, CYP3A5, HTR3A, ABCB1, TNF, EGFR, IL6, IL10, CXCL8, BDNF, IL1B, LEP, TLR4, SLC6A4, UGT1A1, GPR39, UGT1A, MYLK, RAB27A, DPYD, TRPV1, CACNA1A, TREM1, AGR2, HLA-DQB1, RELA, ABCG2, S100A9.	**CYP3A5, ABCB1, TLR4,GPR39, MYLK, RAB27A,**
Nausea	POLE2, CYP3A4, TNFRSF10, TNFRSF10A, MAPRE1, ABCB1, CASP8, MTHFR, CGB5, SLC6A4, DRD2, CYP2D6, ABCG2, OPRM1, ERCC1, MAOA, ADH1B, PAPPA, TACR1, FAAH, TBX19, POU2F1, HTR3A, TRAP1, SERPINA6, HTR3B, HTR3C.	**TNFRSF, ABCB1, ADH1B**
Fatigue	TNFRSF10A, CASP8, CYP3A5, ABCB1, CYP3A7, CYP3A4, TNFRSF10, AR, PARP1, STX17, RIN2, IKZF4, IL2RA, TNFRSF10A, VDR, TP53, CASP8, CYP3A4, TNFSF10, RELA, ABCG2, CASP9, UGT1A1, NFKBIA, ABCC2, EGFR CASP3, ABCB1, CYP3A5, SUMO1, PTGES3, CDH1, CASP8,	**CYP3A5, ABCB1, IGF1**
Bradycardia	HCN4, Chrm2, COMT, SLC6A4, NPPB, ATP2A2, CYP2D6, SCN5A, KCNQ1, crhr1, CHRM2, SCN5A, NPPB, ATP1A3, ATP2A2, PRKAG2, ESRRA, KCNQ1, HCN4, ESRRA, EPB41, PRKAG2.	
Abdominal pain	ABCG2, CYP3A5, CYP3A7, ABCB1, CYP3A4, CRP, IL10, BDNF, IL1B, CDH1, IGF1, PTX3, S100A9, TNFRSF10A, DMD, TRPV1, CACNA1A, TREM1.	**CYP3A5, ABCB1, IGF1,**

| Bone marrow depression | TP53, TERT, S100A4, CD82, IL24, KLF6, RECK, TNF, VEGFA, IL6, TGFB1, MMP9, EGFR, CD274, NFKB1, HIF1A, IL10, PTGS2, ST7, AKT1, STAT3, ERBB2, TLR4, ESR1, CXCR4, IL1B, CTNNB1, MIR21, IFNG, SIRT1, PTEN, ST13, CXCL8, BCL2, NOTCH1, ADIPOQ, KRAS, MYC, CDKN1A, MTOR, MMP2, PPARG, AR, BRCA1, NFE2L2, BRAF, CDKN2A, SNCA, BIRC5, PDCD1, IL17A, JAK2, MAPK1, ITGB1, MAPK14, HLA-B, EZH2, MDM2, BRCA2, ABCB1, CD44, ZNF24, LEP, CDH1, ST7L, FOXP3, MIR146A, APP, BCL2L1, RB1, HGF, VDR, RELA, CDKN1B, GSK3B, HMGB1, RHOA, TLR2, HMOX1, MTHFR, ICAM1, SPP1, CXCL1, MCL1, IGF1, FOXP3, JUN, CRYBG1, KIT, BMP2, MAPK3, SRC, PIK3CA, LCN2, SP1, RPA1, E2F1, ATM, WT1, YAP1, FGF2, RAC1, CASP8, INS, CTLA4, RUNX2, CCL2, MDM4, STAT1, NR3C1, IGF1R, IL4, TNFSF11, RUNX1, TNFRS11B, FOXM1, CD4, IDO1, NLRP3, FAS, PTK2, PROM1, SERPINE1, NOS3, LGALS3, FGFR2, MAPK8, CREBBP, MIR34A, PARP1, TP63, HMGA2, HLAG, FLT3, MET, PTPN11, COMT, CCR5, FOXO1, POU5F1, PLAU, TWIST1, DKK1, VHL, IL2, CHEK1, IL33, SMAD3, H19, TNFSF10, NPM1, DNMT1, PML, AURKA, EP300, IL18, MYD88, ZEB1, EPO, MIF, MMP1, APOBEC3G, BAX, KDR, ITGB3, CASP3, MIR145, NOS2, TARDBP, TP73, PTH, HRAS, STK11, FLT1, NPPB, TIMP1, SNAI1, SOCD3, KCNH2, IL1RN, MAMT1, BECN1, ESR2, HLADQB1, SOD1, PLAUR, APC, CYP19A1, BMI1, SMAD4, GSTP1, CXCL10, AGT, RAD51, NOD2, GDF15, FGFR1, SOCS1, VIM, FN1, HDAC1, ABL1, MSH2, ABCA1, MIR221, PLK1, XRCC1, MECP2, SKP2, TNFSF13B, XIAP, TLR9, CD34, IL2RA, CHI3L1, EDN1, HAMP, PTPRC, CD40LG, CREB1, FTO, S100A9, NF1, VCAM1, EPAS1, SOD2, GJA1, FGF23, CD14, ABCG2, CCL5, VWF, CHEK2, MYCN, RAF1, FASLG, APOA1, YBX1, ROCK1, ELAVL1, HTT, CX3CL1, COL1A1, MLH1, CCN2, BSG, MGM2, TNFRSF1A, TGFBR2, HSPA5, PSEN1, SMAD7, AHR, LGALS1, CFLAR, HDAC2, LMNA, ATF3, RETN, EIF2AK2, SREBF1, IRF3, CHUK, SOX2, KLF4, PRKCD, GRB2, HSPB1, PRKAA1, BTK, FMR1, CDK2, SQSTM1, JAK1, DICER1, APOB, SMAD2, ILR6R, PDCD4, LDLR, RASSF1, NAMPT, IGFBP3, NOTCH3, CYP3A4, IL15, BMP7, SLC2A1, IL12B, PKM, FBXW7, CDK1, NFKBIA, TCF7L2, PAK1, BCR, SYK, CDC42, CD40, HSP90AA1, MMP14, AURKB, PCNA, P2RX7, EGF, CDK4, GRN, SERPINA1, KLRK1, INSR, IL7, KCNQ1, ERCC2, IFNB1, HNF4A, CALR, BCL2L11, TPMT, PIK3R1, MIR143, BMP4, HOTAIR, TNFRSF1B, EGRF1, ITGAV, PTPN22, STAT5A, TNFAIP3, THBS1, ENG, SMARCA4, TGFBR1, ANXA2, DNMT3A, MIR126, HAVCR2, IKZF1, ALOX5, STIM1, TYMS, JAG1, BRD4, AXL, CSNK2A1, SIRT6, NF2, TFRC, RUNX3, OGG1, IL21, MICA, HSPA4, ERBB3, TLR3, ADAM17, TRPV1, CCNE1, GZMB, DNMT3B, STAT6, HSF1, TET2, TIMP2, S100A8, CSF3, IL13, PIN1, NRAS, PINK1, PTPN6, YY1, SERPINF1, NME1, KWAP1, IKBKB, SPARC, SHC1, TOP2A, CXCL1, RIGI, CBL, USP7, MAP3K7, ANGPT2, SMARCB1, FCGR2A, WNT5A, MIR223, BCL6, IRF4, MIR222, SHH, ERG, CCL3, NBN, ID1, HSPD1, PARK7, FUS, CDH2, ITGB2, NGF, ARID1A, NDRG1, VCP, FKBP5, ADM, S100B, CD28, STMN1, PIM1, MAP2K1, PRKDC, IDH2, EIF4E, TGM2, CD163, BAP1, FYN, NANOG, IFIH1, MTDH, AMH, XPO1, PPIA, ADORA2A, FOS, DAPK1, CAMP, IRF1, ABCC1, MECOM, MEN1, NEAT1, TSC2, GATA2, HSP8, MYB, GAS6, SPHK1, NRP1, PDGFB, MEG3, IL27, IL12A, MIR30A, SUMO1, CDK9, STING1, HPSE, ITGA2, KDM1A, ATR, GAPDH, MIR214, SIRT3, XBP1, PDGFRB, VEGFC, ERN1, TSHR, IL1RL1, ARG1, VKORC1, PPARD, ITGA2B, WRN, MYH9, POSTN, MITF, AFP, NGFR, AGO2, ETS1, FOXA1, RXRA, NTRK1, DUSP1, PRKCB, RPS6KB1, PTPN1, TBK1, PDPN, INHBA, PTTG1, HDAC6, MIR200B, MIR16-1, ORAI1, FLNA, ITGA4, TJP1, CTTN, HDAC3, RACK1, SELE, PRKCE, CALM1, PGF, EWSR1, SOST, ATF4, IRAK1, ADAR, CASP9, TRIM28, SAMHD1, PVT1, NES, TGFB3, ILK, TGFB2, DNM1L, CASP2, PLCG1, SCARB1, FHIT, TBX21, PIK3CG, YWHAZ, TXN, MFN2, TP53BP1, BTRC, METTL3, LDHA, CDKN2B, TLR7, NOTCH2, CTCF, TNFRSF10B, HMGA1, TRIM21, ITGA6, MIR29B1, CCNT1, GP1BA, NCOA3, DDIT3, CSF2, XRCC6, POMC, CHGA, ACKR3, KPNA2, CHRNA7, ST7OT3, PHB1, PF4, ATG7, RAN, STUB1, CEACAM1, MMP13, HNRNPK, PKD1, NCL, TRAF3, BARD1, BLM, TRAF2, MSH6, CYLD, WWOX, MIR27B, RARB, XRCC5, FANCD2, DISC1, GDNF, SLC9A1, UHRF1, | **KLF6, ABCB1, HMGB1, IGF1, FAS, FGFR2, PML, GDF15, CDK1, PTPN22, THBS1, ANGPT2, HSPD1, DUSP1, PRKCB, PDPN, CDKN2B, TRPM7, GSN, PTGS1, NT5E, CD47, DCN, ARRB1, WAS, NEDD4L, SMAD1, BRIP1, RAB27A, ROR1, NR2F2, ETS2, SOCS2, AHNAK** |

BAK1, NEDD4, NR4A1, MIR182, RARA, STAT5B, OPA1, PTK2B, CTSB, TEK, TXNIP, TREM1, PRMT5, UCA1, GAS5, CTSD, XIST, PPP2CA, NFATC1, GNAQ, ABCC2, ADIPOR1, TRPM7, AREG, AXIN1, SMURF1, CXCR3, MTA1, CDK5, LOX, POLR2A, TBP, UBE3A, LGALS9, ETV6, TRIM5, AKT2, ISG15, CA2, IL32, MAVS, PTBP1, PALB2, SPI1, GSN, BIN1, HDAC4, CASP1, MAP3K5, CCN1, KAT5, PXN, TLR8, CUL1, PTGS1, ZFP36, MIR375, FADD, REST, OSM, ENO1, FLT4, NT5E, RHD, LYN, NR4A2, CD200, TRIM25, BAD, COPS5, ZEB2, BBC3, BID, ATRX, WNT1, SIN3A, KLF2, CNR2, DAXX, MIR144, GATA4, MED12, MAPK7, CD47, IRF5, HK2, RAP1A, WNT3A, MCAM, MIR31, ADA, ROCK2, DCN, NCOR1, TUG1, ULK1, PERP2, KLF5, RASA1, CDH5, SLC7A5, FLI1, SRSF1, MIR15A, DYRK1A, ATF2, APAF1, BAG1, SGK1, NR5A1, TFPI, CFL1, MAD2L1, MIR140, MIR141, AGT16L1, CD9, WEE1, CD1D, DKC1, BRMS1, MIR22, S1PR1, ARRB1, KIF11, MIR137, FEN1, DIABLO, MIR23A, LOXL1, HSP90B1, BAG3, WAS, IRS2, MALT1, YWHAQ, MIR148A, SEMA3A, SIRT2, THY1, SKP1, FCGR2B, HIPK2, PRDX1, PIEZO1, MIR139, PAX5, CTSL, TUBB3, MIR338, APOBEC3B, ATF6, RAD50, TAC1, IL17F, EEF1A1, RIPK3, ENTPD1, UBE2N, PPM1D, CGAS, MIR96, HSPA9, DHX9, CD8A, MIR10A, CD247, NAT1, FADS1, MIR204, NCOR2, TERF2, CTBP1, ATXN3, MTHFD1, SLC16A1, PTGER4, ABCC4, FZR1, NOX1, MX1, TGFA, NEDD4L, MIR196A2, HBEGF, CCND2, MDK, PIK3CB, TIRAP, EIF2S1, NCOA1, RAB5A, IFITM3, JAK3, CUL4A, CD80, ITCH, PRKAB1, ACTN4, LIF, IGF2BP2, PRDM1, IGF2R, ARNT, SMAD1, GAA, MAP1LC3B, SET, MIR93, XRCC4, KHDRBS1, IFI16, NHERF1, ILF3, MSLN, PDPK1, PYCARD, MIR26A1, KDM6B, APOBEC3F, NFATC2, HES1, BRIP1, PDX1, CSF3R, ITGAL, KMT2D, NOP10, ADD1, LILRB1, FLCN, TCF3, SRSF2, MIR101-1, EIF2AK3, PTGER2, GLO1, SP3, PLD1, CCL4, POLE, MUC4, KCNJ2, MERTK, RGS2, TTK, CDC25C, MICB, CD19, PPP1CA, HAX1, GADD45A, CRKL, DHFR, DYSF, FECH, CSK, MAPK9, LOXL2, TYMP, IL11, MYML2, MIR18A, SSB, CAPN3, UBE2C, TFEB, CRBN, ESRRA, C1QBP, SETD2, CD226, CD63, PGK1, ZBTB16, CTSS, ID2, NEK2, FADS2, SLIT2, MIR199A1, PTN, IKBKE, FPR2, RPGR, TXNRD1, CTS5, PLA2G6, MIR378A, ITPA, HOXA9, HNRNPU, PAK2, FHL2, LMNB1, RPL1, RRM1, PSMD4, RUX1T1, FCER2, SFPQ, IRF7, SLPI, ELK1, FGF7, PFKFB3, RRM2, MACC1, IRF8, SDHD, PVR, ADIPOR2, MIR130A, ALOX5AP, MIR181A1, MRTFA, TLR1, RPTOR, VIP, MIR183, EPHB4, TPX2, CBX5, GPX4, PLK4, IL10RA, RAB11A, TIGIT, STAT2, NEDD9, ING4, PRDX6, SUMO2, MAP2K4, CPT1A, CD33, E2F4, LATS1, TERF1, PBRM1, MDC1, CDKAL1, GNL3, HUWE1, ALDOA, IGFBP5, LDHB, SPINT2, PNPLA2, LMO2, RUVBL1, HDGF, HNRNPL, CLIC1, MASP2, DOT1L, TAF1, XRCC2, CTNNA1, LAG3, IMPDH2, TNFRSF4, DUSP6, NUMB, RBL2, SRSF3, S100A10, TNFRSF9, SPOP, STNNA1, DDIT4, PAK4, RPS19, GNAI2, PTGES, GLB1, MAPRE1, RBBP4, LONP1, GTF2B, TRIB3, KAT2A, MAP2K2, PIAS1, TAFAZZIN, CARM1, SUZ12, RBBP8, CSNK1A1, NUDT1, CXCL2, MIR152, TOPBP1, SIAH1, SMURF2, ADAM9, GOLPH3, TRAP1, RUVBL2, SLC25A5, SH2D1A, CBX3, CBLB, DDX21, BCL3, DLL1, MATR3, SCRIB, MIR124-3, RAD21, PCBP2, CASP10, NEU1, HGS, NFAT5, PBK, EXT2, PRDX3, SPTAN1, SERPINB2, SKI, EIF5A, ATXN1, RAD52, GCLC, TRIM27, CHFR, LAMP1, ASPM, PSME3, BUB1, SFRP2, CUL5, MAP3K1, VPS35, HAS2, RNF2, CASP6, ERCC3, KMT5A, SYVN1, SDCBP, BHLHE40, MBD2, PSMC5, ROR1, NR4A3, CSNK1E, PTMA, ATG3, MSX2, NPPC, CDK8, ATP5F1B, ATP5F1A, ACACA, JUNB, SSRP1, SMARCA3, GFER, SIRPA, SOAT1, ELOB, CPT2, MCOLN1, IRF2, RPL5, CREM, TLR6, CXCR6, CKAP4, DNAJB6, CDC25B, RHEB, HOTTIP, ILF2, DANCR, SAT1, NR2F2, EBAG9, NPR2, ETS2, CTBP2, DNAJB1, PELP1, FBL, MIR483, LTBR, GPBAR1, MYH10, SYMYD3, UBTF, DDX6, AMFR, KLRB1, KCNH1, PLSCR1, CARD9, PPP2R2A, FOXO4, RB1CC1, NEUROD1, CCAR2, BCL11B, PTPN13, PSMB5, PRDM2, CPS1, PRC1, TRIB1, FUT8, CAST, DVL2, SOCS2, MEF2D, RPLP0, ALKBH5, CKB, RECQL, NRIP1, RALA, PDK1, PSMD2, GRK5, CTNNBIP1, TIMELESS, TRADD, BANF1, XAF1, UROD, LILRB2, FIS1, PIAS3, ABCE1, SERPINA5, METTL14, ETF1, S100A11, APOBEC3C, CD2, ACD, OLFM4, SMAD5, RPS14, NME2, GFI1, CFP, DDX39B, GDF11, CLCN3, SLC6A8, CKS1B, PSMC2,

SIAH2, MAP2K7, TBL1XR1, RPL7A, CRNDE, SRD5A1, TOLLIP, TRAF4, TARBP2, PPP5C, TAB1, PRPS1, CAMKK2, PSMC3, PTPRA, CRY2, PEX5, SKIL, MAP2K6, FERMT3, MIR196A1, CRY1, RNF31, AGO1, CDH11, OUTB1, SETD1A, GARS1, BCL2L2, PCLAF, EIF6, MIR485, PHF6, MAP3K11, CSTA, MIR181A2, ARHGEF7, UBE2T, PRPF19, CAD, LIMS1, MGAT5, REV3L, CCT3, DDAH2, EGLN2, DNAJA3, PSMB9, NUP62, AHNAK, PLCD1, TNFAIP8L2, TRIM11, SNAP23, RPS15A, USP39, ANLN, ZFHX3, PSMC4, PSMD1, BLK, PHLPP1, SELENBP1, RPS2, IER3, PSMA3, HIF1AN, TAF15, NCBP1, LAMA1, MYO9B, MIR30E, BIK, MIR92A2, KIF14, ATAD2, MELK, IL1RAP, TRAF5, CHD8, GRB10, TRIM22, HOXD13, AFF1, CCNH, CHCHD2, RPS8, RPS3A, SP100, PIM2, POLR3A, SUFU, PSMC1, RASSF5, TNRC6A, KAT8, SRRT, GALNT3, MIR199A2, MAP4K4, DVL3, MAP2K3, RPL3, CAMK4, MR1, RPS4X, FBXW11, CRISP3, MYBBP1A, MTSS1, MBD3, CIB1, TNFRSF10C, AKAP9, SPAG2, LILRB4, FLII, NCOA4, APOBEC3H.

3.4. Discussion

Colorectal cancer, the most common cancer, continues to have high incidence and mortality rates worldwide despite advancements in understanding molecular mechanisms. For our study, we utilized two datasets. In one GSE62322 dataset of gene expression data from tumor colon samples of twenty-one patients with advanced colorectal cancer. After analyzing the dataset, we identified 953 upregulated genes, showing higher expression in tumor samples than normal samples, and 941 downregulated genes, exhibiting lower expression in tumor samples. These genes play a role in different pathways of cancer progression such as angiogenesis p53 mediated apoptosis, RTK-RAS, lipid metabolism, PI3K/Akt, ubiquitylation, β-catenin/Wnt signaling, Notch signaling mechanisms, cell cycle regulation, cytokine signaling mechanisms; cell proliferation process and filament assembly.

The second dataset(GSE72484) was also analyzed using the GEO2R tool. The patient data set consists of gene expression profiles from irinotecan-treated colorectal cancer samples that had received chemotherapy versus the colorectal cancer sample of patients who did not receive any chemotherapeutic treatment. The analysis revealed 528 upregulated genes and 786 downregulated genes in post-chemotherapy. These genes are linked to pathways related to cancer progression and adverse effects, such as vascularization, natural killer cell-mediated cytotoxicity, Rap1 signaling, necroptosis, hepatitis B, and aldosterone-regulated sodium reabsorption.

Therapeutic genes that were upregulated and downregulated in dataset one were analyzed for their impact on dataset two. Upon comparison, it was found that 280 genes were upregulated and 132 genes were downregulated in a manner that consisted of tumor treatment. However, Topoisomerase inhibitor (irinotecan) treatment is known to suffer from multiple side effects like bone marrow depression, abdominal pain, bradycardia, neutropenia, decreased appetite, thrombocytopenia, anemia, and cholinergic syndrome (diarrhea, fatigue, nausea). We studied the literature to identify genes that were directly or indirectly involved in such side effects. Two thousand fifty-seven such genes and their pathways were studied, and it was found that several pathways that indirectly affected tumor progression were impacted, decreasing the therapeutic impact of topoisomerase inhibitor therapy. Also, several genes were known to be affecting stimulated pathways due to the nonspecific binding of these topoisomerase inhibitors to non-target receptors.

In our study, we looked at the genes that were potentially related to side effects based on our literature review, and it was found that 46 genes were associated with direct and indirect side effects of irinotecan treatment.

DEGs from colorectal tumors (953 genes) with the downregulated DEGs from irinotecan-treated samples (786 genes), and the downregulated DEGs from CRC samples (941 genes) with the upregulated DEGs from irinotecan-treated samples (528 genes), we identified 46 common genes. These genes are significantly affected by chemotherapy and may play roles in tumor progression and side effects pathways.

Functional Validation of Common Genes

Among the 46 common genes, 36 were identified with a logFC value ≥ 1 and 10 with a logFC value < 1. These genes are potentially involved in pathways associated with tumor progression (such as cell proliferation and metastasis) and chemotherapy-related side effects (including anemia, bone marrow depression, nausea, fatigue, neutropenia, bradycardia, decreased appetite, diarrhea, and abdominal pain). Functional annotation from the literature validated their association with these processes.

Furthermore, gene enrichment analysis shows the direct impact on pathways such as signal transduction, cell migration, anti-apoptosis, cell cycle regulation, and protein metabolism that directly support tumor progression. These genes are also involved in side effects pathways like hepatitis B, Fanconi anemia pathway, TGF beta pathway,

serotonergic synapses, ubiquitin-mediated proteolysis, Rap 1 signaling pathway, etc. (Fig.3.14); therefore, overexpression of these genes can lead to the enhancement of the above biological pathways which could adversely affect cancer progression and side effects. The PPI network analysis pinpointed critical regulatory nodes and intermediate hubs within the gene interactions, emphasizing significant genes with crucial roles in the network. This discovery underscores the importance of these shared genes in elucidating the molecular mechanisms behind the adverse effects of irinotecan. It raises the possibility of their involvement in the detected changes in gene expression. Hence, this necessitates the exploration of natural compounds that would potentially impact cancer remediation but would not suffer from the side effects associated with irinotecan treatment.

Identification of natural compounds to restore the function of dysregulated genes
The study also investigated the differential gene expression of 102 naturally occurring compounds known for their anticancer property, which were further studied in the context of colorectal cancer treatment. The 102 natural compounds (NC) included in our study were shown to have anticancer properties similar to topoisomerase inhibitor therapy by direct or indirect impact on differentially expressed genes (DEGs). It was also elucidated whether these NCs had any role to play specifically on the genes associated with topoisomerase inhibitor therapy-mediated side effects. The most commonly associated side effects related to irinotecan treatment were found to be thrombocytopenia, fatigue, nausea, neutropenia, decreased appetite, diarrhea, abdominal pain, and fatigue that were the direct or indirect impact of commonly founded genes(ABCB1, BRIP1, FANCI, TNFRSF10A, WAS, THBS1, CYP3A5, ABCB1, PDE4D, MLXIP, BAALC, KRT19, ANGPT2, SOCS3, TLR4, GPR39, MYLK, RAB27A, TNFRSF, ADH1B, KLF6, HMGB1, FAS, FGFR2, PML, GDF15, CDK1, PTPN22, HSPD1, DUSP1, PRKCB, PDPN, CDKN2B, TRPM7, GSN, PTGS1, NT5E, CD47, DCN, ARRB1, NEDD4L, SMAD1, BRIP1, RAB27A, ROR1, NR2F2, ETS2, SOCS2, AHNAK. GPR39, BAALC, KRT19). The natural compounds studied were investigated for their impact on some of the genes related to side effects. By comparing these common DEGs with those altered by each natural compound, we identified compounds that most effectively reversed the expression of these genes. The NC were ranked based on their ability to reverse the maximum number of DEGs, with

results summarized in Table 3.1 showing the number of genes affected by each compound. For example, TNFRSF10A, WAS, THBS1, ABCB1, and CYP3A5 were related to thrombocytopenia, fatigue, nausea, and decreased appetite. TLR4, GPR39, MYLK, and RAB27A were related to diarrhea, abdominal pain, and fatigue, while dysregulation in PDE4D, MLXIP, BAALC, KRT19, ANGPT2, CYP3A5, SOCS3, CYP3A5, TNFRSF10A leads to neutropenia condition. Natural compounds, being multitargeting, can influence multiple pathways involved in tumor suppression, reducing the likelihood of drug side effects. This multitargeting nature makes them promising candidates for combination therapies in cancer treatment. Drug resistance and adverse side effects may be reduced by this combination, which shows positive synergistic benefits.

3.5.Conclusion

The present study provides a comprehensive analysis of alterations in gene expression in colorectal cancer and the effects of irinotecan chemotherapy (topoisomerase inhibitor) and their relationship to the emergence of severe side effects using datasets GSE62322 and GSE72484. Through differential gene expression, we identified upregulated and downregulated genes in colorectal cancer samples versus normal tissue samples to identify the manifested targets of colorectal cancer. Furthermore, we analyzed gene expression in post-chemotherapy samples compared to untreated samples to determine the impact of irinotecan. Irinotecan, although an FDA-approved topoisomerase inhibitor, suffers from many side effects. By cross-referencing these findings with pre-existing literature on genes associated with irinotecan-induced side effects, we identified a significant overlap. Specifically, we found common genes that were significantly affected by chemotherapy. These genes are involved in critical cancer progression pathways. They are linked to adverse effects commonly observed with topoisomerase inhibitor therapy, such as anemia, bone marrow depression, nausea, fatigue, diarrhea, and neutropenia, which is collectively known as cholinergic syndrome. Natural compounds have long been explored as alternate cancer treatments due to their reduced side effects. This study emphasizes the complex correlation between gene expression changes caused by chemotherapy and the side effects of irinotecan, offering valuable insights that might help reduce such adverse effects

throughout the treatment of colorectal cancer by using natural compounds. However, natural compounds can also exert some side effects. Therefore, molecular targets directly associated with the side effects were identified for irinotecan treatment. Afterward, an assessment of the side effects of natural compounds with similar interactions to these molecular targets was performed to investigate whether they had the potential to cause adverse effects similar to those exerted by irinotecan therapy.

CHAPTER: IV

Objective 2

> ➢ *Mitigation of side effects of chemotherapeutic drugs using Natural compounds*

CHAPTER: IV: OBJECTIVE 2

4.1. Rationale of the study:

The term cancer refers to a group of diseases characterized by the out-of-control growth of cells caused by the accumulation of errors or mutations in their DNA and the potential for invasion or spread to other organs or parts of the body[275]. Two drugs that have received FDA (Food and Drug Administration) approval and are currently being used to treat particular forms of cancer are Topotecan and Irinotecan. In contrast to Irinotecan, which is used to treat colon cancer, rectal, and lung cancers, Topotecan is predominantly used to treat ovarian cancer. It works by inhibiting the activity of an enzyme called DNA Topoisomerase I (TOPO I)[276]. The TOPO I enzyme plays a crucial role in the regulation of DNA structure and function. Its primary function involves the cleavage and resealing of a single strand of DNA, enabling the unwinding and untangling of the DNA molecule. This process is necessary for relieving supercoiling, which can only be resolved locally due to the large size of eukaryotic chromosomes[277]. Due to a temporary nick in the DNA strand, the broken segment has the ability to rotate around its intact complementary strand, allowing it to eliminate any local supercoils. The transesterification of an active-site tyrosine (Tyr-723) at a DNA phosphodiester linkage facilitates the development of a covalent complex between the enzyme and DNA, which in turn triggers the nicking of the strand. The damaged strand's released 5-OH group then undergoes a second transesterification event, in which it attaches to the phosphotyrosine intermediate, effectively reversing the covalent state [278]. This process is necessary for DNA replication and transcription, which are essential for cell division and growth.

Irinotecan functions by interacting with the TOPO I enzyme, inhibiting its ability to reseal the DNA strand that has been cut during normal cellular processes. As a result, this inhibition leads to an accumulation of DNA strand breakage. The presence of excessive DNA strand breaks can activate cell death pathways, ultimately leading to the elimination of cancer cells (Fig.4.1)[279].
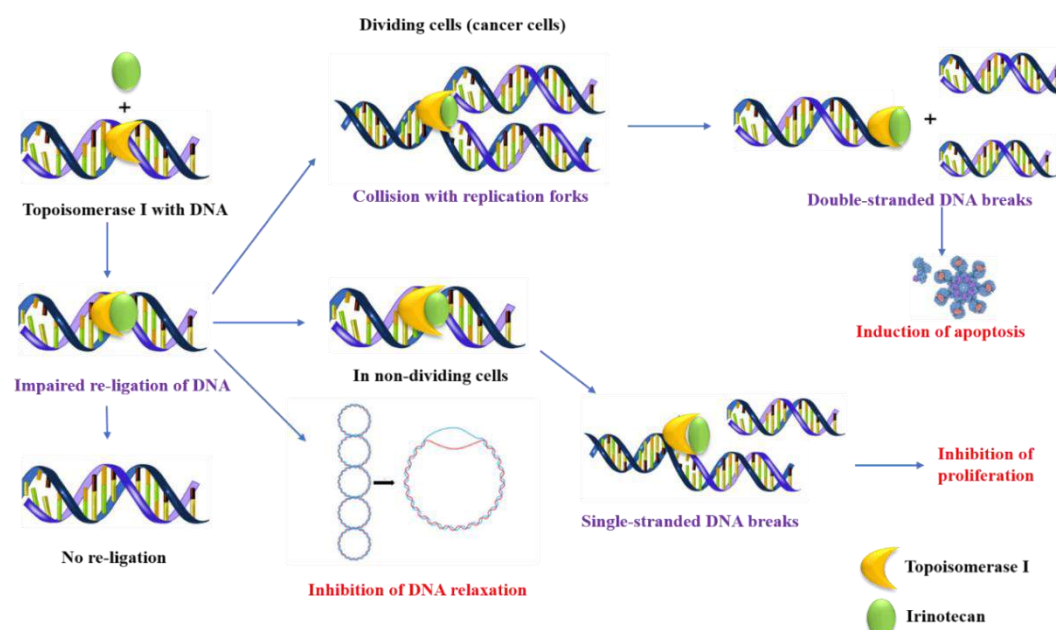
Figure 4. 1. Irinotecan, a topoisomerase I inhibitor, functions by binding to the complex formed between topoisomerase I and DNA. This interaction hinders the resealing of DNA single-strand breaks (SSBs), resulting in the accumulation of DNA double-strand breaks (DSBs). The resulting stable ternary complexes between irinotecan, topoisomerase I, and DNA trigger cellular responses for DNA repair. However, excessive accumulation of DSBs overwhelms the repair mechanisms, leading to cell death. The disruption of DNA structure and impaired repair processes hinder normal cell division and replication, effectively inhibiting cancer cell growth and reducing tumor size. Nevertheless, irinotecan can also affect normal cells, causing side effects such as gastrointestinal toxicity, myelosuppression, and hair loss.

Irinotecan is a successful cancer treatment because cancer cells are more sensitive to this procedure than normal cells.

However, Irinotecan can also have side effects on normal cells that are dividing rapidly, such as those in the bone marrow and digestive tract. These side effects can include nausea, vomiting, diarrhea, and decreased blood cell counts[279, 280]. This investigation aims to tackle the unfavorable side effects of Irinotecan, specifically the emergence of cholinergic syndrome.

4.2. The Cholinergic Syndrome and Adverse Effects:

Irinotecan is a prodrug that is extensively metabolized by the enzyme carboxylesterase in the liver, resulting in the production of the active metabolite 7-ethyl-10-hydroxycamptothecin (SN-38). Irinotecan has both antitumor and toxic effects, and its active metabolite, 7-ethyl-10-hydroxy camptothecin (SN-38) has antitumor activity

but is also toxic because it is bearing 4-piperidinopiperidine moiety is reported to inhibit Acetylcholinesterase (AChE) predominantly through this moiety, which is known to be a major factor determining enzyme activity loss[281]. AChE is an enzyme that breaks down acetylcholine, a neurotransmitter that is involved in many processes in the body, including the regulation of the gastrointestinal tract[282]. The interaction between AChE and its substrate acetylcholine (ACh) is crucial for the regulation of ACh levels at the synapse. AChE is an enzyme that belongs to the serine hydrolase family[283]. The breakdown of acetylcholine by AChE involves a series of steps. Initially, AChE forms a complex with ACh, and this interaction triggers the hydrolysis and inactivation of ACh. The active site of AChE contains a catalytic triad, which consists of three amino acid residues: serine, histidine, and an acidic residue. The catalytic triad facilitates the creation of a tetrahedral intermediate through acid-base reactions. Histidine plays a crucial role in transferring a proton between the oxygen molecules in serine and ACh[284]. This transfer leads to the removal of choline from ACh, resulting in the formation of a new acylated serine residue. Subsequently, the acylated serine undergoes deacylation, where it is deacylated to regenerate the free AChE enzyme. In this step, aspartate stabilizes the protonated histidine, leading to the release of acetic acid and the generation of a new, free enzyme. In addition to the catalytic site, AChE possesses a peripheral anionic site, which is formed by specific amino acid residues such as tyrosine, phenylalanine, and tryptophan. The interaction between these amino acids influences the conformational binding of ACh to the peripheral anionic site[285]. This binding can modulate the activity of AChE and affect the overall enzymatic function. Overall, the interaction between AChE and ACh, mediated by the catalytic triad and the peripheral anionic site, ensures the efficient breakdown of ACh, preventing its excessive accumulation at the synapse and allowing for precise control of neurotransmission. Irinotecan is not directly related to AChE . However, one of the side effects of irinotecan treatment is the development of cholinergic syndrome, which is characterized by symptoms such as diarrhea, nausea, vomiting, and abdominal cramps (Fig.4.2) [222]. Irinotecan and its active metabolite SN-38 have the ability to block AChE, causing the body to accumulate acetylcholine and the onset of cholinergic syndrome[281]. It has been shown in clinical studies that patients who receive irinotecan often experience effects associated with the cholinergic

syndrome, such as hypotension (low blood pressure), hypersalivation (excessive saliva production), bradycardia (slow heart rate), abdominal cramps, acute diarrhea, and diaphoresis (excessive sweating) [233].
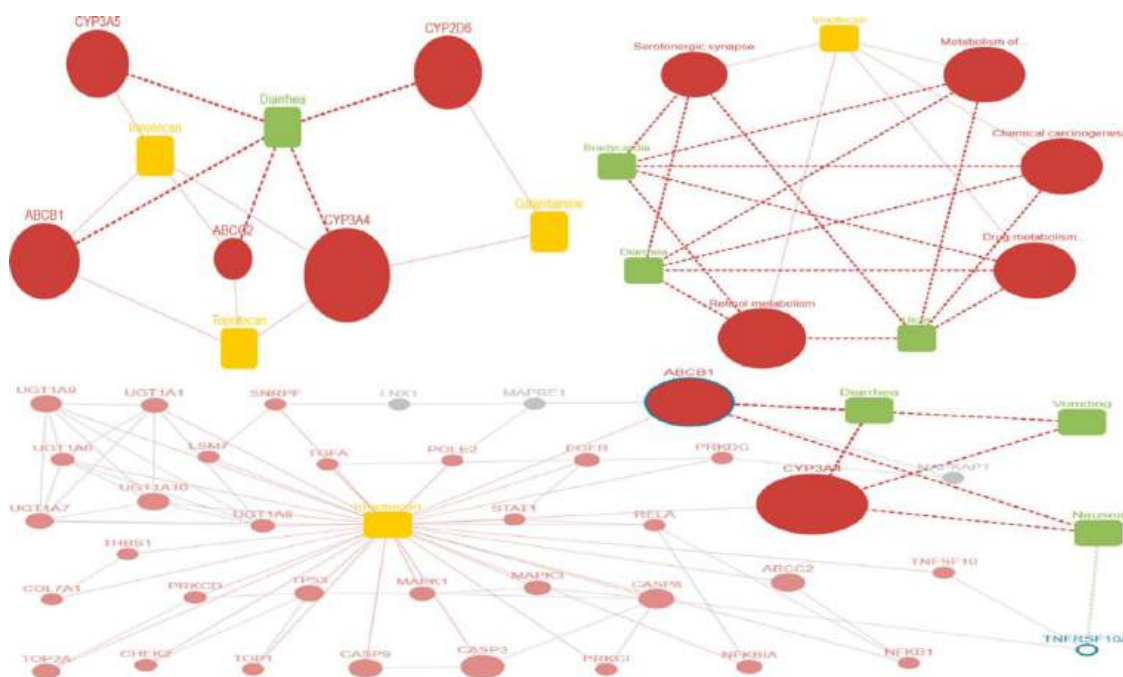
Figure 4. 2. This illustrates how irinotecan works effectively against cancer by interacting with different genes and transporters. Additionally, it interacts with another gene to cause different side effects. Furthermore, the figure shows the interactions between our control drugs with the same gene and a mechanism that is similar to the drug that causes cholinergic symptoms.

Cholinergic syndrome is caused by the accumulation of acetylcholine in the body due to the inhibition of AChE [286]. It is estimated that about 15%–20% of patients who take irinotecan will experience diarrhea and myelosuppression. A rapid cholinergic surge from acetylcholinesterase inhibition causes diarrhea within hours after administration[287]. It has been found that 23-31% of patients with late diarrhea develop severe or life-threatening complications within 24 hours (Fda, n.d.). Several in vitro studies show irinotecan inhibits AChE to cause cholinergic syndrome. The pathophysiology of irinotecan-induced cholinergic syndrome is not yet fully understood, and there are several aspects that remain unexplained. To further understand the pathophysiological processes that underlie this syndrome's particular pathogenesis and its underlying mechanisms, more research is required. According to Dodds and Rivory, the mechanism of inhibition of irinotecan was instantly reversible and non-competitive at clinically relevant concentrations[288]. Numerous studies

demonstrate fusion leads to rhinitis, lacrimation, miosis, increased salivation and diaphoresis, more salivation, flushing, cholinergic syndrome after drug infusion, and intestinal hyperperistalsis leading to diarrhea(Fig.4.2). To prevent or manage cholinergic syndrome in patients undergoing irinotecan treatment, medications such as atropine and loperamide may be prescribed [236]. Atropine is an anticholinergic medication that can block the effects of acetylcholine in the body, while loperamide is an antidiarrheal medication that can relieve the symptoms of diarrhea [289]. Consequently, the development of more potent and targeted antitumor agents remains a significant concern and challenge within the field of medicinal chemistry.

4.4. Natural compounds as an alternative

In the quest for potential therapeutic drugs, researchers have traditionally turned to natural substances or their synthetic derivatives. Specifically, natural or derived compounds that inhibit the activity of the enzyme TOPO I have demonstrated effectiveness in chemotherapy for the treatment of cancer. These TOPO I inhibitors have shown promise as anticancer agents and continue to be an area of active research and development. There are many Asian traditional medicine systems that use *Phyllanthus emblica Linn* (PE) to treat a wide array of diseases, including cancer[290]. The *P. emblica* plant possesses multiple biological effects, including analgesics, antibacterial, antifungals[291], antimutagens[292], antioxidants[293], antipyretics, antitumours, chemopreventatives and hepatoprotectives[294], some of which can be detrimental to human health. The most prevalent and biologically active polyphenol in *Phyllanthus emblica,* Epigallocatechin Gallate (EGCG), is believed to be responsible for many of the beverage's health advantages.

Tea, derived from the Camellia sinensis plant, is a globally favored beverage, with green tea being particularly notable for its abundance of catechins, among which (-)-epigallocatechin-3-gallate (EGCG) stands out. EGCG constitutes over 50% of total catechins in green tea and is renowned as its most potent and extensively studied component[295].The mechanisms underlying EGCG's anticancer effects are multifaceted and include antioxidant activities, modulation of carcinogen metabolism, prevention of DNA damage, induction of cell cycle arrest and apoptosis, inhibition of

metastasis, proteasome inhibition, and modulation of multiple signal transduction pathways such as EGFR, HER2, VEGF receptor, IGF1R, PI3K/AKT, MAPK, and NF-κB signaling[296–298].

Combination therapy involving EGCG and other anticancer agents has shown promising synergistic effects in preclinical studies, although caution is warranted as EGCG may interfere with the efficacy of certain anticancer drugs.
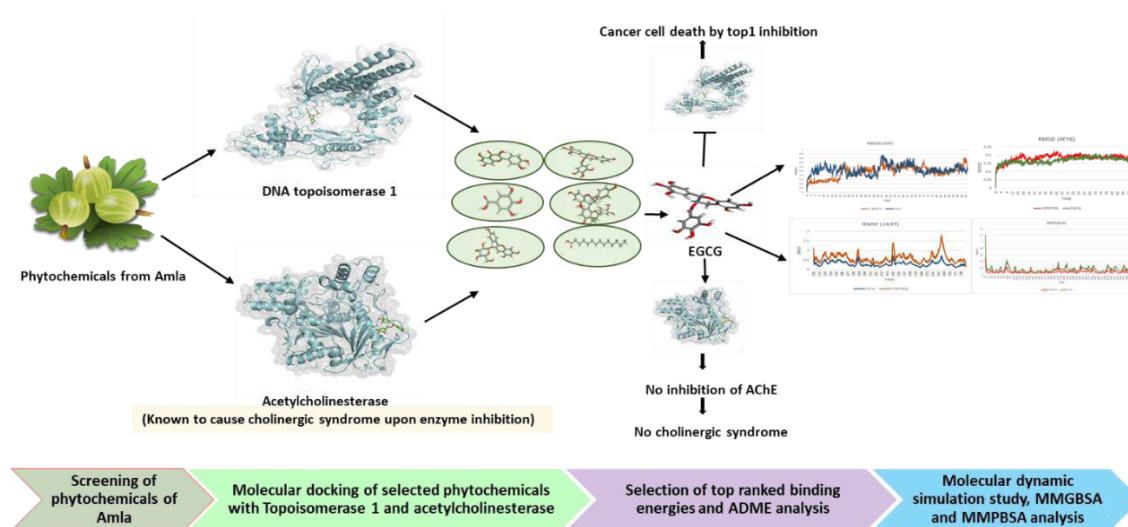
Figure 4. 3 figure illustrating the overall methodology of screening the molecular targets for natural compounds.

4.5.The collection and data analysis

4.5.1. Analysis of the active site and sequence for the chosen target molecule (Receptor)

A PDB file containing the crystal structure of human topoisomerase I and its inhibitor topotecan (FDA-approved drug and analog of irinotecan) PDB ID 1K4T, with the DOI:10.1073/pnas.242259599, is available through the RCSB (https://www.rcsb.org/). Topotecan is a chemotherapy medication categorized as a TOPO I inhibitor and serves as the reference ligand in this study. To investigate the side effects, the crystal structure of the AChE enzyme (4EY6) obtained from the Protein Data Bank. In this analysis (-)-galanthamine, a widely recognized and approved inhibitor of AChE was employed as the reference ligand. By utilizing these references, the aim was to explore potential interactions and elucidate the mechanisms underlying the side effects of the investigated compounds. Using the Protein-Ligand

Interaction Profiler (PLIP) (https://plip-tool.biotec.tu-dresden.de/plip-web/plip/index), it has been confirmed that 1K4T and 4EY6 possess functional domains and amino acid residues within the pocket of the active site. Based on the Co-crystallized ligands in crystal structures, these findings were confirmed and used to determine the binding site.

4.5.2. Screening of natural compounds

A set of sixty-three ligand structures in the "sdf" file format was obtained from the freely available IMPPAT database (https://cb.imsc.res.in/imppat/) for the study (Table 4.1). To ensure compatibility and facilitate further analysis, the three-dimensional structures of these ligands were downloaded from PubChem, a database maintained by the National Center for Biotechnology Information (NCBI) (www.pubchem.ncbi.nih.gov) [28]. The downloaded "sdf" files were then processed using BIOVIA Discovery Studio Visualizer to generate the corresponding PDB files for further analysis.

i. The preparation of ligands (Phyllanthus emblica active compounds) and proteins

To facilitate the analysis, the BIOVIA Discovery Studio Visualizer software was used to prepare the X-ray crystal structures of the TOPO I complex (PDB ID: 1K4T) and the AChE complex (PDB ID: 4EY6). These structures were processed and visualized using the aforementioned software. This step allowed us to examine and explore the structural details of these complexes for the study. Applying an all-atom force field added hydrogen atoms to the fixed structure after fixing structures, removing unwanted chains and water, and Polar hydrogens were added to it. The ionization power, energy minimization, torsion level, degree of freedom, and stereochemical variation of the Ligand were adjusted using EasyDock vina Tool. The gasteiger charges were calculated using the Easy Dock vina Tool, and stored in the form of PDBQT files. The AutoDock Grid tool created 25Å, 25 Å, 25 Å grid boxes with 0.375 Å spacing and 21.242 Å, 03.973 Å, 28.129 Å grid box dimensions in X, Y, Z for 1K4T and -2.435 Å, -30.710 Å, 53.141 Å for 4EY6 respectively.

ii. Molecular Docking Analysis of Active Compounds from Phyllanthus emblica with their Target Proteins

The crystal structure of TOPO I obtained from the RCSB Protein Data Bank (PDB ID: 1K4T) has a resolution of 2.1 Å. Its free R-value is reported as 0.269, while the work R-value is 0.229. Similarly, the crystal structure of AChE enzyme from the RCSB Protein Data Bank (PDB ID: 4EY6) has a resolution of 2.40 Å. Its free R-value is reported as 0.206, and the work R-value is 0.167. These values provide information about the quality and reliability of the crystal structures, with lower R-values indicating better agreement between the observed data and the model. Sixty-three phytochemicals from *Phyllanthus emblica* docked individually against 1K4T as well as for 4EY6 using an in silico docking program, Easy Dock Vina. Before docking was performed, the ligand and enzyme preparation conditions must be met. The phytochemicals with the highest rankings were selected based on their strong binding affinities with the proteins. To visualize these interactions, PyMol, a software tool developed by Schrödinger (http://www.pymol.org/pymol), and BIOVIA Discovery Studio Visualizer were employed.

Table 4.1. An analysis of the binding energies between macromolecules and natural compounds (phytochemicals of Phyllanthus emblica)

Phytochemical name	Source of phytochemicals	Binding energies with topoisomerase-I (1K4T)	Binding energies with Acetylcholinesterase (4EY6)
Procyanidin	bark	-7.8	-7.3
Proanthocyanidin	bark	-9.1	-6.5
Tannic acid	bark	-8.9	-7.7
Leucodelphidin	bark	-4.4	-5.4
Pyrogallol	fruit	-4.0	-5.2
1,3,6-tri-O-galloyl-beta-D-glucose	fruit	-8.6	-7.0
Riboflavin	Fruit and seed	-6.6	-5.7
Furosin	fruit	-8.3	-7.0
Terchebin	fruit	-8.6	-7.4
Phloroglucinol	fruit	-5.2	-6.9
trans-Zeatin	fruit	-5.2	-6.2

Catechol	fruit	-5.2	-6.4
Quercetin	fruit	-9.1	-6.5
Chebulagic acid	Fruit and leaf	-6.4	-7.6
Ellagic acid	Fruit ,Leaf and root	-7.9	-7.0
Methyl gallate	fruit	-6.0	-5.5
Ascorbic acid	Fruit, seed and leaf	-5.7	-5.9
Kzeyiyxacmutrm-uhfffaoysa-	fruit	-8.6	-7.3
Phyllantidine	Fruit and leaf	-7.6	-6.7
Ethyl gallate	fruit	-6.0	-5.6
beta-Glucogallin	fruit	-7.6	-7.0
Galactaric acid	Fruit, leaf and seed	-5.5	-5.9
Chebulinic acid	Fruit and leaf	-9.1	-8.2
Corilagin	Fruit and leaf	-8.3	-7.8
Chebulic acid	Fruit and leaf	-6.4	-6.6
Geraniin	fruit	-8.6	-6.0
Gallic acid	Fruit and leaf	-8.8	-5.8
Trigalloylglucose	fruit	-5	-5.6
Tryptase	fruit	-9.0	-6.7
Kaempferol	leaf	-4.4	-5.6
Lupeol	Leaf, bark and root	-6.4	-6.4
Astragalin	leaf	-6.6	-6.2
beta-Sitosterol	Leaf, seed and stem	-8.0	-6.8
Oleanolic aldehyde	root	-7.0	-6.4
Epigallocatechin gallate	root	-9.1	-4.4
Myristic acid	seed	-9.0	-8.0
Stearic acid	seed	-8.7	-7.0
Palmitic acid	seed	-7.9	-6.7
Nicotinic acid	seed	-5.5	-5.0
alpha-Carotene	seed	-7.7	-6.9
Oleic acid	seed	-8.9	-7.8
Linolenic acid	seed	-5.6	-8.6
D-Galacturonic Acid	seed	-6.0	-5.8
Eriodictyol-7-O-glucoside	stem	-7.0	-8.9
Inositol		-7.3	-5.5
Linoleic acid		-4.6	-6.5

4.5.3. Drug likeness prediction

In order to forecast the pharmacokinetic characteristics of the top six compounds displaying the highest binding affinities, SWISSADME server (http://www.swissadme.ch/) was used. This server facilitated the assessment and prediction of various pharmacokinetic parameters for these compounds. Through this platform, an analysis of the chosen compounds was performed to evaluate their ADME (absorption, distribution, metabolism, excretion) properties. The major ADME-associated parameters that were assessed included drug solubility, pharmacokinetic properties, and predictions related to absorption, metabolism, distribution, excretion, and toxicity. This comprehensive analysis provided valuable insights into the ADME characteristics of the potential compounds and aided in evaluating their potential as drug candidates.

4.5.4. Molecular dynamic simulation

The molecular dynamic simulation method provides an initial understanding of the dynamics of protein-ligand interactions, but it is critical to understand how these connections are maintained and how they affect the protein. The goal was to determine whether the drug-like properties of the model would be met as well as how the interaction would play out. The dynamics of docked complexes can be analyzed through MD simulations. In this research, molecular dynamics simulations were emplyoed to explore how the top-ranking compounds with high binding energies interact with both TOPO I and AChE enzymes. The initial configurations of Top1 and AChE were described using docked crystal structures 1K4T and 4EY6, respectively. The GROMACS molecular dynamics (MD) package version 3.3.3 was employed for the simulations. To accurately represent the intermolecular interactions and dynamics of the systems, the AMBER03 all-atom force field was utilized. The complexes of TOPO I and AChE with the highest ranked phytochemicals were positioned within a rectangular container measuring 93 Å x 110 Å x 130 Å. This arrangement was accomplished using the genion feature of the GROMACS package, which substitutes solvent molecules with ions in areas demonstrating optimal electrostatic potential. To simulate a realistic environment, the container was filled with TIP3P water molecules (34) representing the solvent. To maintain overall electro neutrality, 23 or 24 Na+

counter ions were added to balance the system's charge. This setup ensured that the simulations accurately represented the physiological conditions and allowed for the study of the protein-ligand complexes in a realistic aqueous environment. Various analyses were conducted, including direct hydrogen bonding analysis, RMSD (root mean square deviation) calculations, RMSF (root mean square fluctuation) calculations, and MMGBSA (Molecular Mechanics Generalized Born Surface Area) and MMPBSA (Molecular Mechanics/Poisson-Boltzmann Surface Area) analyses. The simulations were run for a duration of 100 nanoseconds to examine the sustained interactions between the proteins and ligands. Prior to analyzing the ligand-receptor interactions, the trajectory obtained from the simulation was evaluated to ensure structural stability.

4.6. Result and discussion

4.6.1. Molecular docking

The docking studies performed on TOPO I demonstrated that the six compounds exhibited a free binding energy of 9.1 kcal/M, indicating a strong interaction between the compounds and the protein(Fig 4.4). However, it was observed that only a subset of these compounds displayed favorable binding affinities with AChE. The observed inhibition of enzyme activity in our study was primarily attributed to non-covalent interactions established between the ligand and TOPO I or AChE. These interactions included hydrogen bonds, steric interactions, and van der Waals interactions. The strength and specificity of these non-covalent interactions played a crucial role in determining the overall inhibitory effect of the ligand on the enzyme's activity. Through the formation of these interactions, the ligand disrupted the normal functioning of the enzyme, leading to the observed inhibition. Figure 4.6 illustrates the relative bindings of the highest ranked compounds with 1K4T and 4EY6, along with their corresponding reference molecules.

These types of interactions played a significant role in determining the binding affinity and stability of the receptor-drug complex. Hydrophobic interactions occur between nonpolar regions of the receptor and drug, while Van der Waals forces involve attractive forces between atoms or molecules due to fluctuations in their electron

distribution. These interactions contribute to the overall binding strength and specificity between the receptor and drug molecule, ultimately influencing their pharmacological effects. Due to its hydrophobic properties, EGCG was also believed to interact with TOPO I at first, before modifying TOPO I's receptor protein via the active hydrophobic pocket. It was shown that EGCG interacts with Asp 533, Lys 532, and Arg 364 in TOPO I 's active site (Table 4.2), where previously reported Asp 533 and Arg 364 were required for DNA TOPO I to bind topotecan (Table 4.3)[29]. H-bonds formed between the hydroxyl group of EGCG and the TOPO I residues Arg 364, Asp 533, Glu 418, Lys 493, Ala493, Thr501 improved binding capacity, indicating an important role for H-bonds in EGCG binding (Fig.4.5). According to the molecular docking studies discussed above, EGCG impacts amino acid residues and stabilises the TOPO I cleavage complex to effectively reduce TOPO I's activity. The residual phytochemicals similarly engage with comparable affinities, primarily interacting with alternate binding sites within the hydrophobic pocket of TOPO I. For instance, Quercetin demonstrates hydrophobic interactions with Glu 418, Hse 367, and Ser 423, whereas Astragalin predominantly engages in hydrophobic interactions with Arg 434, Asn 408, and Asp 344. The comprehensive depiction of these additional comparative interactions for the top ranked compounds is presented in Figure 4.4. The reference molecule [(-)-galantamine] associated with AChE exhibits a hydrophobic interaction with Arg 13, as well as numerous hydrogen interactions involving Pro 52(A), Leu 178, Gln 181(A), Glu 185, Pro 55(A), Lys 53, Asn 186, Gly 14, Pro 36, Trp 56, Phe 37, and Trp 182. The detailed comparative interactions of AChE with the top ranked compounds are elaborated in Figure 4.6. The interaction of AChE with EGCG shows hydrophobic and hydrogen bonding on Pro36, Trp56, Val60, Tyr98, and 57Ser, 61Asp, 66Gln, Tyr98, respectively which does not have any match with its reference drug (-)-galantamine (approved acetylcholinesterase inhibitor) (Table 4.5). EGCG has been found to not bind to its specific binding residue of AChE (4EY6), indicating that it does not inhibit AChE activity (Fig. 4.6). This suggests that the presence of EGCG results in a decrease in the levels of acetylcholine within the cell. These findings imply that related ligand may be a key ingredient in the creation of anticancer drugs.
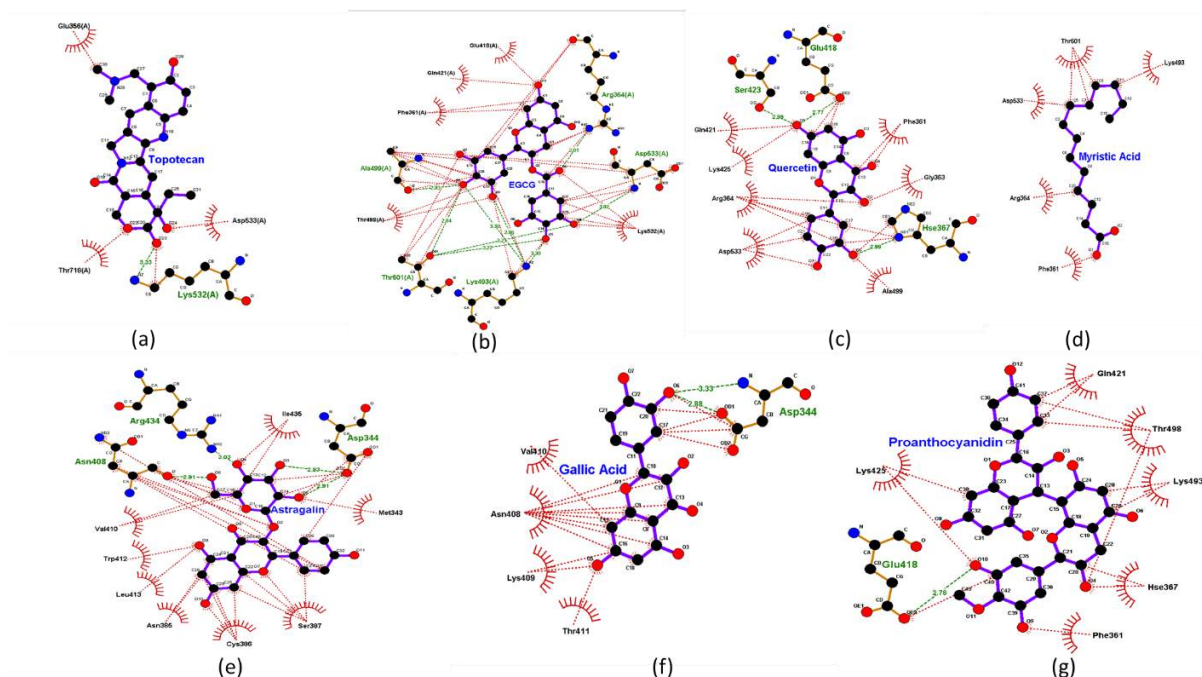
Figure 4. 4 Ligplot representations illustrating the interactions between TOPO I and a) Topotecan, b) EGCG, c) Quercetin, d) Myristic Acid, e) Astragalin, f) Gallic Acid, and g) Proanthocyanidin. Hydrogen bonds are denoted by green lines, while red dotted lines highlight hydrophobic interactions.
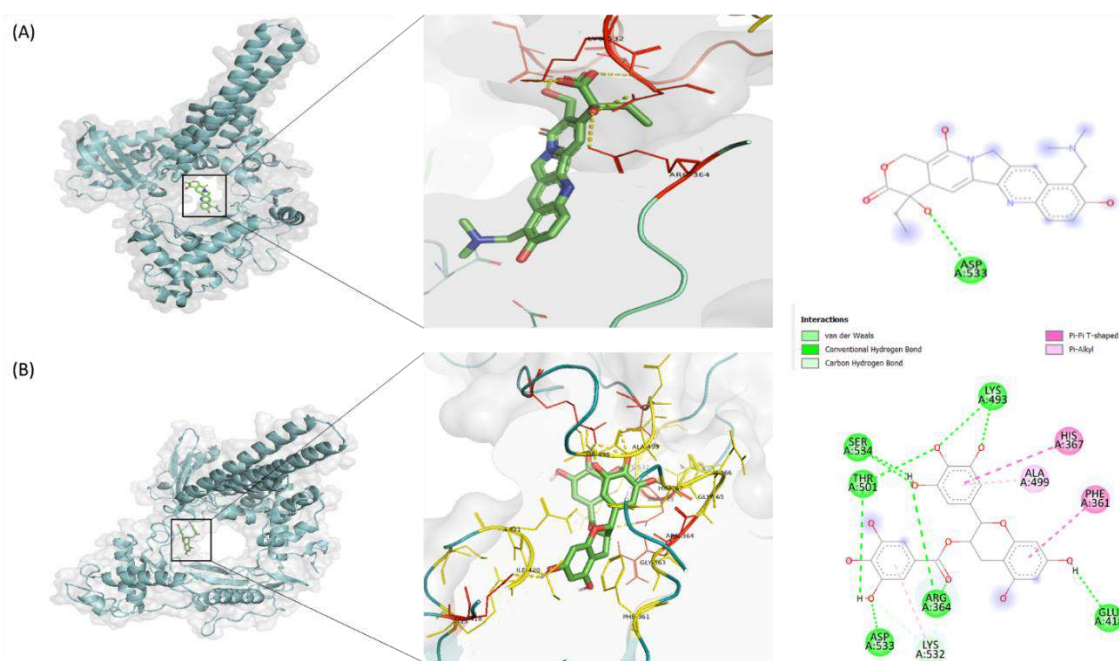
Figure 4. 5. The figure presents an analysis of the docked complex of Topotecan, an structure analog of approved anticancer drug Irinotecan, on the upper side (A), and the DNA TOPO I-EGCG complex on the lower side (B). The middle portion of the figure illustrates the 3D structure, highlighting the interactions between DNA TOPO I with the reference ligand and EGCG. In this representation, polar interactions are denoted by the color red, while non-polar interactions are depicted in yellow color. The 2D structure on the right side showcases the interactions in a

simplified form, where green color represents hydrogen bonds and Van der Waals interactions between amino acid residues, protein atoms, and the ligand.

Table 4.2. This table shows the interaction between TOPO I and EGCG.

Hydrophobic Interactions					
Index	**Residue**	**AA**	**Distance**	**Ligand Atom**	**Protein Atom**
1	364A	ARG	3.99	5816	1712
2	532A	LYS	3.63	5810	3435

Hydrogen Bonds						
Index	**Residue**	**AA**	**Distance H-A**	**Distance D-A**	**Donor Angle**	**Donor Atom**	**Acceptor Atom**
1	364A	ARG	2.81	3.66	146.08	5827 [O3]	1711 [O2]
2	418A	GLU	2.47	2.81	100.06	5831 [O3]	2265 [O.co2]
3	493A	LYS	2.00	2.86	135.53	3074 [N3+]	5829 [O3]
4	499A	ALA	2.34	2.83	110.30	5828 [O3]	3126 [O2]
5	499A	ALA	3.15	3.75	116.23	3123 [Nam]	5829 [O3]
6	501A	THR	2.27	2.84	112.39	3144 [O3]	5828 [O3]
7	501A	THR	2.79	3.21	106.41	5824 [O3]	3144 [O3]
8	533A	ASP	2.07	3.02	145.53	3443 [Nam]	5824 [O3]

π-Stacking						
Index	**Residue**	**AA**	**Distance**	**Angle**	**Offset**	**Stacking Type**	**Ligand Atoms**
1	361A	PHE	5.09	67.76	1.79	T	5802, 5803, 5804, 5805, 5806, 5807

Salt Bridges					
Index	**Residue**	**AA**	**Distance**	**Ligand Group**	**Ligand Atoms**
1	364A	ARG	4.25	Carboxylate	5822, 5823
2	532A	LYS	5.39	Carboxylate	5822, 5823

Table 4.3. A table showing the interaction between Topotecan (control) ligand and TOPO I.

Hydrogen Bonds							
Index	**Residue**	**AA**	**Distance H-A**	**Distance D-A**	**Donor Angle**	**Donor Atom**	**Acceptor Atom**
1	364A	ARG	2.97	3.95	175.00	2299 [Ng+]	5634 [Nar]

Salt Bridges					
Index	**Residue**	**AA**	**Distance**	**Ligand Group**	**Ligand Atoms**
1	532A	LYS	3.88	Carboxylate	5624, 5625
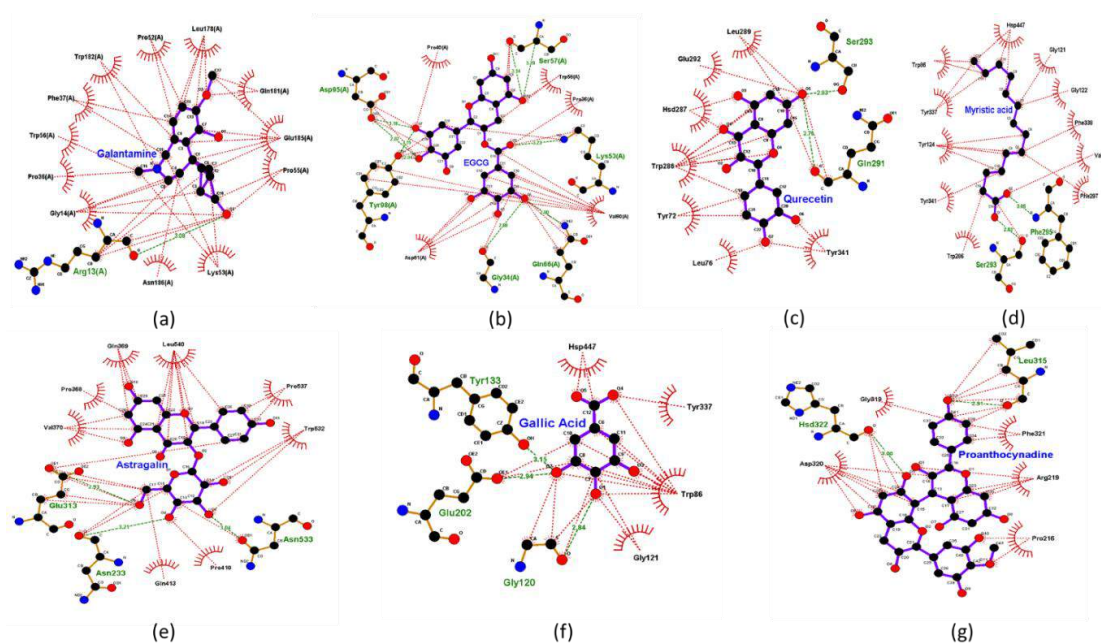
Figure 4. 6 Ligplot representations illustrating the interactions between AChE and a) Galantamine, b) EGCG, c) Quercetin, d) Myristic Acid, e) Astragalin, f) Gallic Acid, and g) Proanthocyanidin. Hydrogen bonds are denoted by green lines, while red dotted lines highlight hydrophobic interactions.
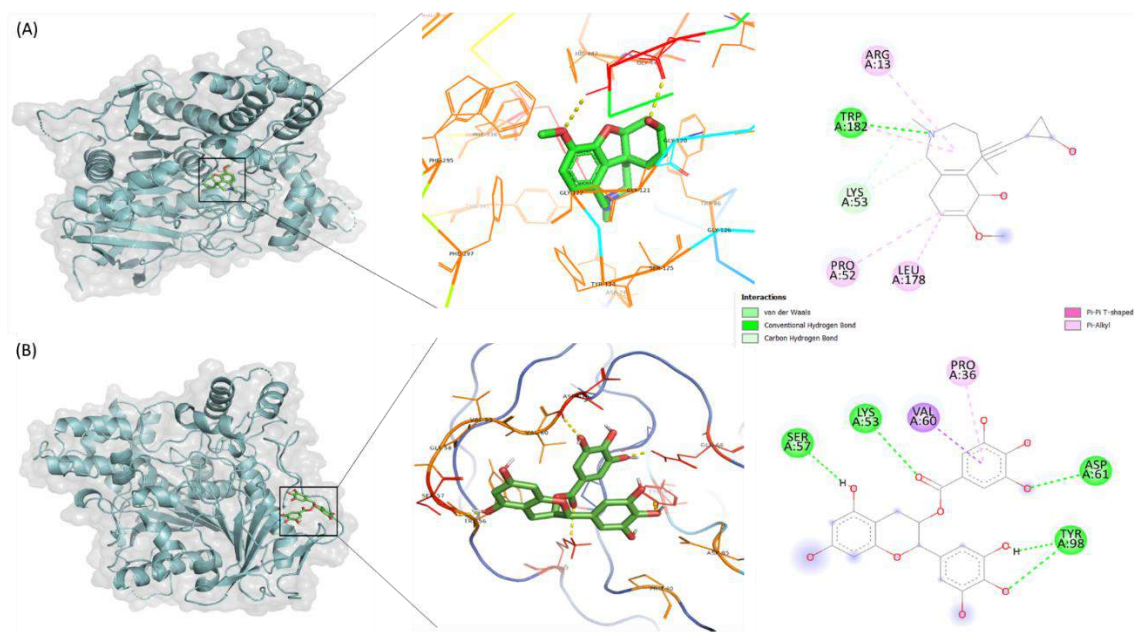
Figure 4.7   A detailed Analysis of the docked complex of (-)-galantamine, an approved acetylcholinesterase inhibitor, on the upper side (A), and the AChE-EGCG complex on the lower side (B). The middle panel displays a 3D structure illustrating the interactions between acetylcholinesterase with the reference ligand and EGCG. Polar interactions are highlighted in red, while non-polar interactions are depicted in orange. The right panel shows a 2D representation, where hydrogen bonds and van der Waals interactions are denoted by green color. The bonds between amino acid residues, protein atoms, and the ligand are visualized in the 2D representation.

Table 4.4. this table describes the different types of interactions between acetylcholinesterase and EGCG.

				Hydrogen interactions			
Index	**Residue**	**AA**	**Distance H-A**	**Distance D-A**	**Donor Angle**	**Donor Atom**	**Acceptor Atom**
1	57A	SER	2.37	3.20	132.94	498 [Nam]	5024 [O3]
2	57A	SER	2.98	3.80	135.65	503 [O3]	5024 [O3]
3	57A	SER	2.87	3.80	161.29	5024 [O3]	503 [O3]
4	61A	ASP	2.36	3.37	157.04	527 [Nam]	5018 [O3]
5	66A	GLN	3.13	3.97	136.05	579 [Nam]	5019 [O3]
6	98A	TYR	2.32	2.94	115.75	898 [O3]	5022 [O3]
7	98A	TYR	2.25	3.15	153.87	5021 [O3]	898 [O3]
				Hydrophobic interactions			
	Residue	**AA**	**Distance**	**Ligand Atom**	**Protein Atom**		
8	36A	PRO	3.93	5008	299		
9	56A	TRP	3.72	4995	486		
10	60A	VAL	3.55	5003	525		

11	60A	VAL	3.87	5008	524
12	98A	TYR	3.99	5008	895
Salt Bridges					
Index	**Residue**	**AA**	**Distance**	**Ligand Group**	**Ligand Atoms**
1	53A	LYS	3.84	Carboxylate	5017, 5016

Table 4.5. In this table, different types of interactions between acetylcholinesterase and (-)-galantamine are presented.

Water Bridges									
Index	**Residue**	**AA**	**Distance A-W**	**Distance D-W**	**Donor Angle**	**Water Angle**	**Donor Atom**	**Acceptor Atom**	**Water Atom**
1	120A	GLY	3.30	2.62	154.92	84.25	936 [Nam]	8469 [O3]	8557
2	122A	GLY	3.12	2.89	156.95	82.89	944 [Nam]	8468 [O3]	8710
3	125A	SER	3.80	2.63	112.90	90.76	976 [O3]	8461 [N3]	8665
4	133A	TYR	2.84	3.30	116.36	80.15	8469 [O3]	1032 [O3]	8557
5	204A	ALA	3.04	3.08	169.54	73.55	1562[Nam]	8469 [O3]	8710
Hydrogen interactions									
Index	**Residue**	**AA**	**Distance H-A**	**Distance D-A**	**Donor Angle**	**Donor Atom**	**Acceptor Atom**		
1	203A	SER	2.89	3.83	163.70	1561 [O3]	8456 [O3]		
2	337A	TYR	2.19	2.86	128.04	2544 [O3]	8461 [N3]		
Hydrophobic Interactions									
Index	**Residue**	**AA**	**Distance**	**Ligand Atom**	**Protein Atom**				
1	86A	TRP	3.86	8463	649				
2	86A	TRP	3.60	8451	654				
3	86A	TRP	3.79	8453	657				
4	124A	TYR	3.80	8459	968				
5	297A	PHE	3.65	8458	2229				
6	337A	TYR	3.97	8463	2542				

| 7 | 338A | PHE | 3.87 | 8458 | 2554 | |

4.6.2. ADME analysis

Drug molecules need to have a balance between hydrophilicity and lipophilicity in their physicochemical qualities in order to pass through the cell membrane and connect with the target receptor. The cell membrane is hydrophilic because of the protein and water in the cytoplasm, while lipophilic because of the phospholipid content. Two variables—Log P and Topological Polar Surface Area (TPSA)—are used to assess a compound's lipophilicity. The majority of the substances utilised in this investigation were found to be lipophilic substances, with log P = 5 and TPSA = 140. Proanthocyanidin, astragalin, and quercetin are three substances with low log P values and TPSA values above 140, which suggest that they will have a hard time passing through lipophilic cell membranes and have a low bioavailability (Figs. 4.8 and 4.9). The acceptable ranges of all ADME parameters are summarized in table 4.6. There was no violation of Veber rule for ECGC and Myristic acid in the selected hits. However, gallic acid, and quercetin violated one parameter in the selected hits. The selected hits appear to have drug-like properties based on these results. Out of the initial 6 compounds, 3 molecules were identified to adhere to Lipinski's rule of five, exhibiting characteristics such as non-mutagenicity, non-irritation, non-tumorigenicity, and no adverse effects on reproductive health (Table 4.6). The five parameters that make up Lipinski's rule of five are molecular weight (MW), cLogP (partition coefficient between n-octanol and water), the number of hydrogen bond donors (HBD), and the number of hydrogen bond acceptors (HBA). A compound is considered orally bioactive if it satisfies these criteria.
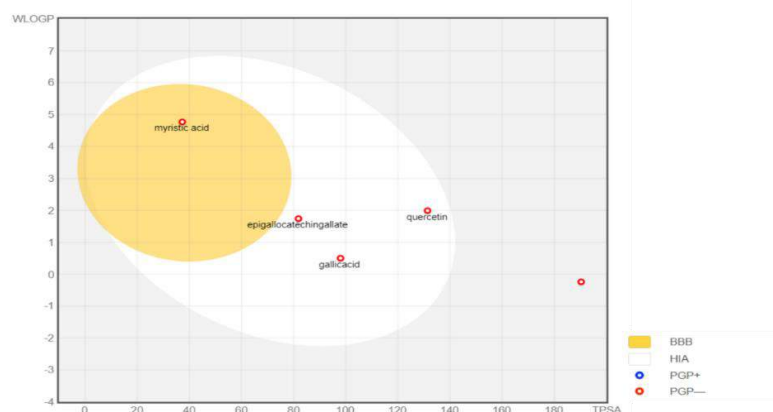
Figure 4. 8. Boiled egg diagram showing the pharmacokinetic behavior and bioavailability of 6 herbal phytochemicals. The diagram was created using Swiss ADME and represents gastrointestinal absorption and brain access capability. The size of the yolk indicates brain access capability, while the size of the white indicates gastrointestinal absorption.

Table 4.6. Using computational parameters of drug likeness (swiss ADME analysis) to assess the compliance of compounds. (BBB- Blood Brain Barrier, PAINS-Pan Assay interference compounds, TPSA- Topological Polar Surface Area).

Parameters	Epigallocatec hingallate	Gallic acid	Quercetin	Myristic acid	Proanthocy anidin	Astragalin
BBB	No	No	No	Yes	No	No
Human intestinal absorption	High	High	High	High	Low	Low
Log P	2.05	0.21	1.23	4.45	1.85	-0.25
TPSA(Å)	81.86	97.99	131.36	37.30	209.76	190.28
Molecular weight	320.38 g/mol	170.12	302.24	228.37	592.55	448.38
Class	Soluble	Moderately soluble	soluble	Moderately soluble	Poorly soluble	Moderately soluble
Log Kp(skin permeation)	-6.57 cm/s	-6.84	-7.05	-3.35	-8.00	-8.52
Lipinski	Yes	Yes	Yes	Yes	No	No
Ghose	Yes	No	Yes	Yes	No	Yes
Veber	Yes	Yes	Yes	No	No	No
PAINS	0 alert	1 alert	1 alert	0 alert	0 alert	0 alert
Bioavailability score	0.55	0.56	0.55	0.85	5.45	5.29
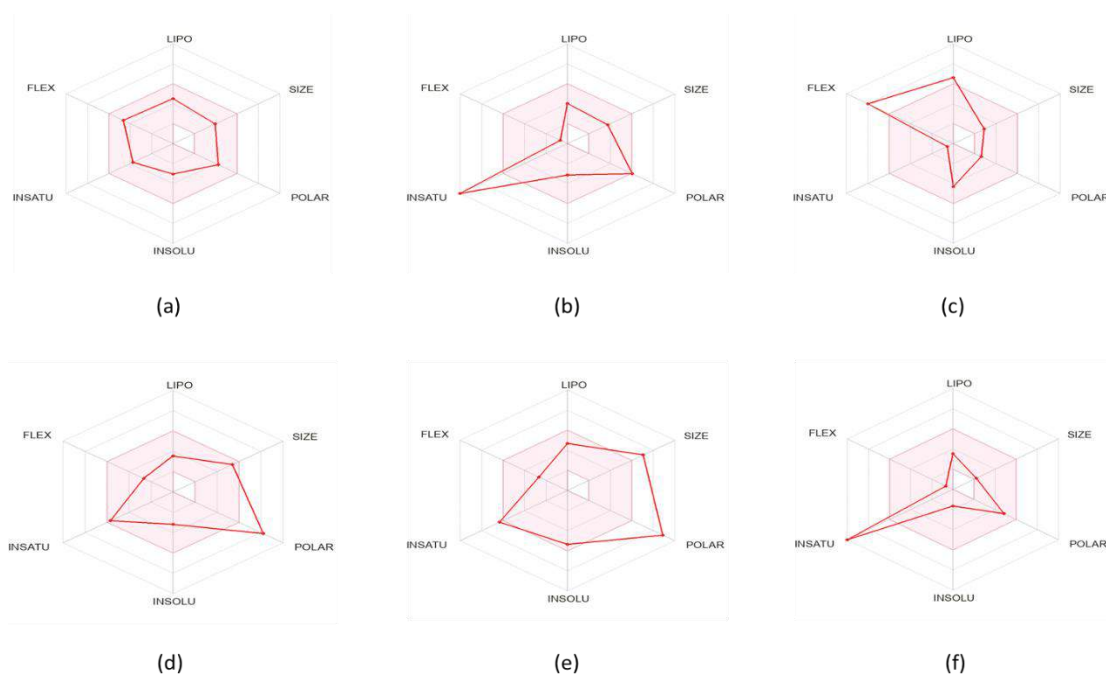
Figure 4. 9. A bioavailability radar was developed based on the physicochemical properties of an isolated compound from Phyllanthus emblica to evaluate its potential for oral bioavailability. The radar serves as a tool to assess the likelihood of the compound being absorbed and utilized by the body through oral ingestion. The radar takes into account various chemical characteristics of the compound, including solubility, molecular weight, stability, and permeability, to provide insight into its suitability for oral administration.

4.6.3. MD simulation

To assess the stability of the six docked complexes, we performed molecular dynamics simulations. The outcomes of these simulations revealed that EGCG forms a robust binding with the active site of TOPO I. This binding is characterized by the establishment of multiple hydrogen bonds with crucial amino acid residues, consequently enhancing the stability of the protein-ligand complex. Moreover, the analysis of binding energies indicates that the interaction between EGCG and TOPO I was notably favorable when compared to other top-ranked compounds. A comprehensive compilation of comparative energies can be found in the Table 4.7. Throughout the simulation, the EGCG-topoisomerase complex demonstrated remarkable stability, exhibiting notably fewer conformational alterations when

contrasted with the dynamic simulations of other molecules(fig.4.10). In the first 10 ns, the ligand (EGCG) demonstrated remarkable stability, with RMSD values remaining steady between 0.4-0.6Å until a slight fluctuation occurred at around 25 ns. EGCG is a substantial molecule with flexible sections and is similar in size to the control molecule (topotecan) simulation for EGCG. The LINCS algorithm ensured that the lengths of all bonds remained consistent. Every ten steps, the neighbour list was updated. The ligand engaged in significant interactions with several residues, such as Arg364, via H-bond interactions and with Lys532 via hydrophobhic interactions till the last step of simulation. Additionally, stacking interactions were observed between EGCG and Trp203. Previous research has shown that TOPO I interacts with several crucial residues, such as Asp364, Lys 532[30]. In each frame, we measured the displacement and average distance between atoms as compared to the original structure by using root mean square deviation (RMSD) and root mean square fluctuation (RMSF), and observed the primary structural changes in proteins and ligands (Fig. 4.11). The RMSD and RMSF graphs displayed in figure 4.10 illustrate the RMSD for the ligands and protein receptors. Figure 4.11 displays the analogous binding interactions of the selected ligands with the TOPO I complex, elucidating their consistency across diverse stages of molecular dynamic simulation. As for AChE, it was observed that AChE's docked structure remained stable throughout simulation, but its inhibitory pocket was not occupied by its ligand based on our docking results. As a result, the ligand does not undergo any conformational changes during the simulation since it binds to enzyme at a separate site from its inhibitory site throughout the 100 ns molecular dynamic simulation. Figure 4.12 illustrates the comparative bindings of various ligands with AChE at distinct stages of molecular dynamic simulation. At the conclusion of the MD simulation, the results indicated that both the AChE control [(-)-galantamine] and the AChE-EGCG complex remained stable at their respective sites, as determined by the molecular docking studies conducted earlier. Interestingly, our natural compound (EGCG) was observed to occupy a distinct site on the AChE molecule, which differed from the known inhibitory sites targeted by approved AChE inhibitors [(-)-galantamine]. This suggests that EGCG may exert its effects on AChE through a different mechanism or site of action compared to the approved inhibitors.

Analysis of the simulation results also suggests that EGCG may inhibit the activity of topoisomerase by blocking access to the DNA substrate. Topotecan interacted mainly with Arg364 and Lys532 during most of the simulation run. Arg364 and Lys532 were also the interacting sites for EGCG and TOPO I complex. Molecular docking and Molecular dynamic simulations demonstrated that EGCG interacted with the residues Arg364 and Lys532, forming a sustained H-bond with Arg364 and Lys532. These results offer fresh insights into the molecular mechanism of inhibition while being compatible with earlier research on the interaction between EGCG and TOPO I.
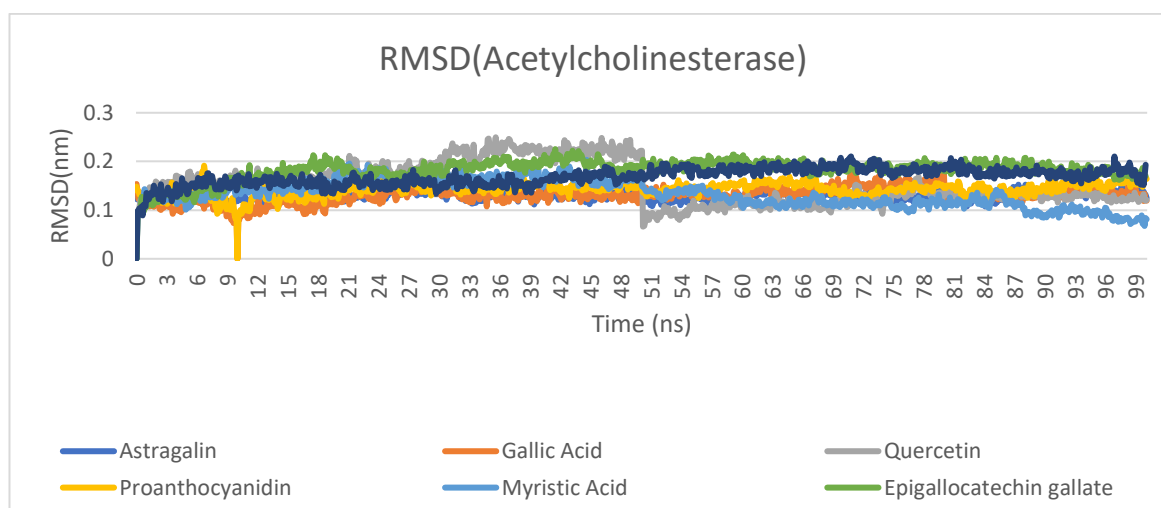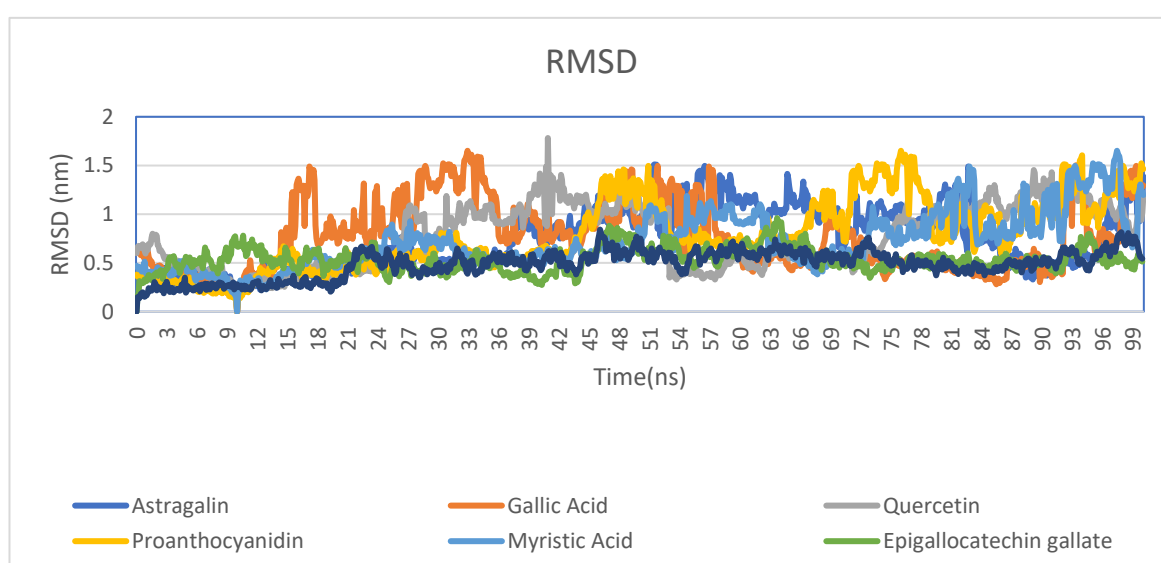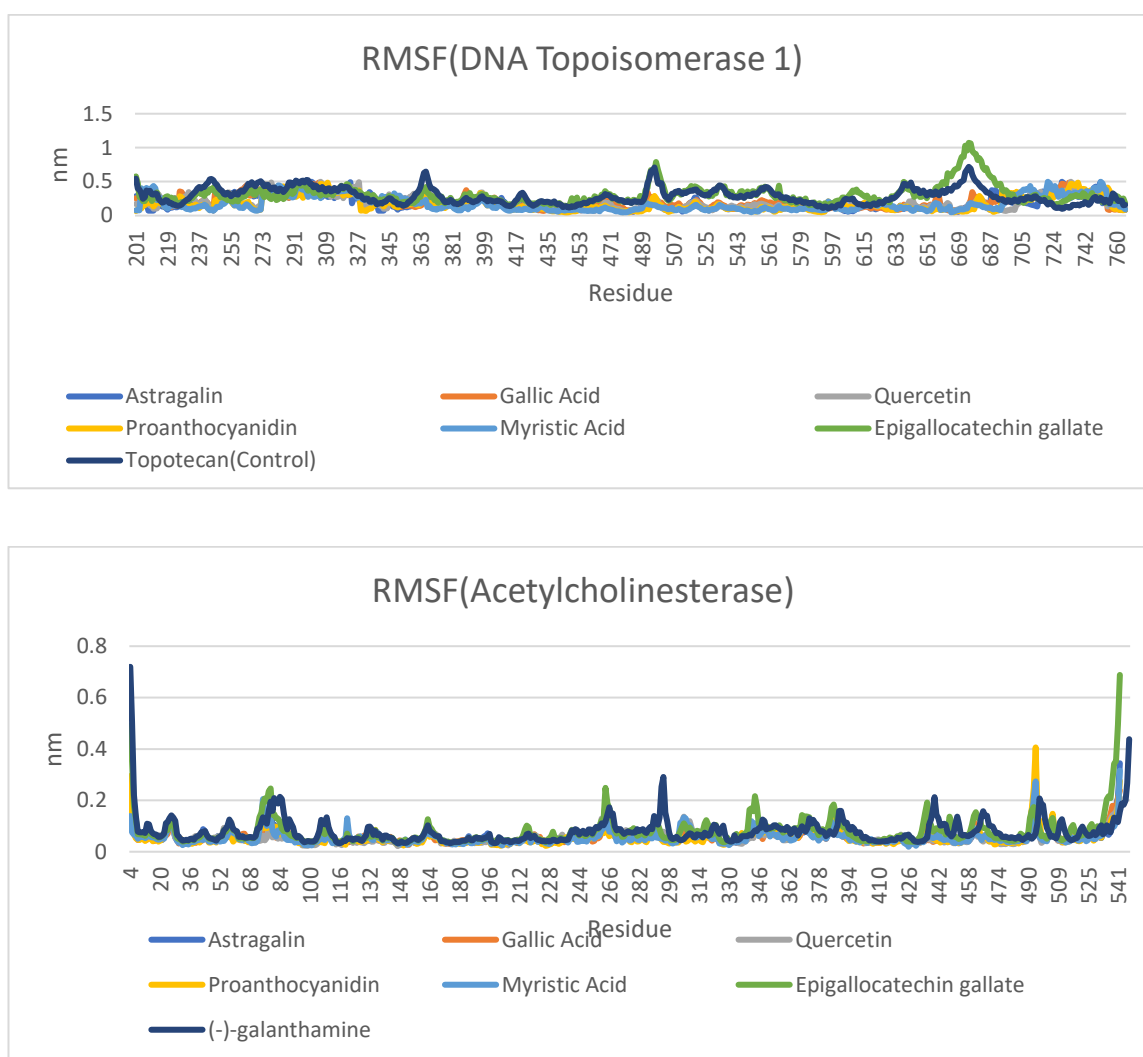
Figure 4.10 Plotting the root mean square deviation (RMSD) and root mean square fluctuation (RMSF) for the 1K4T complex and the 4EY6 complex, respectively. Based on the protein-ligand docked complexes (blue for 1k4t and green for 4ey6), RMSD values are extracted from protein fit ligand (orange for 1k4t and red for 4ey6). In a 100-ns MD simulation, the RMSF graph was plotted for each complex along with the protein.

DNA Topo 1 (complex)	0 ns	50 ns	100 ns
Topotecan			
Epigallocatechin gallate			
Proanthocyanidin			
Myristic acid			
Astragalin			
Quercetin			
Gallic Acid			
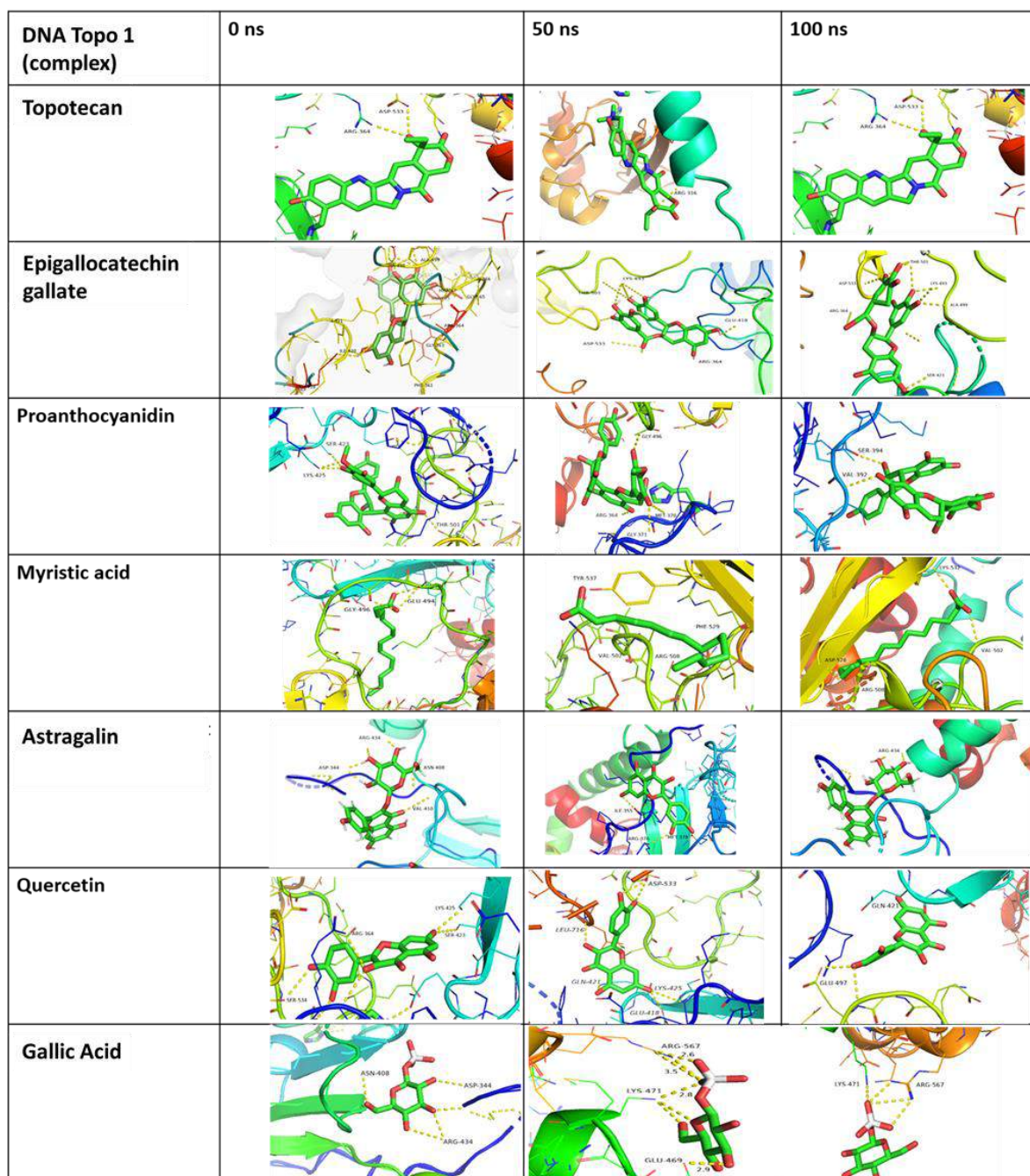
Figure 4. 11. Variations in residue interactions and their spatial relationships around TOPO I complexes are examined across distinct time frames during molecular simulations.

Acetylcholinesterase (complex)	0 ns	50 ns	100 ns
Galantamine(control)			
Epigallocatechingallate			
Proanthocyanidin			
Myristic acid			
Gallic acid			
Quercetin			
Astragalin			
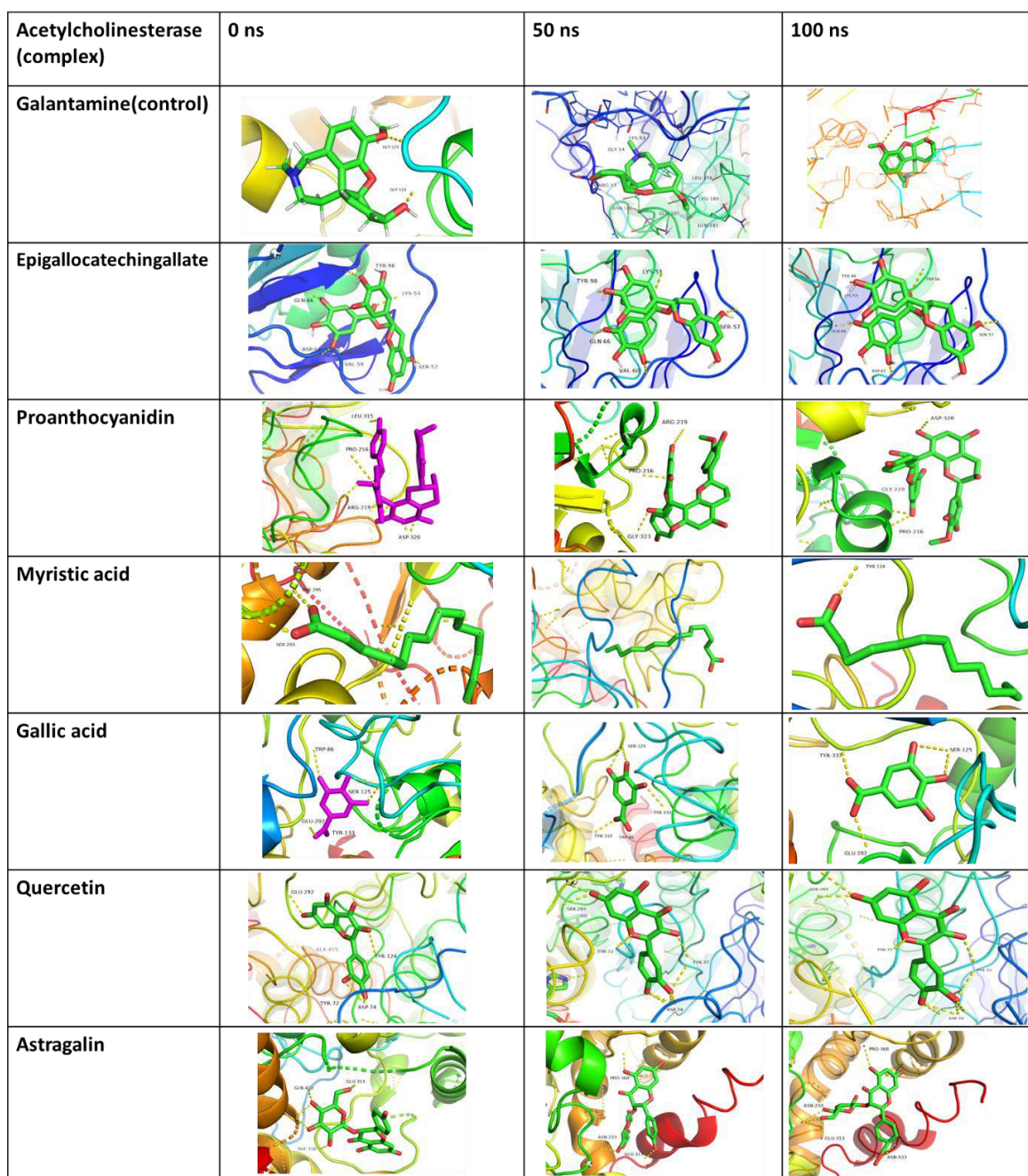
Figure 4. 12. Variations in residue interactions and their spatial relationships around AChE complexes are examined across distinct time frames during molecular simulations.

Table 4.7. This table compares the binding energy components calculated using two commonly used computational methods, AMBER MM-PBSA and MMGBSA. The table shows the values of four different energy components: van der Waals , polar solvation, nonpolar solvation, and total binding free energy, obtained from each method for a given protein-ligand complex(1K4T- TOPO I and 4EY6 - Acetylcholinesterase).

Energy component (average)	MM/GBSA (Delta complex-receptor-ligand)		MM/PBSA (Delta complex-receptor-ligand)	
1K4T	**control**	**EGCG**	**Control**	**EGCG**
ΔVan der waal	-27.35 kcal/mol	-31.01 kcal/mol	-27.35 kcal/mol	**-31.01 kcal/mol**
ΔGGAS	-48.26 kcal/mol	-74.35 kcal/mol	-48.26 kcal/mol	**-74.35 kcal/mol**
ΔGSOLV	32.34 kcal/mol	-49.53 kcal/mol	52.49 kcal/mol	**74.35 kcal/mol**
ΔG$_{binding}$ energy	-15.92 kcal/mol	-24.82 kcal/mol	4.23 kcal/mol	**0.56 kcal/mol**
Energy component (average)	MM/GBSA (Delta complex-receptor-ligand)		MM/PBSA (Delta complex-receptor-ligand)	
4EY6	**control**	**EGCG**	**Control**	**EGCG**
ΔVan der waal	-33.83 kcal/mol	-18.11 kcal/mol	-33.83 kcal/mol	**-18.11 kcal/mol**
ΔGGAS	-67.97 kcal/mol	-49.63 kcal/mol	-67.97 kcal/mol	**-49.63 kcal/mol**
ΔGSOLV	47.84 kcal/mol	-31.08 kcal/mol	70.56 kcal/mol	**43.61 kcal/mol**
ΔG$_{binding}$ energy	**-20.13 kcal/mol**	**-18.55 kcal/mol**	**2.59 kcal/mol**	**-6.02 kcal/mol**

To substantiate the binding energies of the protein-ligand complexes, we additionally conducted MMGBSA and MMPBSA analyses. Table 4.7 within the study presents the energy constituents and corresponding numerical values for both topotecan and EGCG, acquired through the employment of MM/GBSA and MM/PBSA methodologies. The results of the calculations indicate that EGCG has a binding free energy of -24.82 kcal/mol according to MM/GBSA and 0.56 kcal/mol according to MM/PBSA. These noteworthy findings suggest that EGCG could potentially function as a Top1 inhibitor by binding to interaction sites, ultimately leading to the inhibition of tumor growth and replication process. On the other hand, the results also exhibits the energetic constituents and quantitative estimates for (-)-galantamine and EGCG for AChE, acquired via MM/GBSA and MM/PBSA methodologies. The outcomes of the computations indicate that EGCG has a binding free energy of -18.55 kcal/mol (MM/GBSA) and -06.02 kcal/mol (MM/PBSA). As compare to its control results, these consequential findings propose that EGCG do not have enough potential to function as an AChE inhibitor by binding at different interaction sites, thereby do no obstract the function of AChE.

4.7. Comparative analysis of EGCG with other approved topoisomerase inhibitors:

A comparative study on the toxicity and drug-likeness properties of EGCG was conducted with other approved topoisomerase inhibitors. These were camptothecin, irinotecan, topotecan, epirubicin, etoposide, teniposide, amsacrine, and anthracyclines. This comparison would therefore enable the evaluation of the potential of EGCG as a topoisomerase inhibitor with desirable pharmacological properties.

Drug-Likeness Property: Drug-likeness is the qualitative approximate "drug-like" nature of a compound, considering such parameters as bioavailability, solubility, and chemical stability. These properties have been considered very important for the efficacy and safety of a pharmaceutical compound. On this note, EGCG showed quite promising drug-likeness. In this regard, it resulted in very good Lipinski's Rule of Five parameters, often considered an index for drug-likeness. These parameters include molecular weight, hydrogen bond donors, hydrogen bond acceptors, and partition coefficient log P. Compliance of EGCG with these criteria indicates that it holds all the desirable pharmacokinetic properties, and thus its potential as a very effective therapeutic agent is raised(Fig.4.13) & (Table 4.8).

Comparison of Toxicity: The toxicity assessment for the plausible therapeutic compounds is an exercise that cannot be evaded if safe clinical applications must be ensured. We compared the toxicity profile of EGCG with other topoisomerase inhibitors using in silico prediction. Our results indicated that EGCG has lower values of toxicity compared to camptothecin, irinotecan, topotecan(Fig.4.14).
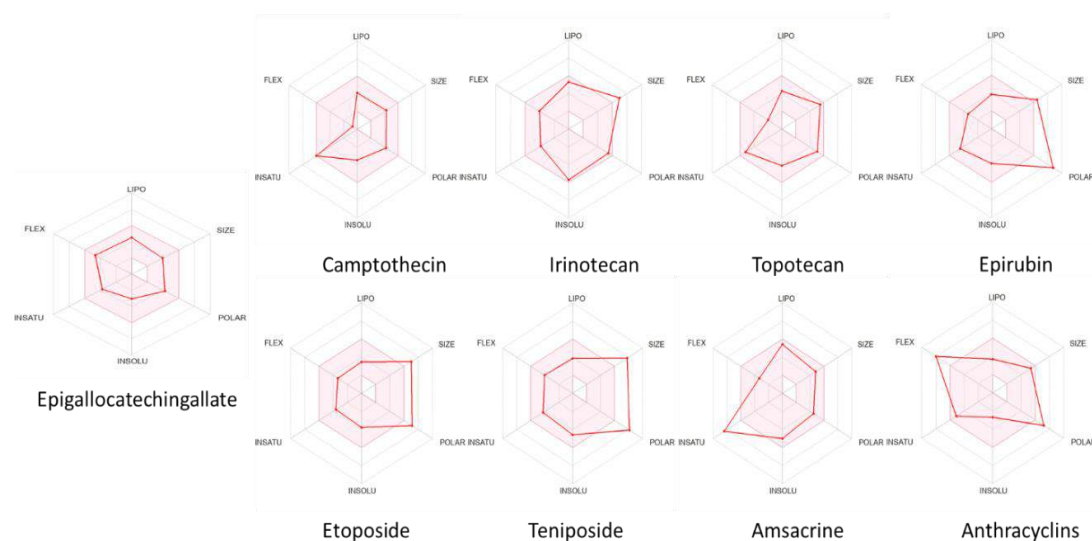
Figure 4. 13. bioavailability radar was created using the physicochemical attributes of approved inhibitory drugs for Top I and EGCG. Its purpose is to gauge the compound's viability for oral bioavailability. This radar functions as a tool for estimating the compound's potential absorption and utilization within the body through oral ingestion. The radar incorporates a range of chemical properties such as solubility, molecular weight, stability, and permeability to offer an assessment of the compound's appropriateness for oral administration.

Table 4.8. A comparative of drug likeness prediction of EGCG and approved Top 1 and Top 2 inhibitors. These parameters encompass factors such as BBB (Blood Brain Barrier) permeability, the potential for PAINS (Pan Assay Interference Compounds), and TPSA (Topological Polar Surface Area).

	Topoisomerase 1 inhibitor				Topoisomerase II Inhibitor				
Parameters	EGCG	Camptothecin	Irinotecan	Topotecan	Etoposide	Teniposide	Amsacrine	Anthracyclins	Epirubin
BBB	No	No	No	No	No	No	No	No	No
Human intestinal absorption	High	High	High	Low	Low	Low	High	Low	Low
Log P	2.05	2.49	3.73	1.67	1.15	1.98	3.47	0.69	0.44
TPSA(Å)	81.86	81.42	114.20	104.89	160.83	189.07	88.70	163.18	206.07
Molecular weight	320.38 g/mol	348.35	586.68	457.97	588.56	656.65	393.46	444.48	543.52
Class	Soluble	Soluble	Moderately soluble	Moderately soluble	Soluble	Moderately soluble	Poorly soluble	Moderately soluble	Soluble
Log Kp(skin permeation)	-6.57 cm/s	-7.19	-7.22	-7.66	-9.46	-9.43	-5.85	-8.30	-8.71
Lipinski	Yes	Yes	Yes	Yes	No	No	Yes	Yes	No
Ghose	Yes	Yes	No	Yes	No	No	Yes	No	No
Veber	Yes	Yes	Yes	Yes	No	No	Yes	No	No
PAINS	0 alert	0 alert	0 alert	1 alert	0 alert	0 alert	1 alert	2 alert	1 alert
Bioavailability score	0.55	0.55	0.55	0.55	0.17	0.17	0.55	0.55	0.17
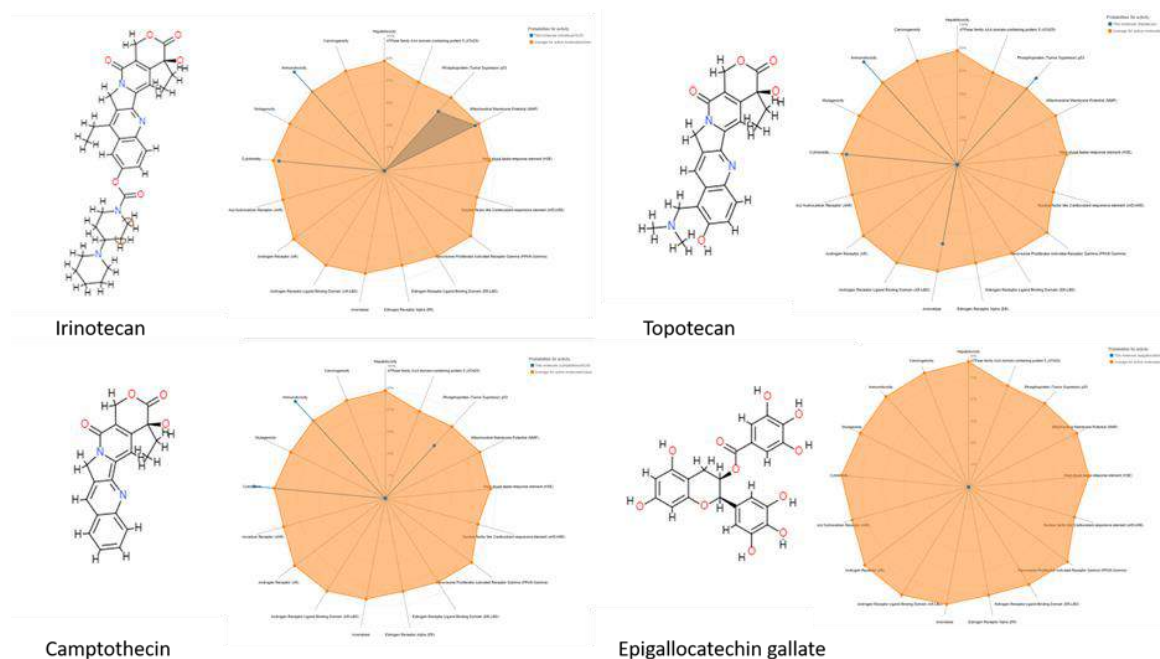
Figure 4. 14. Comparative assessment of the toxicity profiles between the approved Top1 inhibitor and EGCG.

4.8. Discussion

The current landscape of tumor treatment encompasses surgical resection and chemotherapy administration, with several FDA-approved medications such as Irinotecan hydrochloride liposome, Topotecan hydrochloride, Erlotinib, Mitomycin, and Olaparib targeting various signaling pathways and DNA synthesis processes. These chemotherapeutic agents have effectively slowed cancer progression by disrupting key cellular processes within rapidly dividing cells. Among these, Irinotecan and Topotecan have demonstrated a focused approach by targeting TOPO 1, a crucial enzyme involved in DNA replication and transcription. By impeding the repair of single-strand DNA breaks generated by this enzyme, these drugs accumulate DNA strand breaks in tumor cells, thereby hindering their ability to replicate and transcribe. This selective action offers a promising strategy for curbing malignant growth while minimizing damage to healthy cells.

However, the use of these chemotherapeutic agents is not devoid of adverse effects, ranging from gastrointestinal disturbances to severe cholinergic syndrome. Notably, the cholinergic syndrome associated with Irinotecan has been linked to its potential to

inhibit acetylcholinesterase (AChE), resulting in the accumulation of acetylcholine. To address these undesirable effects, research has shifted towards exploring natural compounds that mimic the functionalities of approved medications while mitigating their negative consequences. The congruity between the inhibitory mechanisms of topotecan and phytochemical compounds arises from their shared ability to replicate critical interactions involving Arg364 and Asp533 amino acids. This emulation facilitates a parallel inhibitory effect similar to Camptothecin (CPT), disrupting the enzyme-DNA complex. Through molecular docking and dynamics simulations, our study suggests that the novel inhibitor can access the enzyme-DNA interface and position itself akin to the established Topotecan inhibitor. This augments the potential for inhibiting DNA replication and transcription, which is crucial for cancer proliferation. Significantly, their interaction with acetylcholinesterase does not hinder the enzyme's function in non-dividing cells, suggesting a more targeted approach to intervention. The present study employs a comprehensive methodology involving virtual screening, molecular docking, and dynamics simulations to elucidate the structural insights into the binding mechanisms of bioactive compounds derived from Phyllanthus emblica (P. emblica). These compounds have demonstrated interactions with molecular targets crucial to cancer pathogenesis, hinting at their potential in advancing cancer treatment. Notably, Epigallocatechin gallate (EGCG) stands out among these compounds due to its minimal side effects compared to standard treatments like Irinotecan. The study's findings highlight EGCG's superior binding energy to TOPO I protein, which was -9.1 kcal compared to topotecan (-8.2 kcal), an FDA-approved drug. Additionally, our study shows a weak binding affinity of EGCG to acetylcholinesterase (-4.4 kcal), suggesting a reduced likelihood of inducing associated side effects.

A notable finding is the consistent interaction of EGCG with the active site of topoisomerase 1, as evidenced by molecular docking and dynamics simulations. Simultaneously, its limited interaction with acetylcholinesterase further supports its potential as a therapeutic agent. This evidence collectively underscores EGCG's promise to address not only cancer but also other ailments associated with chemotherapy.

In conclusion, the research findings shed light on the potential of naturally occurring compounds, particularly EGCG from P. emblica, as viable candidates for cancer treatment. These compounds offer a dual advantage of effective cancer intervention and reduced side effects through their ability to interact selectively with TOPO I and limited interaction with acetylcholinesterase. Further studies and clinical trials are warranted to validate and translate these findings into clinical practice, potentially revolutionizing the landscape of cancer therapy and advancing toward more targeted and safer treatment options.
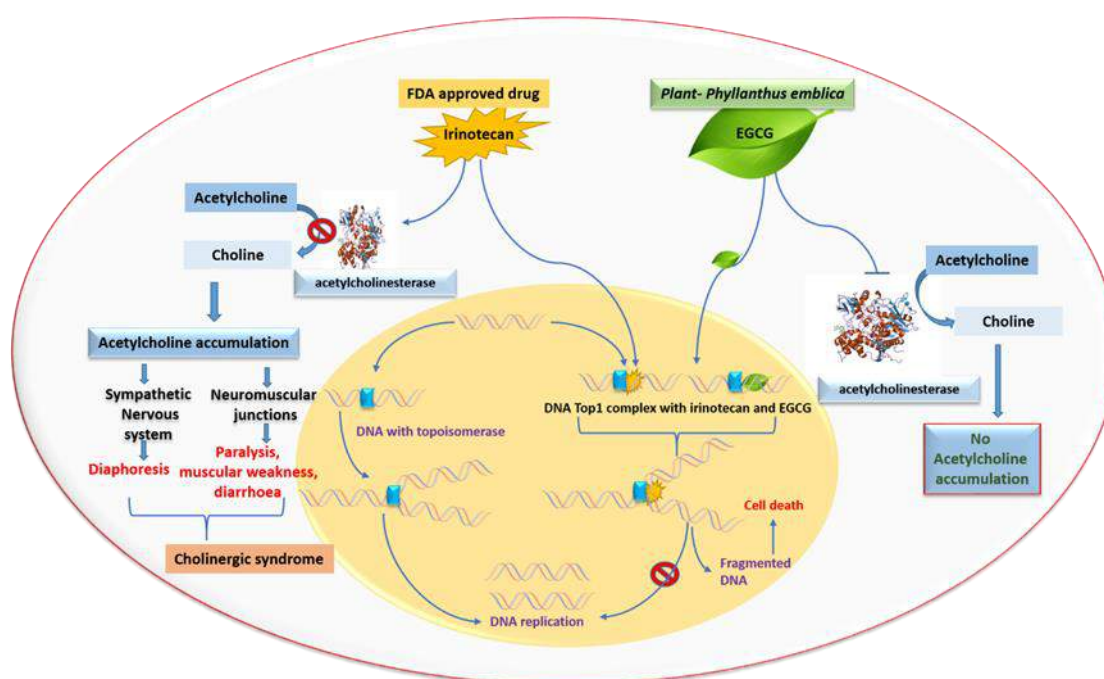
Figure 4. 15. Topoisomerase I inhibitors' cellular effects on both proliferating and non-dividing cells. To reduce torsional stress, topoisomerase I attaches to double-stranded DNA and causes single-strand breaks. A topoisomerase I inhibitor called irinotecan stops the enzyme from mending these fractures. DNA double-strand breaks and the consequent induction of apoptosis can result from the complex made up of DNA, topoisomerase I, and irinotecan colliding with replication forks in rapidly growing cells. AChE, an enzyme involved in the neuromuscular junction, catalyses the conversion of acetylcholine (ACh) substrate to choline. This inhibition of AChE by Irinotecan can lead to an accumulation of ACh, resulting in a condition known as cholinergic syndrome. Cholinergic syndrome is characterized by a range of symptoms, diaphoresis, including abdominal cramping, diarrhoea, and excessive salivation, sweating, and flushing of the skin. On the other hand Epigallocatechin gallate (EGCG), derived from Phyllanthus emblica, exhibits minimal binding affinity towards acetylcholinesterase. Consequently, it is unlikely to effectively inhibit the enzyme and is thereby associated with a low probability of causing any side effects typically attributed to AChE inhibition.

4.9.Conclusion

In the landscape of global health concerns, cancer stands as the second leading cause of mortality worldwide, following cardiovascular disease. Given the drawbacks of conventional therapies, including drug resistance and adverse effects, mounting evidence suggests that plant-derived remedies hold significant potential for effective cancer treatment.

Our study has addressed a significant complication associated with chemotherapy. Our findings underscore the latent capacity of natural compounds to selectively inhibit human TOPO I, impeding the progression of tumors. Our molecular dynamics study sheds light on the interaction between EGCG and TOPO I. It gives evidence for the valuable potential of the natural compound in inhibiting the replication process in cells. To deepen our understanding, it is imperative to delve into the intricacies of the EGCG-TOPO I interaction and to probe the broader potential of other natural substances in cancer treatment. These natural agents hold the promise of equaling or surpassing FDA-approved drugs while evading interactions with AChE that trigger the cholinergic syndrome. However, it is important to note that natural compounds can also exhibit concentration-dependent toxicity to healthy cells.

In our study, we have therefore evaluated the potential risk of side effects for natural compounds with efficient anticancer properties by evaluating their direct binding capabilities with receptors associated with side effects of irinotecan cancer therapy. Clinical application of these natural compounds was limited by several challenges in solubility, stability, bioavailability, and targeted delivery. In this context, nanoparticle-mediated drug delivery systems have been an up-and-coming solution for these problems, more especially in improving the therapeutic efficacy of natural compounds against cancer.

Adding nanoparticles in drug delivery systems improves the potential of using natural compounds in cancer treatment. These agents can be made more potent and degradable by nanoparticles, effectively delivering them only to cancer cells, thereby reducing the harm caused to healthy tissues due to their toxicity. Specifically, the drug delivery method increases plant extracts' effectiveness and lowers their side effects, meaning better outcomes for patients generally.

CHAPTER:V

Objective 3:

- ➢ **Synthesis and characterization of nanoparticles for drug loading, Response study for drug toxicity and drug delivery.**

CHAPTER V : OBJECTIVE 3

5.1. Rationale of study

Although several natural compounds have advantages for cancer therapy, the frequent limitations are poor solubility and poor bioavailability[299]. Nanoparticle-mediated delivery of drugs resolved such problems by increasing stability and solubility of natural compounds, hence improving the therapeutic effects[300]. Here are several reason to choose nanoparticle mediated drug delivery system to enhance the therapeutic efficacy of natural compounds in cancer treatment:

- Nanoparticles further make it possible to bypass putative cellular mechanisms of resistance in cancer cells, hence a possible solution to drug resistance. The EPR effect, coupled with an increased permeability and retention, allows for nanoparticle accumulation in tumor tissues, increasing treatment efficacy[301].

- Some of the benefits which can be attained by utilizing NPs as vehicles for drug delivery include: i) Overcoming the problems associated with the low solubility and bioavailability of the drug[302], ii) Increasing permeability of the drug across cancer cell and controlling its release, iii) NPs are non-toxic, biodegradable, highly fluorescent particles of small size, 1–100 nm, on which the cancer drug is effortlessly loaded[303].

- Nanoparticles could be engineered for targeted delivery into certain types of cancerous cells to reduce any possible impacts on normal tissues and thus minimize adverse side effects[304]. They provide controlled release of the drug, hence sustained therapeutic levels at the site of the tumor.

- Nanoparticles protect natural compounds from degradation and can carry multiple therapeutic agents to allow for combination therapy. It is the versatility and the customizability of nanoparticles that allow them to be optimized according to certain compounds and targets, which blend with the trends of personalized medicine and promise great potential for clinical translation into effective therapies against cancer[305, 306].

Calcium carbonate ($CaCO_3$) is highly valued in biomedical applications due to its abundance, cost-effectiveness, safety profile, biocompatibility, pH responsiveness, and gradual biodegradability[307]**.** CCNPs are especially potential candidate for cancer therapy because they have the potential to induce the death of tumor cells, increase intracellular $Ca2+$ levels, and even cause mitochondrial damage(Fig. 5.1)[308]. They are normally engineered in a way that makes dissolution, entrapment, or covalent adsorption attach them to drugs, thereby releasing the drugs onto the cancer tissues with remarkable precision and minimizing exposure on healthy cellular levels[309]. The specific properties of CCNPs include very high loading capacity and biocompatibility, thereby making them very excellent choices for drug delivery systems[310].

Within these nanoparticles, drugs can be dissolved, entrapped, adsorbed, or covalently attached. The size of colloidal particles is a critical determinant of their drug delivery effectiveness. Particles larger than 1 μm cannot passively diffuse through epithelial membranes and typically remain localized at the site of administration.

They've been also utilized for biosensing, and encapsulating proteins in pharmaceuticals[311]. Despite their extensive use, there have been no significant reports of hazardous properties associated with $CaCO_3$ nanoparticles.
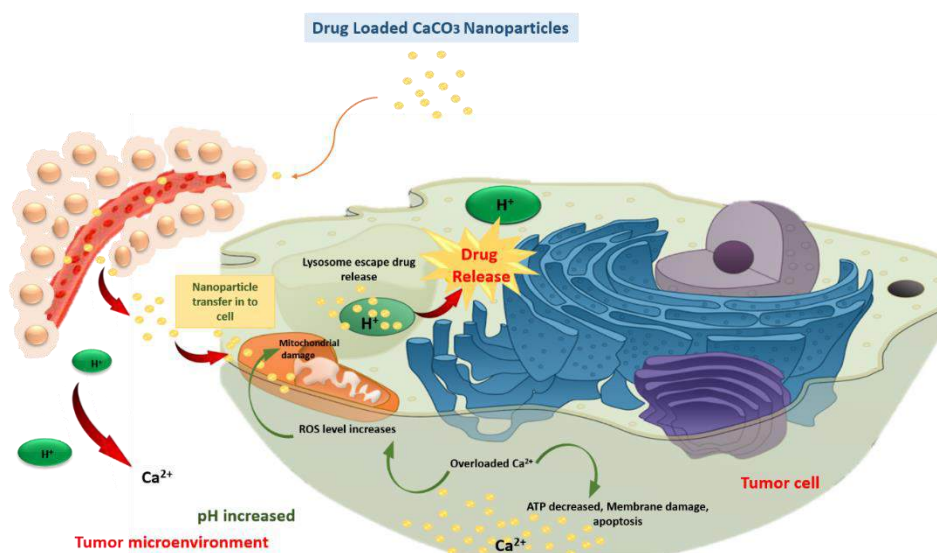
Figure 5. 1 Schematic representation of drug-loaded calcium carbonate nanoparticles within cells, illustrating their role in various mechanisms of cell apoptosis. The nanoparticles facilitate targeted drug delivery and induce mitochondrial damage by increasing ROS levels, leading to cell apoptosis.

$CaCO_3$ can exist in three crystalline forms: calcite, aragonite, and vaterite. Calcite is the most stable form, while aragonite and vaterite are less stable and can transform into calcite over time. The choice of crystalline form depends on synthesis conditions like reactant concentration and temperature[312]. Each form has unique properties and applications. For example, vaterite's high porosity and surface area make it ideal for controlled drug delivery systems, while aragonite's biocompatible properties make it suitable for bone repair and tissue engineering[313].

- *Calcite:* Calcite, being the most thermodynamically stable phase, is often used in industrial applications, especially when combined with copolymers for targeted drug release in cancer treatment[313].
- *Vaterite:* Vaterite's rapid decomposition under mild conditions makes it a promising candidate for controlled drug delivery systems[314].
- *Aragonite:* Aragonite, denser than calcite, can integrate well with bone tissue, making it valuable for bone repair and as a carrier for anticancer drugs[315].

These diverse properties highlight the versatility of $CaCO_3$ in biomedical applications. In particular, $CaCO_3$ nanoparticles have emerged as promising candidates for delivering drugs to cancer tissues and cells.

5.2. Materials and methods

Calcium chloride, sodium bicarbonate salts, fetal bovine serum, RPMI-1640, and trypsin ethanol were purchased from Sigma Eldritch. Glasswares for cell culture and nanoparticle synthesis were purchased from Tarson Pvt Limited and NEST. Colorectal cancer cell lines (COLO320 DM) were obtained from the National Centre for Cell Science (NCCS) Pune. The compound 3-(4,5-dimethyl-2-thiazolyl)-2,5-diphenyl-2-H-tetrazolium bromide (MTT) was acquired from Krishgen Biosystems Pvt Ltd. All the remaining reagents were of high purity and were acquired from commercially accessible sources.

5.2.1. Preparation of calcium carbonate nanoparticles

In the present study, nano-sized calcium carbonate has been synthesized through chemical precipitation. For this process, the aqueous solutions of sodium carbonate and calcium chloride were mixed, which immediately resulted in precipitates of calcium carbonate. The powder obtained was characterized further in detail for structure and morphology.

- *Chemical precipitation:* One of the most used procedures in the synthesis of $CaCO_3$ micro and nanoparticles is the precipitation technique. This technique involves a straightforward process without additives and is conducted by the mere mixing of supersaturated solutions of Na_2CO_3 and $CaCl_2$[316]. Control over the size and morphology of synthesized particles was attained by tuning parameters such as reactant concentration, reaction time, and temperature[317]. The solutions of sodium carbonate Na_2CO_3, 0.1M, and calcium chloride $CaCl_2$ (0.1) solutions were stirred together and mixed at various speeds ranging from 300 to 30,000 rpm with a temperature range of 25 °C to 37 °C followed by continuous stirring for 20 minutes. The obtained solution was then taken in falcon tubes for centrifugation. After centrifugation, the pellet was washed a few times with ethanol and dried to be stored for further use (Fig.5.2).
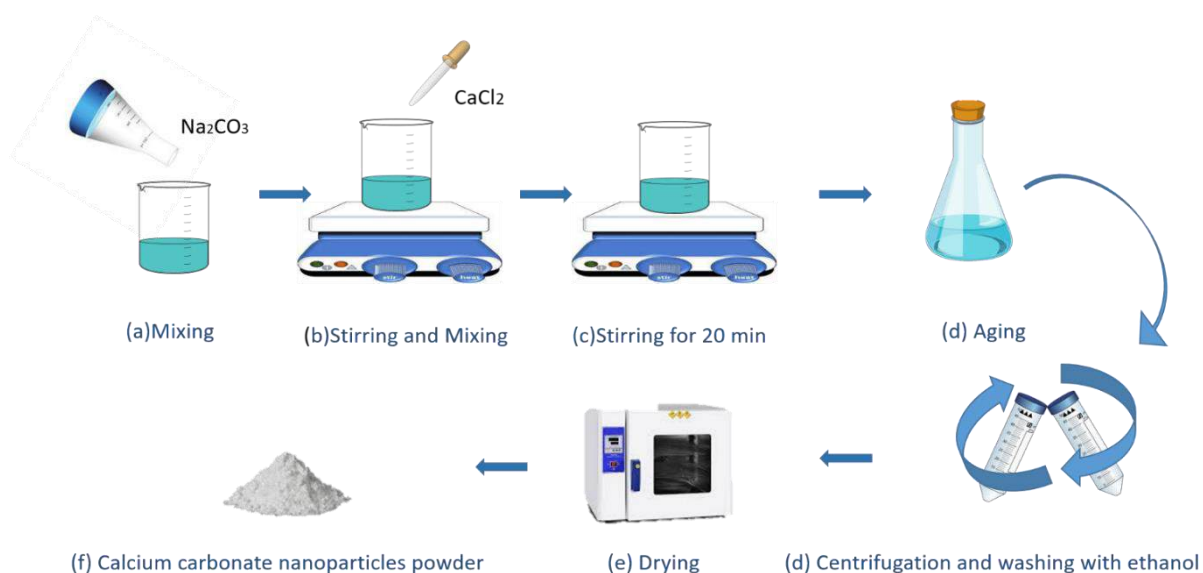
Figure 5. 2 Synthesis process of calcium carbonate nanoparticles through the chemical precipitation method. The controlled chemical reaction between calcium chloride ($CaCl_2$) and sodium carbonate (Na_2CO_3), under well-defined environmental conditions, should yield calcium

carbonate (CaCO₃) nanoparticles. Thereafter, the said nanoparticles shall be collected, washed, and dried for reuse.

5.2.2. Characterization of calcium carbonate nanoparticles

The characterization of synthesized nanoparticles was done using several techniques. Scanning Electron Microscopy and transmission electron microscopy was conducted to study the morphology of synthesized calcium carbonate nanoparticles and drug loaded nanoparticles respectievely. XRD /max 2500 V diffractometer was used to measure the X-ray diffraction patterns, and an FTIR-7600 instrument was used to get the Fourier transform infrared spectra. Dynamic light scattering (DLS) was used to determine the particle size distribution of calcium carbonate nanoparticles.

5.2.3. Drug loading to synthesized nanoparticle

Two dilutions of EGCG were prepared with distilled water at 2 mg/ml and 4 mg/ml concentrations to conjugate nanoparticles with EGCG. 10mg of $CaCO_3$ was dispersed in 2 ml of ethanol. The 1 ml of the EGCG solution was added to 2 ml of ethanol-$CaCO_3$ nanoparticles mixture. The obtained mixture was ultrasonicated for 20 minutes for the conjugation of EGCG with the $CaCO_3$ nanoparticles. After sonication, dark incubation was carried out using an orbital shaker for up to 24 hours. Then, the samples were ultra-centrifugated for 10 min at 2000 rpm(Fig.5.3). The supernatant from each sample was taken to measure the percentage encapsulation using the UV–vis spectrophotometer at a wavelength of 480 nm. The loading efficiency and loading capacity were determined from the readings in the UV–vis spectrophotometer at 480 nm.

5.2.4. Drug Release Study

The release behaviors of EGCG from calcium carbonate nanoparticles were studied at pH 4.8 and 7.4 in PBS buffers. Drug release kinetics was investigated using a standard curve to calculate the concentration of EGCG. Centrifuge pellet containing the EGCG-loaded Calcium Carbonate nanoparticles was placed in dialysis tubing along with 3 ml of buffer solution. First, the test sample suspension of 3 mL EGCG-loaded sample (4mg/mL and 6 mg/mL) was added to the dialysis bag (34 kDa). This dialysis bag was then immersed in a PBS buffer of 100 mL and shaken at 70 rpm in a water bath at 37 °C. At a preset time interval, 3 mL of the PBS buffer was withdrawn from the medium,

which was replaced by an equal volume of fresh PBS. The released EGCG was determined in triplicate using a UV–vis spectrophotometer at 424 nm. The experiment was conducted at two different pH, 4.8 and 7.4, to find out any effect of pH on the drug release property(Fig.5.3).
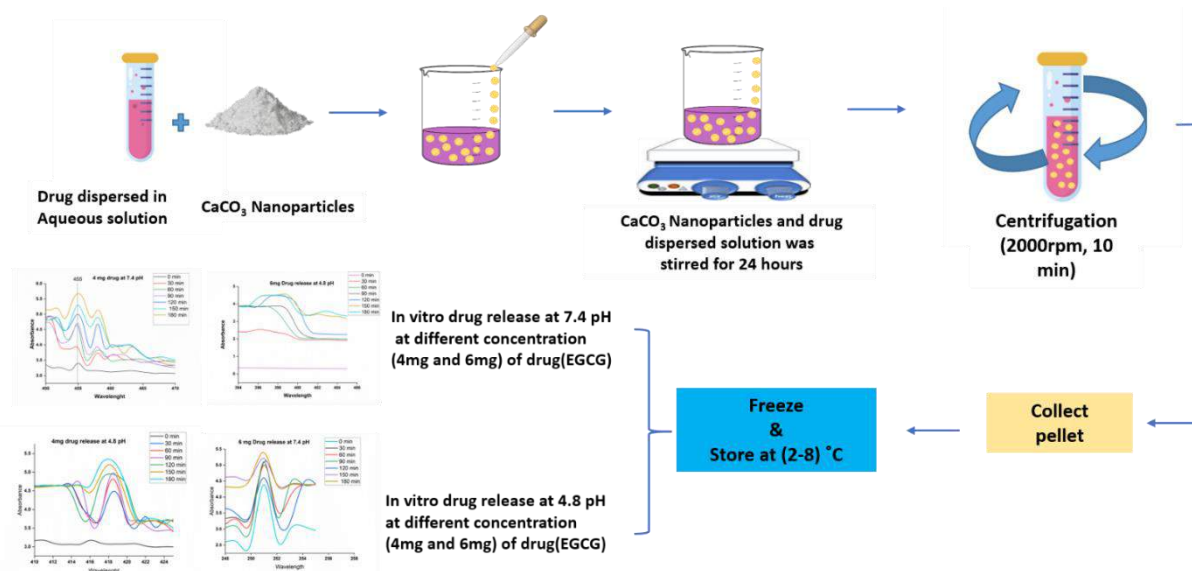
Figure 5. 3 Schematic representation of EGCG drug loading and release in CaCO3 nanoparticles. The process involves EGCG solution and dispersing CaCO3, followed by mixing and ultra-sonication. After incubation on an orbital shaker, the mixture is ultra-centrifuged, and the supernatant is analyzed for loading efficiency. The EGCG-loaded CaCO3 is then used for UV–vis analysis, and Drug release is compared at pH 4.8 and 7.4.

5.2.4. Cell cytotoxicity analysis

The human colon cell line, derived from the colon of a 55-year-old male and procured from NCCS Pune, was cultured on a 96-well plate using complete Roswell Park Memorial Institute (RPMI-1640) medium at a density of 1×10^4 cells per well. Cytotoxicity of calcium carbonate nanoparticles (CCN), EGCG loaded-CCN, and EGCG alone were tested on a colorectal cancer cell line (COLO-320 DM). The cells were subjected to different concentrations of Calcium carbonate nanoparticles (1-150µg/L), EGCG-loaded Calcium carbonate nanoparticles (1-150µg/L), and EGCG (1-150µg/L). The cells were cultured at 37 °C. Then, 50 µL of MTT solution (with a concentration of 5 mg/mL in PBS) was introduced to the plates. The ELISA plate reader manufactured by Bio-rad was employed to measure the absorbance at 570 nm

and 630 nm (with 630 nm serving as the reference wavelength). The cells were incubated in 96 well plates at 37˚C, 5% CO2 for 24 hours.

5.2.5. Cell apoptosis study

The flow cytometry test was employed to quantify apoptosis in COLO320 DM. The cells were seeded in six-well plates at a density of 3×105 and 4×105 cells per well, respectively. The plates were then incubated at 37 °C in a 5% CO2 environment for 24 hours. Subsequently, the cells were subjected to varying concentrations of Calcium carbonate nanoparticles (100µg/L), EGCG-loaded Calcium carbonate (100µg/L), and EGCG (100 µg/L) for 48 hours. The cells were harvested by trypsinization. Subsequently, the cells were rinsed twice with PBS. The cells were treated with a binding buffer (100 mL), Annexin V-fluorescein isothiocyanate (FITC) (2.5 µL), and propidium iodide (PI) (2.5 µL) as directed by the kit instruction manual from Krishgen Biosystem, Mumbai. Subsequently, the cells were placed in a dark environment and kept at room temperature for 20 minutes. The assay findings were detected using flow cytometry (BD FACSCalibur™).

5.3. Results and Discussion

5.3.1. Scanning Electronic Microscope and transmission electron microscope analysis

The SEM image represented that the synthesized particles used to form several quasi-spherical particles with a rough surface texture. Figure 5.4 shows the existence of particle agglomeration as well. This was more obvious in the samples synthesized by lower molarity concentrations of reactants. A low vacuum mode of operation was used with the imaging process since the $CaCO_3$ nanopowder is nonconductive. As observed from the SEM images themselves, these $CaCO_3$ nanoparticles are primarily made of flower-shaped crystal formations. Many aggregates are also identifiable, making it appear that the NPs might have an inherent tendency to agglomerate (Fig.5.4). The likely reason for their very probable agglomeration is the very high surface energy expected from the small particle size, an allegation that is later verified from the results of the XRD phase study. The morphology investigation revealed that the nanoparticles are circular and flower-like in shape, with diameters from 80 to 300 nm. The TEM

images indicated irregular aggregates, proving the homogeneous distribution and encapsulation of the drug. These images proved that the drug was uniformly loaded and highly integrated into the calcium carbonate nanoparticles(Fig.5.5).
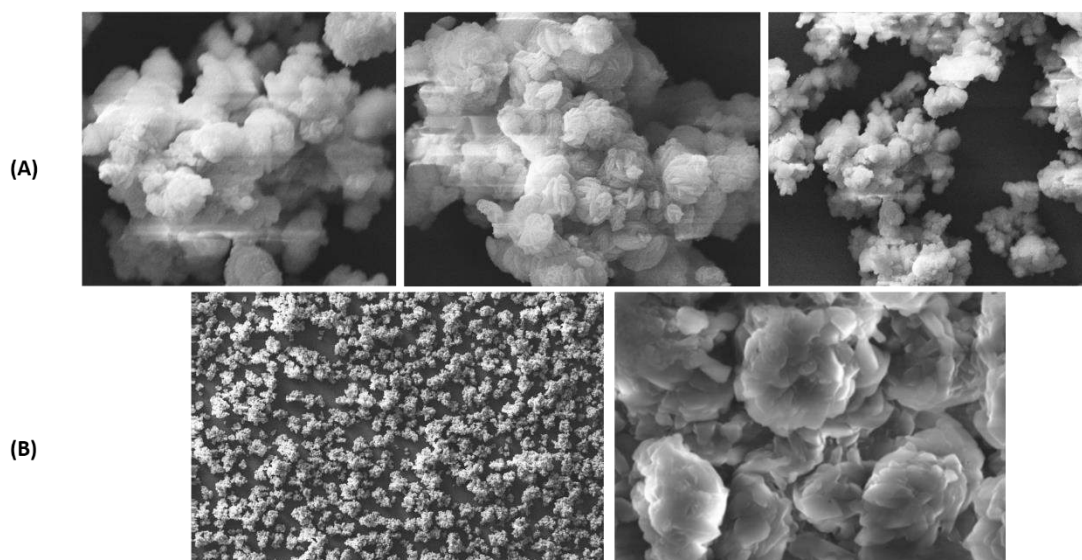
Figure 5. 4(A)SEM images of synthesized calcium carbonate nanoparticles, confirming particle sizes in the range of 100-200 nanometers.(B) Drug loaded CaCO$_3$ nanopartilces.
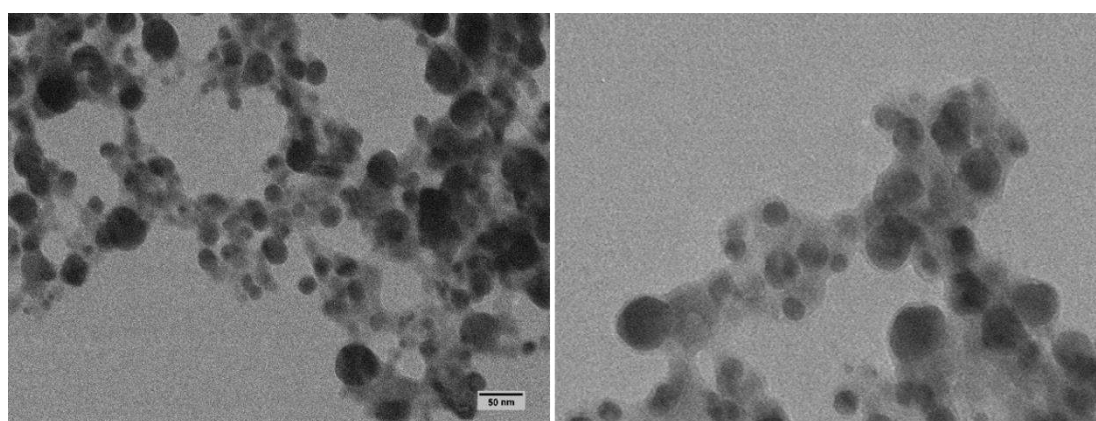
Figure 5. 5 TEM for morphology analysis of drug loaded calcium carbonate nanoparticles.

5.3.3. XRD Analysis

The crystalline structure of the synthesized samples was characterized by X-ray Diffraction analysis. Obtained XRD patterns demonstrated that the formed samples have a single-phase structure and calcite crystal symmetry, which substantiated the formation of pure calcium carbonate without the signature of any detectable secondary phases. The crystal size of the particles was also estimated from the obtained XRD

data, which again confirmed the nanoscale dimensions of the synthesized material. The intensity and sharpness of the XRD peaks reflect the degree of crystallinity of the $CaCO_3$ nanoparticles. The predominant XRD peak signifying calcite was typically observed at approximately $2\theta = 26.5, 27.7, 37.4$ degrees[318]. Additional notable peaks were observed at 2θ values of 45.9, 48.6, and 51.4 degrees, thereby confirming the formation of calcite. Calcite is the most stable polymorph of $CaCO_3$(Fig.5.6).
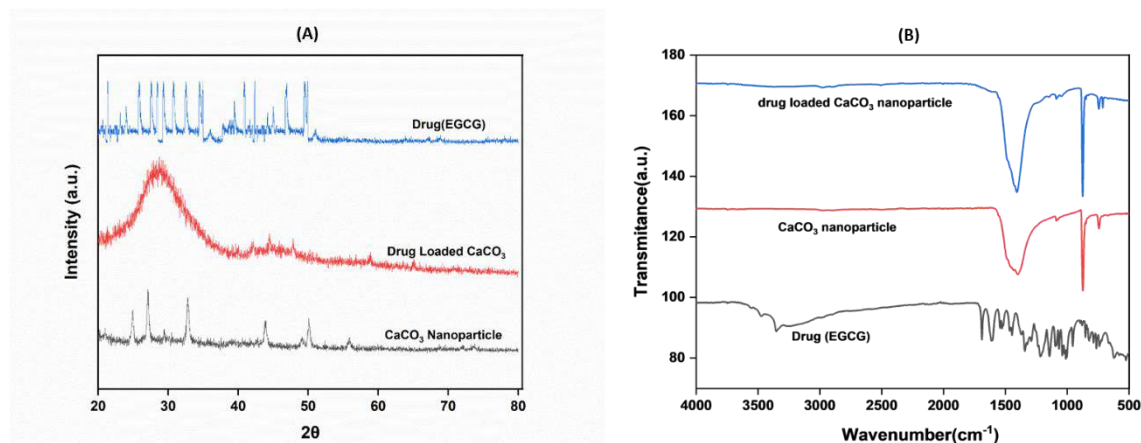
Figure 5. 6(A) X-ray diffraction and (B) FTIR spectra of CaCO₃ nanoparticles, drug(EGCG) loaded CaCO₃ nanoparticles, and Drug alone.

5.3.4.FTIR analysis

FTIR spectroscopy is essential in identifying various phases of organic and inorganic compounds, mainly calcium carbonate phases, due to differences in their carbonate ions, $CO_3{}^{2-}$[319]. Carbonate ions and similar molecules exert four normal modes of vibration peaks: The bands at 712, 848, and 872/cm were assigned to the calcite vibration mode of a calcium carbonate nanoparticle(Fig.5.6).

5.3.5. DLS analysis

To further elucidate the nanoparticles' size distribution, Dynamic Light Scattering measurements were performed. From DLS analyses, information related to average particles' size in synthesized samples, as well as their size distribution, emerges. The evidence established that variations of synthesis parameters alter the size of the particles, clearly expounding on the phenomenon involved in the synthesis process affecting the final characteristics of the particles[320]. The particle size distributions of drug-loaded and blank $CaCO_3$ nanoparticles are shown in Figure 5.7. The $CaCO_3$

nanoparticles without EGCG and those with it loaded had average diameters of 114.64 nm and 289.09 nm, respectively. With polydispersity index (PDI) values of 0.465 for the drug-loaded $CaCO_3$ nanoparticles and 0.196 for the blank $CaCO_3$ nanoparticles, both formulations showed comparatively monodisperse particle size distributions.
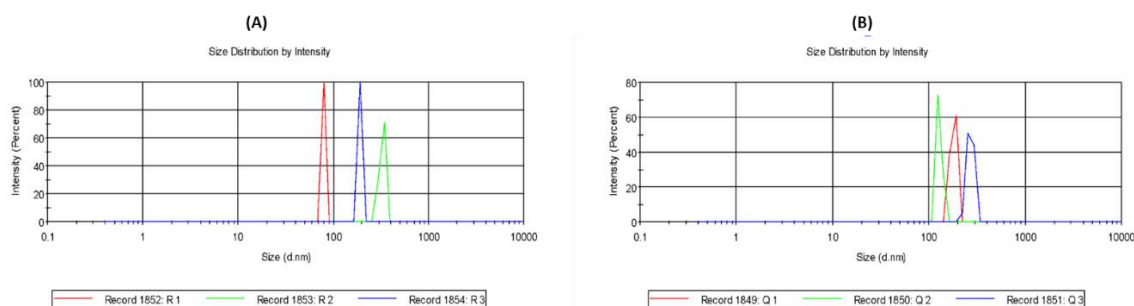
Figure 5. 7 The graph illustrates the size distribution of (A) CaCO3 nanoparticles and (B)EGCG Loaded CaCO3 nanoparticles

5.3.6. In-vitro drug release kinetics

The drug release properties of EGCG-loaded CCNPs were performed at a temperature of 37 °C with a gentle and consistent stirring motion. At fixed time intervals (0, 30, 60, 90, 120, 150, and 180 minutes), 1000 µl of each solution was transferred into a cuvette for spectrophotometry absorbance measurements at every time interval Fig. 5.8 (A & B). The encapsulation efficiency of EGCG inside CCNPs was 66.2%. This might be due to a large surface area of the CCNPs and/or protective effects of calcium carbonate, leading to the awry of premature drug release within the biological system. The drug release profile showed a controlled release of EGCG from CCNPs at both pH 7.4 and 4.8 PBS (Fig. 5.8). A burst drug release was followed by a much slower and steady release until the equilibrium stage at both pH levels. Results indicate that CCNPs loaded with EGCG are suitable drug carriers for targeting pH-specific cancer cells, with a leveled reduction of early drug release in nontarget body regions.

Further evaluavation of EGCG release in the presence of acidic conditions at pH 4.8 (mimicking the tumor microenvironment) also showed much faster release at pH 4.8 compared to pH 7.4. Precisely, at pH 4.8, around 50% of EGCG was monitored to be released within the first hour, while it was nearly 20% at pH 7.4, as demonstrated in Fig 5.8 (A&B). The acidic medium assists in the solubilization of the calcium

carbonate nanoparticles, thus liberating calcium ions (Ca^{2+}) along with carbon dioxide (CO_2) gas, as represented in the reaction:

$$CaCO_3(s) + 2H^+(aq) \rightarrow Ca_2^+(aq) + CO_2(g) + H_2O(l)$$

This rapid dissolution of the calcium carbonate matrix leads to an immediate release of the Drug encapsulated inside the matrix. All these results taken together demonstrated that CCNPs exhibited a good response in the release profile of EGCG in the presence of ROS, indicative of the potential of the nanoparticles to be used as a carrier for the site-specific delivery of drugs in the cancer treatment process.

5.3.7. Cell cytotoxicity analysis

The cytotoxicity of calcium carbonate nanoparticles (CCNPs), EGCG-loaded CCNPs, and free EGCG was evaluated in the COLO-320 DM cell line. EGCG-loaded CCNPs showed a more significant cytotoxic effect on the COLO-320 DM cell line compared to CCNPs and free EGCG. These results could suggest that EGCG-loaded CCNPs had effective interaction with the outer layer of the cancer cells. Controlled release of EGCG, specifically at the site of cancer, will facilitate robust interaction between EGCG and the DNA base pair of the cancer cells, leading to apoptotic cell death.
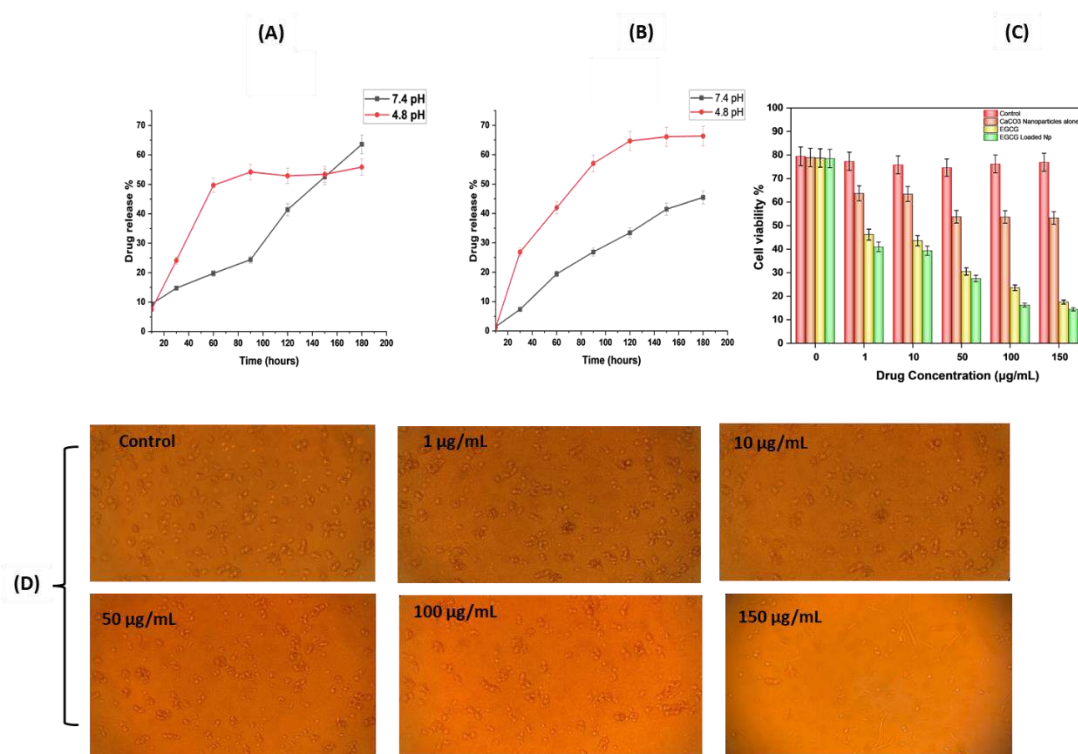
Figure 5. 8 The drug release profiles of EGCG-loaded CCNPs were evaluated at pH 7.4 and pH 4.8, with concentrations of 4mg/ml (A) and 6mg/ml (B). Initial burst followed by the extended release of the Drug until equilibrium favors pH-specific targeting in cancer. (C) The MTT assay results demonstrated a significant cytotoxic effect of the EGCG-loaded CCNPs compared to CCNPs and free EGCG. This validates the successful targeting of cancer cells and induction of apoptotic cell death. (D) More dose dependency towards the apoptotic and morphological changes in EGCG-loaded NNPs treated COLO-320 DM cell against the varying concentrations with a minimum side effect in control groups.
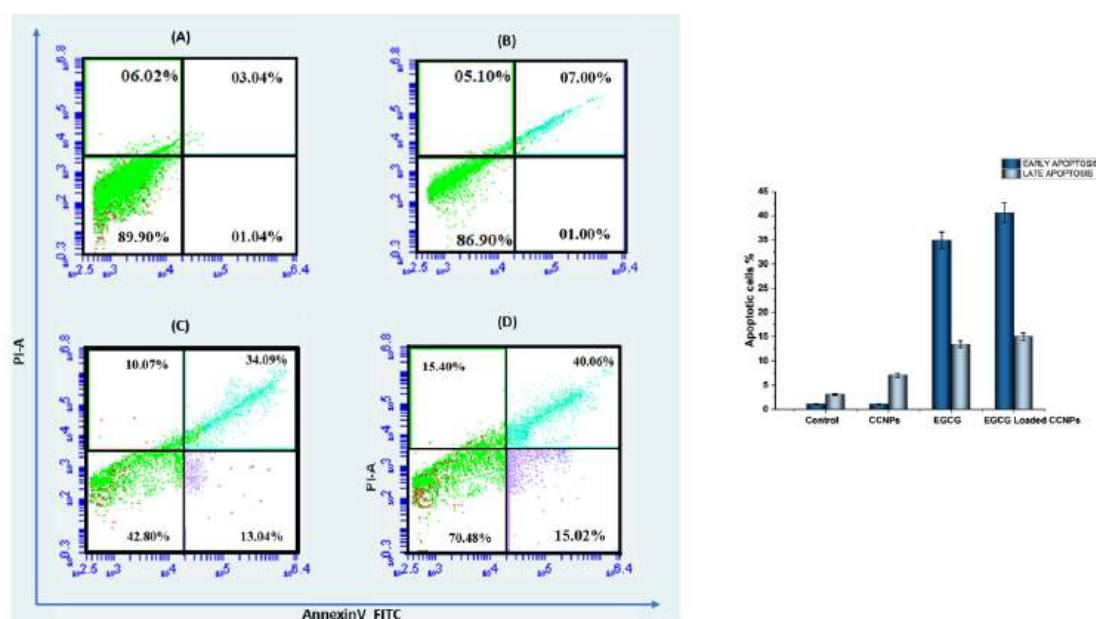
Figure 5. 9 Flow cytometry analysis was performed to assess cancer cell death using Annexin V-FITC/PI staining in COLO320DM cells. The quantification of the percentage of cell death was determined. The infusion of EGCG-loaded calcium carbonate nanoparticles (CCNPs)(D) results in a notable increase in both early (Q3) and late (Q2) apoptosis when compared to the control COLO-320 DM cells(A), CCNPs(B) alone and free EGCG(C). The control flask was treated with DMSO control for 24 hours.

5.3.8.Apoptosis analysis

The incidence of early and late apoptosis in the COLO-320 DM cell line treated with EGCG-loaded CCNPs increased considerably compared to other treatment methods(CCNPs alone and EGCG alone). The percentage of cell fractions in early (Q3) and late (Q2) apoptosis increased in the EGCG-loaded CCNPs treated group, indicating the cytotoxic effects of the developed nanoparticles against the COLO-320 DM cell line. No significant changes were seen between the control group and the other groups, which confirms that the NPs had minimal side effects on normal cells. The results align with the MTT findings, suggesting that the EGCG-loaded calcium

carbonate NPs exhibit more significant cytotoxic effects on the malignant cell line than the other treatment(Fig.5.9).

5.4. Discussion

Surgery, radiotherapy, and chemotherapy are some of the conventional modalities, but they have considerable side effects and long-term disadvantages. In that direction, the dose-dependent and insolubility-related toxicities of drugs also become a significant challenge in cancer treatment. Therefore, nanoparticle-mediated Drug Delivery Systems are feasible to ensure targeted and effective delivery for better therapy outcomes. Many types of NPs have been studied to determine their possibility of being used as nanocarriers. The present study describes the successful synthesis, detailed characterization, and biological evaluation of calcium carbonate nanoparticles as carriers for the anticancer agent epigallocatechin gallate. Chemical precipitation produced the nanoparticles with the desired properties in structure and morphology. SEM results showed the formation of quasi-spherical nanoparticles with a rough surface and aggregation behavior that could be due to high surface energy. The crystalline nature of the powder was confirmed by the XRD pattern, which shows calcite crystal symmetry and hence indicates the purity of calcium carbonate. FTIR spectra indicated characteristic peaks of carbonate ions, thereby justifying the preparation of calcium carbonate. According to DLS analysis, size distribution, and average particle size were noted whereby blank $CaCO_3$ nanoparticles were about 114.64 nm, and that of the drug-loaded nanoparticle was 289.09 nm; hence, EGCG was successfully loaded.

Drug release patterns of EGCG from the prepared calcium carbonate nanoparticles were carried out in PBS buffers at pH 4.8 and 7.4. Release kinetics indicated that EGCG-loaded CCNPs provided controlled and sustained drug release. The release rate was pH-dependent, with faster release at the lower pH of 4.8, simulating the acidic tumor microenvironment. This is typical pH-responsive release behavior, which is advantageous for targeted cancer therapy by ensuring preferential drug release at the tumor site and, therefore, reducing system toxicity. The cytotoxic effects on the human colorectal cancer cell line COLO-320 DM were evaluated for CCNPs, EGCG-loaded CCNPs, and free EGCG. Results demonstrated that EGCG-loaded CCNPs exhibited

more significant cytotoxicity than CCNPs alone and free EGCG. Flow cytometry analysis revealed a substantial increase in early and late apoptosis in cells treated with EGCG-loaded CCNPs compared to the other treatments. This underscores their potent apoptotic-inducing effects on colorectal cancer cells, which agrees with the cytotoxicity results.

5.5 Conclusion

Our study demonstrates the successful synthesis of EGCG-loaded calcium carbonate nanoparticles as an effective drug delivery system. This approach holds significant promise for developing calcium carbonate nanoparticles as a carrier for EGCG. It showed that such nanoparticles had proper structural properties and controlled release with improved anticancer efficacy. The utilization of calcium carbonate nanoparticles reduced the unfavorable effects in cell lines that were reliant on the dosage and preserved the anticancer efficacy of EGCG in COLO-320 DM cells. Consequently, it demonstrated that, due to the pH-dependent drug release activity of the drug-loaded nanoparticles, EGCG-loaded CCNPs can be employed as a safe, efficient method of targeted cancer therapy. The results demonstrate that the cytotoxicity effects of Calcium carbonate nanoparticles, EGCG-loaded Calcium carbonate nanoparticles, and EGCG were influenced by the dosage and duration of exposure. As a result, such nanoparticle-mediated drug delivery systems would significantly enhance the potential to improve efficacy, as well as enhance safety in cancer treatment. Future studies should aim at clearly resolving mechanisms of selective toxicity, and in vivo testing for evaluating the pharmacokinetics, biodistribution, and therapeutic efficacy of EGCG-loaded CCNPs using animal models is of prime importance. Furthermore, exploring the potential of this nanocarrier system for other therapeutic agents could broaden its application within nanomedicine.

CHAPTER:VI

CONCLUSION

CHAPTER VI: CONCLUSION

Colorectal cancer remains a significant global health challenge, particularly affecting individuals aged 50 and older. Primary prevention strategies, including healthy lifestyle choices, risk avoidance, and early detection through regular screening, are crucial in reducing its incidence and impact. Early detection methods such as stool-based tests and colonoscopies, along with treatments tailored to the cancer stage, play a pivotal role in managing the disease. While current treatments like surgery, radiotherapy, targeted therapy, and immunotherapy are effective, they often come with substantial side effects. The effectiveness of FDA-approved anticancer chemotherapy drugs in treating colorectal cancer is limited, as they often come with significant side effects.

Our research delves into the alterations in gene expression induced by chemotherapeutic agents and explores the potential of various natural compounds to counteract these disruptions. We aim to mitigate the dysregulation in gene expression provoked by chemotherapy administration through the strategic use of natural compounds. By elucidating these mechanisms, we seek to enhance the efficacy of cancer treatment while minimizing adverse effects on gene expression. The current research performs expression profiling of gene alterations in colorectal cancer and the effects of chemotherapy with an irinotecan based on datasets GSE62322 and GSE72484. Parsing differentially expressed genes in colorectal cancer versus normal tissue and in samples after chemotherapy versus not-treated ones helped to explain the effect of irinotecan on gene expression and its relation to serious side effects. Our findings demonstrate that many genes altered by chemotherapy are involved in crucial cancer progression pathways and are thus associated with adverse effects, such as anemia, bone marrow depression, nausea, fatigue, diarrhea, neutropenia, and cholinergic syndrome.

We intended to identify specific molecular targets that could be associated with the side effects of FDA-approved drugs. In this respect, such unintended adverse reactions could be expected when these drugs interact with other unintented targets. While

considering substitutes for traditional chemotherapy, we focused on the potential use of natural compounds, especially EGCG, as potent agents against cancer with minimized side effects. Our study in molecular dynamics revealed a promising interaction of EGCG against Human TOPO I, showing its potential to act as an inhibitor of the tumor as irinotecan does and evade AChE that caused cholinergic syndrome. While EGCG is a naturally occurring substance, it has the potential to produce dose-dependent toxicity to normal human cells. To address this issue, we have developed drug delivery through nanoparticle-mediated mechanisms. Because calcium carbonate nanoparticles (CCN) have been shown in the literature to have the following properties: they are abundant, less harmful to cells, safe, biocompatible, pH-responsive, and gradually biodegradable, we synthesized CCN using the chemical precipitation method.

Calcium carbonate ($CaCO_3$) nanoparticles stay stable in neutral and basic pH conditions but dissolve in acidic conditions. This makes them suitable for delivering drugs specifically to cancer cells throughout therapy. Because cancerous cells have a low pH, they cause $CaCO_3$ to dissolve and release medications that are encapsulated, such as EGCG. The drug releases very little at neutral pH, which is similar to the pH of healthy tissues but a lot more when the pH is acidic (pH 4-6). By maintaining therapeutic levels, this controlled release minimizes potential risks associated with EGCG overdose, including nephrotoxicity and myelosuppression. Furthermore, it was observed that the drug-loaded $CaCO_3$ nanoparticles showed enhanced cell cytotoxicity based on the results of the MTT assay. Flow cytometry analysis revealed significantly higher incidents of both the early and late stages of apoptosis compared to the drug administered alone. The results thus indicate that the $CaCO_3$ nanoparticle delivery system has improved the therapeutic efficacy of the drug while potentially reducing its cytotoxic side effects.

In summary, our findings provide significant insight into the molecular mechanisms underlying irinotecan-mediated side effects and thereby offer a new dimension in cancer therapy through the rational use of natural compounds and nanoparticle-mediated drug delivery. This nanoparticle-mediated delivery system showed promise for safe and efficient targeted cancer therapy. Future research should elucidate the

mechanisms of selective toxicity and conduct in vivo testing to evaluate the pharmacokinetics, biodistribution, and therapeutic efficacy of EGCG-loaded CCNPs using animal models. Additionally, exploring this nanocarrier system for other therapeutic agents could broaden its application within nanomedicine. Expanding studies to include various natural compounds could identify new candidates with superior efficacy and minimal side effects. Our study underscores the potential of integrating bioinformatics, molecular biology, and nanotechnology to develop novel, targeted cancer treatments, enhancing patient care and overcoming limitations of conventional therapies. We shall strive to unravel these mechanisms with the idea of developing better cancer treatment strategies with reduced adverse effects, thus leading to the ultimate goal of personalized medicine and improved patient care in oncology. Further research in this line could lead to nature-inspiring and innovative cancer therapies that will transform treatment landscapes and be more effective for patients with colorectal cancer and beyond.

VIII. PUBLICATIONS SUMMARY

JOURNAL PUBLICATION

- Ritu, Asmita Das, Prakash Chandra "Cholinergic side Effect-Free anticancer drugs: paving the way for safer and more effective cancer treatment" Journal of biomolecular Structure & Dynamics (Taylor & Francis) September 2023 (impact factor 4.4).

- Ritu, Asmita Das, Prakash Chandra "Immune checkpoint targeting antibodies hold promise for combinatorial cancer therapeutics". Clinical and experimental medicine (Springer) September 2023 (impact factor 4.6).

- Ritu, Krishan kumar verma, Asmita Das, Prakash Chandra Phytochemical-Based Synthesis of Silver Nanoparticle: Mechanism and Potential Applications. Bionanoscience (Springer) May 2023 (impact factor 3.0).

- Amit Mathur, Ritu, Asmita Das, Prakash Chandra Autophagy: a necessary evil in cancer and inflammation, 3 Biotech November 2023 (Springer) (impact factor 2.8)

CONFERENCES AND PRESENTATIONS

- Ritu, Asmita Das, Prakash Chandra, "Immunomodulatory antibodies hold promise for combinatorial therapy" accepted for publication in international conference on innovations in Biotechnology and Life Science (ICIBLS 2020).

- Ritu, Asmita Das , Prakash Chandra ,"Predicting phytochemicals from water mint as a potential drug to treat breast cancer: a CI & Molecular docking approach" presented on 2nd international conference on environment agriculture human and animal health 2023 (ICEAHAH2023)

- Ritu, Asmita Das, Prakash Chandra, "Unravelling the therapeutic potential of phyllanthus emblica's Beta-carotene: Insight into NF-κB signalling modulation through molecular docking and dynamics simulations" presented on 2nd international conference on Smart Technologies and System for Nest Generation Computing (ICSTSN2023) (April 2023).

➢ Ritu, Asmita Das , Prakash Chandra, Biogenic Synthesis of Silver Nanoparticles using Shewanella putrefaciens: Characterization and Evaluation of Antimicrobial Activity presented on National conference on Bioentrepreneurship- Academia to Industry 23-24 February, 2023.

BOOK CHAPTER PUBLISHED

➢ Ritu, Apoorva, Simran singh, Prakash Chandra, and Asmita Das Nanotechnological aspects and future perspective of nanocoatings for medical devices and implants Woodhead Publishing Series in Biomaterials 2024, Pages 251-281 book: Next-Generation Antimicrobial Nanocoatings for Medical Devices and Implants. DOI: 10.1016/B978-0-323-95756-4.00005-1.

➢ Ritu, Shruti Sounkaria, Gunjan Sachdeva, Asmita Das , Prakash Chandra , "Potentialities of nanobiotechnology in nutrient management in the livestock products", January 2023, Elsevier

➢ Shweta Gulia, Ritu ,Asmita Das , Prakash Chandra , "Bioremediation of PAHs using nanotechnology" June 2023, Elsevier

BOOK CHAPTER ACCEPTED

➢ Ritu, Prachi Pannu, Pooja, Asmita Das and Prakash Chandra "Safety and Biocompatibility of Nanogels: Addressing Current Concerns") for Inclusion in Our Approved Book entitled Nanogels: Fundamentals to Pharmaceutical and Biomedical Applications Elsevier.

➢ Ritu, nida e falak, Bharmjeet, Asmita Das and Prakash Chandra "Nanoscience in controlled drug release in the GI tract", " IOP Publishing.

IX. **REFERENCES**

1. Sachdeo RA, Charde MS, Chakole RD (2020) Colorectal cancer: An overview. *Asian Journal of Research in Pharmaceutical Science 10:211*

2. Siegel RL, Miller KD, Goding Sauer A, Fedewa SA, Butterly LF, Anderson JC, Cercek A, Smith RA, Jemal A (2020) Colorectal cancer statistics, 2020. *CA Cancer J Clin 70:145–164*

3. Sung H, Ferlay J, Siegel RL, Laversanne M, Soerjomataram I, Jemal A, Bray F (2021) Global Cancer Statistics 2020: GLOBOCAN Estimates of Incidence and Mortality Worldwide for 36 Cancers in 185 Countries. *CA Cancer J Clin 71:209–249*

4. Granados-Romero JJ, Valderrama-Treviño AI, Contreras-Flores EH, Barrera-Mera B, Herrera Enríquez M, Uriarte-Ruíz K, Ceballos-Villalba JC, Estrada-Mata AG, Alvarado Rodríguez C, Arauz-Peña G (2017) Colorectal cancer: a review. *Int J Res Med Sci 5:4667*

5. Man J, Zhang T, Yin X, Chen H, Zhang Y, Zhang X, Chen J, Yang X, Lu M (2022) Spatiotemporal Trends of Colorectal Cancer Mortality Due to Low Physical Activity and High Body Mass Index From 1990 to 2019: A Global, Regional and National Analysis. *Front Med (Lausanne). https://doi.org/10.3389/fmed.2021.800426*

6. Debela DT, Muzazu SG, Heraro KD, Ndalama MT, Mesele BW, Haile DC, Kitui SK, Manyazewal T (2021) New approaches and procedures for cancer treatment: Current perspectives. *SAGE Open Med 9:205031212110343*

7. Amirkhah R, Naderi-Meshkin H, Shah J, Dunne P, Schmitz U (2019) The Intricate Interplay between Epigenetic Events, Alternative Splicing and Noncoding RNA Deregulation in Colorectal Cancer. *Cells 8:929*

8. Bardhan K, Liu K (2013) Epigenetics and Colorectal Cancer Pathogenesis. *Cancers (Basel) 5:676–713*

9. Qingwei Z, Dongsheng H, Duo L, Youlei W, Songxia Y, Ziqi Y, Lanjuan L (2020) Fluorouracil Supplemented With Oxaliplatin or Irinotecan for Solid Tumors: Indications From Clinical Characteristics and Health Outcomes of Patients. *Front Oncol. https://doi.org/10.3389/fonc.2020.01542*

10. Wang Y, Probin V, Zhou D (2006) Cancer Therapy-Induced Residual Bone Marrow Injury: Mechanisms of Induction and Implication for Therapy. *Curr Cancer Ther Rev 2:271–279*

11. Nakamura H, Maeda H (2023) Cancer Chemotherapy. *Fundamentals of Pharmaceutical Nanoscience 401–427*

12. *Vaillant AAJ, Rout P, Reynolds SB, Zito PM (2024) Neutropenia. Mayo Clinic Medical Manual 661–665*

13. *Wang J (2012) Natural compounds as anticancer agents: Experimental evidence. World J Exp Med 2:45*

14. *Du Y-X, Mamun A Al, Lyu A-P, Zhang H-J (2023) Natural Compounds Targeting the Autophagy Pathway in the Treatment of Colorectal Cancer. Int J Mol Sci 24:7310*

15. *Mokhtari RB, Homayouni TS, Baluch N, Morgatskaya E, Kumar S, Das B, Yeger H (2017) Combination therapy in combating cancer. Oncotarget 8:38022–38043*

16. *Talib WH, Alsayed AR, Barakat M, Abu-Taha MI, Mahmod AI (2021) Targeting Drug Chemo-Resistance in Cancer Using Natural Products. Biomedicines 9:1353*

17. *Harada S, Morlote D (2020) Molecular Pathology of Colorectal Cancer. Adv Anat Pathol 27:20–26*

18. *Grady WM, Carethers JM (2008) Genomic and Epigenetic Instability in Colorectal Cancer Pathogenesis. Gastroenterology 135:1079–1099*

19. *Armaghany T, Wilson JD, Chu Q, Mills G (2012) Genetic alterations in colorectal cancer. Gastrointest Cancer Res 5:19–27*

20. *Hari DM, Leung AM, Lee J-H, Sim M-S, Vuong B, Chiu CG, Bilchik AJ (2013) AJCC Cancer Staging Manual 7th Edition Criteria for Colon Cancer: Do the Complex Modifications Improve Prognostic Assessment? J Am Coll Surg 217:181–190*

21. *Aiderus A, Barker N, Tergaonkar V (2024) Serrated colorectal cancer: preclinical models and molecular pathways. Trends Cancer 10:76–91*

22. *Fleming M, Ravula S, Tatishchev SF, Wang HL (2012) Colorectal carcinoma: Pathologic aspects. J Gastrointest Oncol 3:153–73*

23. *Pino MS, Chung DC (2010) The Chromosomal Instability Pathway in Colon Cancer. Gastroenterology 138:2059–2072*

24. *Zhang L, Shay JW (2017) Multiple Roles of APC and its Therapeutic Implications in Colorectal Cancer. JNCI: Journal of the National Cancer Institute. https://doi.org/10.1093/jnci/djw332*

25. *Yan W-F, Wu G, Sun P-C, Qiu D (2015) P53 mutations occur more commonly than KRAS mutations in colorectal adenoma. Int J Clin Exp Med 8:1370–5*

26. *Szylberg Ł, Janiczek M, Popiel A, Marszałek A (2015) Serrated Polyps and Their Alternative Pathway to the Colorectal Cancer: A Systematic Review. Gastroenterol Res Pract 2015:1–7*

27. *Boland CR, Goel A (2010) Microsatellite Instability in Colorectal Cancer. Gastroenterology 138:2073-2087.e3*

28. *Schöniger S, Rüschoff J (2022) Mismatch Repair Deficiency and Microsatellite Instability. Encyclopedia 2:1559–1576*

29. *Roudko V, Cimen Bozkus C, Greenbaum B, Lucas A, Samstein R, Bhardwaj N (2021) Lynch Syndrome and MSI-H Cancers: From Mechanisms to "Off-The-Shelf" Cancer Vaccines. Front Immunol. https://doi.org/10.3389/fimmu.2021.757804*

30. *Kahi CJ (2019) Screening Relevance of Sessile Serrated Polyps. Clin Endosc 52:235–238*

31. *Benedict M (2015) Interval colorectal carcinoma: An unsolved debate. World J Gastroenterol 21:12735*

32. *Gryfe R (2009) Inherited Colorectal Cancer Syndromes. Clin Colon Rectal Surg 22:198–208*

33. *Mitchem J, Hall J (2016) Adenomatous Polyposis Syndromes: Diagnosis and Management. Clin Colon Rectal Surg 29:321–329*

34. *Steinke V, Engel C, Büttner R, Schackert HK, Schmiegel WH, Propping P (2013) Hereditary Nonpolyposis Colorectal Cancer (HNPCC)/Lynch Syndrome. Dtsch Arztebl Int. https://doi.org/10.3238/arztebl.2013.0032*

35. *Mishra N, Hall J (2012) Identification of Patients at Risk for Hereditary Colorectal Cancer. Clin Colon Rectal Surg 25:067–082*

36. *Jasperson KW, Tuohy TM, Neklason DW, Burt RW (2010) Hereditary and Familial Colon Cancer. Gastroenterology 138:2044–2058*

37. *Amersi F, Agustin M, Ko CY (2005) Colorectal cancer: epidemiology, risk factors, and health services. Clin Colon Rectal Surg 18:133–40*

38. *Levin B, Lieberman DA, McFarland B, et al (2008) Screening and Surveillance for the Early Detection of Colorectal Cancer and Adenomatous Polyps, 2008: A Joint Guideline From the American Cancer Society, the US Multi-Society Task Force on Colorectal Cancer, and the American College of Radiology. Gastroenterology 134:1570–1595*

39. Schreuders EH, Grobbee EJ, Spaander MCW, Kuipers EJ (2016) Advances in Fecal Tests for Colorectal Cancer Screening. Curr Treat Options Gastroenterol 14:152–162

40. Doubeni CA, Jensen CD, Fedewa SA, Quinn VP, Zauber AG, Schottinger JE, Corley DA, Levin TR (2016) Fecal Immunochemical Test (FIT) for Colon Cancer Screening: Variable Performance with Ambient Temperature. The Journal of the American Board of Family Medicine 29:672–681

41. Tran TN, Peeters M, Hoeck S, Van Hal G, Janssens S, De Schutter H (2022) Optimizing the colorectal cancer screening programme using faecal immunochemical test (FIT) in Flanders, Belgium from the "interval cancer" perspective. Br J Cancer 126:1091–1099

42. Ribbing Wilén H, Saraste D, Blom J (2022) Interval cancers in a population-based screening program for colorectal cancer with gender-specific cut-off levels for fecal immunochemical test. J Med Screen 29:156–165

43. Zorzi M, Battagello J, Selby K, Capodaglio G, Baracco S, Rizzato S, Chinellato E, Guzzinati S, Rugge M (2022) Non-compliance with colonoscopy after a positive faecal immunochemical test doubles the risk of dying from colorectal cancer. Gut 71:561–567

44. Medical Advisory Secretariat (2009) Flexible sigmoidoscopy for colorectal cancer screening: an evidence-based analysis. Ont Health Technol Assess Ser 9:1–23

45. Stracci F, Zorzi M, Grazzini G (2014) Colorectal Cancer Screening: Tests, Strategies, and Perspectives. Front Public Health. https://doi.org/10.3389/fpubh.2014.00210

46. Shaukat A, Levin TR (2022) Current and future colorectal cancer screening strategies. Nat Rev Gastroenterol Hepatol 19:521–531

47. Lopes SR, Martins C, Santos IC, Teixeira M, Gamito É, Alves AL (2024) Colorectal cancer screening: A review of current knowledge and progress in research. World J Gastrointest Oncol 16:1119–1133

48. Medical Advisory Secretariat (2009) Magnetic Resonance (MR) Colonography for Colorectal Cancer Screening: An Evidence-Based Analysis. Ont Health Technol Assess Ser 9:1–35

49. Hausmann J, Tal A, Gomer A, Philipper M, Moog G, Hohn H, Hesselbarth N, Plass H, Albert J, Finkelmeier F (2021) Colon Capsule Endoscopy: Indications, Findings, and Complications – Data from a Prospective German Colon Capsule Registry Trial (DEKOR). Clin Endosc 54:92–99

50. *Koffas A, Papaefthymiou A, Laskaratos F-M, Kapsoritakis A, Epstein O (2022) Colon Capsule Endoscopy in the Diagnosis of Colon Polyps: Who Needs a Colonoscopy? Diagnostics 12:2093*

51. *Eliakim R, Yassin K, Niv Y, et al (2009) Prospective multicenter performance evaluation of the second-generation colon capsule compared with colonoscopy. Endoscopy 41:1026–1031*

52. *Feeney G, Sehgal R, Sheehan M, Hogan A, Regan M, Joyce M, Kerin M (2019) Neoadjuvant radiotherapy for rectal cancer management. World J Gastroenterol 25:4850–4869*

53. *Figueredo A, Zuraw L, Wong RK, Agboola O, Rumble RB, Tandan V (2003) The use of preoperative radiotherapy in the management of patients with clinically resectable rectal cancer: a practice guideline. BMC Med 1:1*

54. *LISCU H-D (2021) Short-Course Radiotherapy versus Long-Course Radio-Chemotherapy as Neoadjuvant Treatment for Locally Advanced Rectal Cancer: Meta-Analysis from a Toxicity Perspective. Maedica - A Journal of Clinical Medicine. https://doi.org/10.26574/maedica.2021.16.3.382*

55. *Liu W-Y, Dinapoli N, Wang X, et al (2016) Possible contribution of IMRT in postoperative radiochemotherapy for rectal cancer: analysis on 1798 patients by prediction model. Oncotarget 7:46536–46544*

56. *Hall EJ (2006) Intensity-modulated radiation therapy, protons, and the risk of second cancers. International Journal of Radiation Oncology*Biology*Physics 65:1–7*

57. *Mohiuddin M, Marks J, Marks G (2008) Management of Rectal Cancer: Short- vs. Long-Course Preoperative Radiation. International Journal of Radiation Oncology*Biology*Physics 72:636–643*

58. *Smyth MJ, Teng MW (2018) 2018 Nobel Prize in physiology or medicine. Clin Transl Immunology. https://doi.org/10.1002/cti2.1041*

59. *Gonzalez H, Hagerling C, Werb Z (2018) Roles of the immune system in cancer: from tumor initiation to metastatic progression. Genes Dev 32:1267*

60. *Davda J, Declerck P, Hu-Lieskovan S, Hickling TP, Jacobs IA, Chou J, Salek-Ardakani S, Kraynov E (2019) Immunogenicity of immunomodulatory, antibody-based, oncology therapeutics. J Immunother Cancer 7:1–9*

61. *Colombo MP, Piconese S (2007) Regulatory-T-cell inhibition versus depletion: the right choice in cancer immunotherapy. Nat Rev Cancer 7:880–887*

62. Rocamora-Reverte L, Melzer FL, Würzner R, Weinberger B (2020) *The Complex Role of Regulatory T Cells in Immunity and Aging. Front Immunol.* https://doi.org/10.3389/FIMMU.2020.616949

63. Hadrup S, Donia M, Thor Straten P (2013) *Effector CD4 and CD8 T Cells and Their Role in the Tumor Microenvironment. Cancer Microenvironment 6:123*

64. Dong Y, Wan Z, Gao X, Yang G, Liu L (2021) *Reprogramming Immune Cells for Enhanced Cancer Immunotherapy: Targets and Strategies. Front Immunol.* https://doi.org/10.3389/fimmu.2021.609762

65. Buchbinder EI, Desai A (2016) *CTLA-4 and PD-1 Pathways: Similarities, Differences, and Implications of Their Inhibition. Am J Clin Oncol 39:98*

66. Quatrini L, Mariotti FR, Munari E, Tumino N, Vacca P, Moretta L (2020) *The Immune Checkpoint PD-1 in Natural Killer Cells: Expression, Function and Targeting in Tumour Immunotherapy. Cancers (Basel) 12:1–21*

67. Sobhani N, Tardiel-Cyril DR, Davtyan A, Generali D, Roudi R, Li Y (2021) *CTLA-4 in Regulatory T Cells for Cancer Immunotherapy. Cancers (Basel) 13:1–18*

68. Sobhani N, Tardiel-Cyril DR, Davtyan A, Generali D, Roudi R, Li Y (2021) *CTLA-4 in Regulatory T Cells for Cancer Immunotherapy. Cancers (Basel) 13:1–18*

69. Shiravand Y, Khodadadi F, Kashani SMA, Hosseini-Fard SR, Hosseini S, Sadeghirad H, Ladwa R, O'Byrne K, Kulasinghe A (2022) *Immune Checkpoint Inhibitors in Cancer Therapy. Current Oncology 29:3044–3060*

70. Ganesh K, Stadler ZK, Cercek A, Mendelsohn RB, Shia J, Segal NH, Diaz LA (2019) *Immunotherapy in colorectal cancer: rationale, challenges and potential. Nat Rev Gastroenterol Hepatol 16:361–375*

71. Waldman AD, Fritz JM, Lenardo MJ (2020) *A guide to cancer immunotherapy: from T cell basic science to clinical practice. Nat Rev Immunol 20:651–668*

72. Tridente G (2014) *Alemtuzumab. Adverse Events with Biomedicines 81*

73. Havrdova E, Horakova D, Kovarova I (2015) *Alemtuzumab in the treatment of multiple sclerosis: key clinical trial results and considerations for use. Ther Adv Neurol Disord 8:31*

74. Freedman MS, Kaplan JM, Markovic-Plese S (2013) *Insights into the Mechanisms of the Therapeutic Efficacy of Alemtuzumab in Multiple Sclerosis. J Clin Cell Immunol 4:152*

75. *Fda, Cder (2016) HIGHLIGHTS OF PRESCRIBING INFORMATION FULL PRESCRIBING INFORMATION: CONTENTS* 1 INDICATIONS AND USAGE 1.1 Locally Advanced or Metastatic Urothelial Carcinoma 1.2 Metastatic Non-Small Cell Lung Cancer 2 DOSAGE AND ADMINISTRATION 2.1 Recommended Dosing 2.2 Dose Modifications 2.3 Preparation and Administration 3 DOSAGE FORMS AND STRENGTHS 4 CONTRAINDICATIONS 5 WARNINGS AND PRECAUTIONS.*

76. *Weinstock C, Khozin S, Suzman D, Zhang L, Tang S, Wahby S, Goldberg KB, Kim G, Pazdur R (2017) U.S. Food and Drug Administration Approval Summary: Atezolizumab for Metastatic Non-Small Cell Lung Cancer. Clin Cancer Res 23:4534–4539*

77. *Rosenberg JE, Hoffman-Censits J, Powles T, et al (2016) Atezolizumab in patients with locally advanced and metastatic urothelial carcinoma who have progressed following treatment with platinum-based chemotherapy: a single-arm, multicentre, phase 2 trial. Lancet 387:1909–1920*

78. *Socinski MA, Jotte RM, Cappuzzo F, et al (2018) Atezolizumab for First-Line Treatment of Metastatic Nonsquamous NSCLC. New England Journal of Medicine 378:2288–2301*

79. *West H, McCleod M, Hussein M, et al (2019) Atezolizumab in combination with carboplatin plus nab-paclitaxel chemotherapy compared with chemotherapy alone as first-line treatment for metastatic non-squamous non-small-cell lung cancer (IMpower130): a multicentre, randomised, open-label, phase 3 trial. Lancet Oncol 20:924–937*

80. *Horn L, Mansfield AS, Szczęsna A, et al (2018) First-Line Atezolizumab plus Chemotherapy in Extensive-Stage Small-Cell Lung Cancer. N Engl J Med 379:2220–2229*

81. *Pillai RN, Ramalingam SS, Carbone DP, Paz-Ares LG, Thayu M, Watson P, Khokhar NZ, Reck M (2017) Randomized, open-label phase Ib/II study of atezolizumab with or without daratumumab in previously treated advanced or metastatic non-small cell lung cancer (NSCLC). Journal of Clinical Oncology 35:TPS9102–TPS9102*

82. *Malhotra J, Lin Y, Gonzales A, Patel M, Chan N, Aisner J, Jabbour S (2021) FP03.02 A Phase I Trial of Atezolizumab and Varlilumab in Combination With Radiation in Patients with Metastatic Non-Small Cell Lung Cancer. Journal of Thoracic Oncology 16:S948*

83. *Mathieu L, Shah S, Pai-Scherf L, et al (2021) FDA Approval Summary: Atezolizumab and Durvalumab in Combination with Platinum-Based Chemotherapy in Extensive Stage Small Cell Lung Cancer. Oncologist 26:433–438*

84. *Infante JR, Hansen AR, Pishvaian MJ, et al (2016) A phase Ib dose escalation study of the OX40 agonist MOXR0916 and the PD-L1 inhibitor atezolizumab in patients with advanced solid tumors. https://doi.org/101200/JCO20163415_suppl101 34:101–101*

85. *Disis ML, Taylor MH, Kelly K, et al (2019) Efficacy and Safety of Avelumab for Patients With Recurrent or Refractory Ovarian Cancer: Phase 1b Results From the JAVELIN Solid Tumor Trial. JAMA Oncol 5:393–401*

86. *Kaufman HL, Russell J, Hamid O, et al (2016) Avelumab in patients with chemotherapy-refractory metastatic Merkel cell carcinoma: a multicentre, single-group, open-label, phase 2 trial. Lancet Oncol 17:1374*

87. *Rodriguez-Vida A, Bellmunt J (2018) Avelumab for the treatment of urothelial cancer. Expert Rev Anticancer Ther 18:421–429*

88. *Chin K, Chand VK, Nuyten DSA (2017) Avelumab: clinical trial innovation and collaboration to advance anti-PD-L1 immunotherapy. Annals of Oncology 28:1658–1666*

89. *Juliá EP, Amante A, Pampena MB, Mordoh J, Levy EM (2018) Avelumab, an IgG1 anti-PD-L1 Immune Checkpoint Inhibitor, Triggers NK Cell-Mediated Cytotoxicity and Cytokine Production Against Triple Negative Breast Cancer Cells. Front Immunol. https://doi.org/10.3389/fimmu.2018.02140*

90. *Yamazaki T, Galluzzi L (2017) Blinatumomab bridges the gap between leukemia and immunity. Oncoimmunology 6:e1358335*

91. *Cesco-Gaspere M, Morris E, Stauss HJ (2009) Immunomodulation in the treatment of haematological malignancies. Clin Exp Med 9:81–92*

92. *Fang W, Yang Y, Ma Y, et al (2018) Camrelizumab (SHR-1210) alone or in combination with gemcitabine plus cisplatin for nasopharyngeal carcinoma: results from two single-arm, phase 1 trials. Lancet Oncol 19:1338–1350*

93. *Ciociola T, Magliani W, Giovati L, Sperindè M, Santinoli C, Conti G, Conti S, Polonelli L (2014) Antibodies as an Unlimited Source of Anti-Infective, Anti-Tumour and Immunomodulatory Peptides. Sci Prog 97:215–233*

94. *Ahmed SR, Petersen E, Patel R, Migden MR (2019) Cemiplimab-rwlc as first and only treatment for advanced cutaneous squamous cell carcinoma. Expert Rev Clin Pharmacol 12:947–951*

95. *Migden MR, Rischin D, Schmults CD, et al (2018) PD-1 Blockade with Cemiplimab in Advanced Cutaneous Squamous-Cell Carcinoma. New England Journal of Medicine 379:341–351*

96. *Saltarella I, Desantis V, Melaccio A, Solimando AG, Lamanuzzi A, Ria R, Storlazzi CT, Mariggiò MA, Vacca A, Frassanito MA (2020) Mechanisms of Resistance to Anti-CD38 Daratumumab in Multiple Myeloma. Cells 9:167*

97. *Frerichs KA, Verkleij CPM, Dimopoulos MA, Marin Soto JA, Zweegman S, Young MH, Newhall KJ, Mutis T, van de Donk NWCJ (2021) Efficacy and Safety of Durvalumab Combined with Daratumumab in Daratumumab-Refractory Multiple Myeloma Patients. Cancers (Basel). https://doi.org/10.3390/CANCERS13102452*

98. *Faiena I, Cummings AL, Crosetti AM, Pantuck AJ, Chamie K, Drakaki A (2018) Durvalumab: an investigational anti-PD-L1 monoclonal antibody for the treatment of urothelial carcinoma. Drug Des Devel Ther Volume 12:209–215*

99. *Lee J-M, Cimino-Mathews A, Peer CJ, et al (2017) Safety and Clinical Activity of the Programmed Death-Ligand 1 Inhibitor Durvalumab in Combination With Poly (ADP-Ribose) Polymerase Inhibitor Olaparib or Vascular Endothelial Growth Factor Receptor 1-3 Inhibitor Cediranib in Women's Cancers: A Dose-Escalation, Phase I Study. Journal of Clinical Oncology 35:2193–2202*

100. *Godwin CD, Gale RP, Walter RB (2017) Gemtuzumab ozogamicin in acute myeloid leukemia. Leukemia 31:1855–1868*

101. *Mahalingam D, Patel M, Sachdev J, et al (2016) PD-011 Safety and efficacy analysis of imalumab, an anti-oxidized macrophage migration inhibitory factor (oxMIF) antibody, alone or in combination with 5-fluorouracil/leucovorin (5-FU/LV) or panitumumab, in patients with metastatic colorectal cancer (mCRC). Annals of Oncology 27:ii105*

102. *Letendre P, Monga V, Milhem M, Zakharia Y (2017) Ipilimumab: from preclinical development to future clinical perspectives in melanoma. Future Oncology 13:625–636*

103. *Khalil DN, Smith EL, Brentjens RJ, Wolchok JD (2016) The future of cancer treatment: immunomodulation, CARs and combination immunotherapy. Nat Rev Clin Oncol 13:273–290*

104. *Lipson EJ, Drake CG (2011) Ipilimumab: an anti-CTLA-4 antibody for metastatic melanoma. Clin Cancer Res 17:6958–6962*

105. *Fda HIGHLIGHTS OF PRESCRIBING INFORMATION.*

106. *Choueiri TK, Fishman MN, Escudier B, et al (2016) Immunomodulatory Activity of Nivolumab in Metastatic Renal Cell Carcinoma. Clinical Cancer Research 22:5461–5471*

107. *Hume DA, MacDonald KPA (2012) Therapeutic applications of macrophage colony-stimulating factor-1 (CSF-1) and antagonists of CSF-1 receptor (CSF-1R) signaling. Blood 119:1810–1820*

108. *Wang-Gillam A, O'Reilly EM, Bendell JC, et al (2019) A randomized phase II study of cabiralizumab (cabira) + nivolumab (nivo) ± chemotherapy (chemo) in advanced pancreatic ductal adenocarcinoma (PDAC). https://doi.org/101200/JCO2019374_supplTPS465 37:TPS465–TPS465*

109. *O'Hara MH, O'Reilly EM, Varadhachary G, et al (2021) CD40 agonistic monoclonal antibody APX005M (sotigalimab) and chemotherapy, with or without nivolumab, for the treatment of metastatic pancreatic adenocarcinoma: an open-label, multicentre, phase 1b study. Lancet Oncol 22:118–131*

110. *Borghaei H, Paz-Ares L, Horn L, et al (2015) Nivolumab versus Docetaxel in Advanced Nonsquamous Non-Small-Cell Lung Cancer. N Engl J Med 373:1627–1639*

111. *Tobinai K, Klein C, Oya N, Fingerle-Rowson G (2017) A Review of Obinutuzumab (GA101), a Novel Type II Anti-CD20 Monoclonal Antibody, for the Treatment of Patients with B-Cell Malignancies. Adv Ther 34:324–356*

112. *Hafeez U, Gan HK, Scott AM (2018) Monoclonal antibodies as immunomodulatory therapy against cancer and autoimmune diseases. Curr Opin Pharmacol 41:114–121*

113. *Larkins E, Blumenthal GM, Yuan W, et al (2017) FDA Approval Summary: Pembrolizumab for the Treatment of Recurrent or Metastatic Head and Neck Squamous Cell Carcinoma with Disease Progression on or After Platinum-Containing Chemotherapy. Oncologist 22:873*

114. *Sanlorenzo M, Vujic I, Daud A, Algazi A, Gubens M, Luna SA, Lin K, Quaglino P, Rappersberger K, Ortiz-Urda S (2015) Pembrolizumab Cutaneous Adverse Events and Their Association With Disease Progression. JAMA Dermatol 151:1206*

115. *Robert C, Schachter J, Long G V., et al (2015) Pembrolizumab versus Ipilimumab in Advanced Melanoma. New England Journal of Medicine 372:2521–2532*

116. *Langer CJ, Gadgeel SM, Borghaei H, et al (2016) Carboplatin and pemetrexed with or without pembrolizumab for advanced, non-squamous non-small-cell lung cancer: a randomised, phase 2 cohort of the open-label KEYNOTE-021 study. Lancet Oncol 17:1497*

117. *Mezquita L, Planchard D (2018) Durvalumab for the treatment of non-small cell lung cancer. Expert Rev Respir Med 12:627–639*

118.   Rosenberg SA, Restifo NP, Yang JC, Morgan RA, Dudley ME (2008) *Adoptive cell transfer: a clinical path to effective cancer immunotherapy. Nat Rev Cancer 8:299–308*

119.   Barrett DM, Grupp SA, June CH (2015) *Chimeric Antigen Receptor– and TCR-Modified T Cells Enter Main Street and Wall Street. The Journal of Immunology 195:755–761*

120.   Brudno JN, Kochenderfer JN (2016) *Toxicities of chimeric antigen receptor T cells: recognition and management. Blood 127:3321–3330*

121.   Parkhurst MR, Yang JC, Langan RC, et al (2011) *T Cells Targeting Carcinoembryonic Antigen Can Mediate Regression of Metastatic Colorectal Cancer but Induce Severe Transient Colitis. Molecular Therapy 19:620–626*

122.   Le I, Dhandayuthapani S, Chacon J, Eiring AM, Gadad SS (2022) *Harnessing the Immune System with Cancer Vaccines: From Prevention to Therapeutics. Vaccines (Basel) 10:816*

123.   Goyal F, Chattopadhyay A, Navik U, Jain A, Reddy PH, Bhatti GK, Bhatti JS (2024) *Advancing Cancer Immunotherapy: The Potential of mRNA Vaccines As a Promising Therapeutic Approach. Adv Ther (Weinh). https://doi.org/10.1002/adtp.202300255*

124.   Fan T, Zhang M, Yang J, Zhu Z, Cao W, Dong C (2023) *Therapeutic cancer vaccines: advancements, challenges, and prospects. Signal Transduct Target Ther 8:450*

125.   Martinis E, Ricci C, Trevisan C, Tomadini G, Tonon S (2023) *Cancer Vaccines: From the State of the Art to the Most Promising Frontiers in the Treatment of Colorectal Cancer. Pharmaceutics 15:1969*

126.   Lacy P, Stow JL (2011) *Cytokine release from innate immune cells: association with diverse membrane trafficking pathways. Blood 118:9–18*

127.   Donnelly RP, Young HA, Rosenberg AS (2009) *An Overview of Cytokines and Cytokine Antagonists as Therapeutic Agents. Ann N Y Acad Sci 1182:1–13*

128.   Chulpanova DS, Kitaeva K V., Green AR, Rizvanov AA, Solovyeva V V. (2020) *Molecular Aspects and Future Perspectives of Cytokine-Based Anti-cancer Immunotherapy. Front Cell Dev Biol. https://doi.org/10.3389/fcell.2020.00402*

129.   Bonati L, Tang L (2021) *Cytokine engineering for targeted cancer immunotherapy. Curr Opin Chem Biol 62:43–52*

130. *Dubbs SB (2018) The Latest Cancer Agents and Their Complications. Emerg Med Clin North Am 36:485–492*

131. *Kim ST, Suarez-Almazor ME (2019) Managing immune dysregulation resulting from immune checkpoint inhibitors: impact of the ASCO guidelines and key take-homes for immunologists. Expert Rev Clin Immunol 15:211–213*

132. *Rojas-Quintero J, Díaz MP, Palmar J, et al (2024) Car T Cells in Solid Tumors: Overcoming Obstacles. Int J Mol Sci 25:4170*

133. *Kaczmarek M, Poznańska J, Fechner F, Michalska N, Paszkowska S, Napierała A, Mackiewicz A (2023) Cancer Vaccine Therapeutics: Limitations and Effectiveness—A Literature Review. Cells 12:2159*

134. *Adebayo AS, Agbaje K, Adesina SK, Olajubutu O (2023) Colorectal Cancer: Disease Process, Current Treatment Options, and Future Perspectives. Pharmaceutics 15:2620*

135. *Gmeiner WH (2024) Recent Advances in Therapeutic Strategies to Improve Colorectal Cancer Treatment. Cancers (Basel) 16:1029*

136. *Taieb J, Gallois C (2020) Adjuvant Chemotherapy for Stage III Colon Cancer. Cancers (Basel) 12:2679*

137. *Anand U, Dey A, Chandel AKS, et al (2023) Cancer chemotherapy and beyond: Current status, drug candidates, associated risks and progress in targeted therapeutics. Genes Dis 10:1367*

138. *Breukink SO, Donovan KA (2013) Physical and Psychological Effects of Treatment on Sexual Functioning in Colorectal Cancer Survivors. J Sex Med 10:74–83*

139. *fda, cder HIGHLIGHTS OF PRESCRIBING INFORMATION.*

140. *fda, cder HIGHLIGHTS OF PRESCRIBING INFORMATION.*

141. *Choi Y Il, Lee SH, Ahn BK, Baek SU, Park SJ, Kim YS, Shin SH (2008) Intestinal Perforation in Colorectal Cancers Treated with Bevacizumab (Avastin®). Cancer Research and Treatment : Official Journal of Korean Cancer Association 40:33*

142. *Hurwitz H, Saini S (2006) Bevacizumab in the Treatment of Metastatic Colorectal Cancer: Safety Profile and Management of Adverse Events. Semin Oncol 33:S26–S34*

143. *Glimelius B (2005) Benefit-risk assessment of irinotecan in advanced colorectal cancer. Drug Saf 28:417–433*

144. *Fujita KI, Kubota Y, Ishida H, Sasaki Y (2015) Irinotecan, a key chemotherapeutic drug for metastatic colorectal cancer. World J Gastroenterol 21:12234–12248*

145. *Camptosar (Irinotecan Hydrochloride) 1996 Diarrhea, neutropenia, nausea, vomiting, alopecia. - Google Search. https://www.google.com/search?q=Camptosar+(Irinotecan+Hydrochloride)+ 1996+Diarrhea%2C+neutropenia%2C+nausea%2C+vomiting%2C+alopeci a.&oq=Camptosar+(Irinotecan+Hydrochloride)+1996%09Diarrhea%2C+ne utropenia%2C+nausea%2C+vomiting%2C+alopecia.&gs_lcrp=EgZjaHJvb WUyBggAEEUYODlBBzUyMGowajeoAgCwAgA&sourceid=chrome&ie=UT F-8. Accessed 8 Jul 2024*

146. *Rider BJ (2017) Capecitabine. xPharm: The Comprehensive Pharmacology Reference 1–4*

147. *Capecitabine BC Cancer Drug Manual.*

148. *Lee JJ, Chu E (2017) Adherence, Dosing, and Managing Toxicities With Trifluridine/Tipiracil (TAS-102). Clin Colorectal Cancer 16:85–92*

149. *Fakih M, Vincent M (2010) Adverse events associated with anti-EGFR therapies for the treatment of metastatic colorectal cancer. Current Oncology 17:S18*

150. *Saleh M, Cassier PA, Eberst L, et al (2020) Phase I Study of Ramucirumab Plus Merestinib in Previously Treated Metastatic Colorectal Cancer: Safety, Preliminary Efficacy, and Pharmacokinetic Findings. Oncologist 25:e1628*

151. *fda, cder HIGHLIGHTS OF PRESCRIBING INFORMATION.*

152. *Fda, Cder Eloxatin (oxaliplatin) powder for solution.*

153. *Sara JD, Kaur J, Khodadadi R, Rehman M, Lobo R, Chakrabarti S, Herrmann J, Lerman A, Grothey A (2018) 5-fluorouracil and cardiotoxicity: a review. Ther Adv Med Oncol. https://doi.org/10.1177/1758835918780140*

154. *Stucchi E, Bartolini M, Airoldi M, Fazio R, Daprà V, Mondello G, Prete MG, Puccini A, Santoro A (2024) Fruquintinib as new treatment option in metastatic colorectal cancer patients: is there an optimal sequence? https://doi.org/10.1080/14656566.2024.2336069*

155. *Tan S, Zhang S, Zhou N, Cai X, Yi C, Gou H (2023) Efficacy and safety of fruquintinib dose-escalation strategy for elderly patients with refractory metastatic colorectal cancer: A single-arm, multicenter, phase II study. Cancer Med 12:22038*

156. *Messmer M, Upreti S, Tarabishy Y, Mazumder N, Chowdhury R, Yarchoan M, Holdhoff M (2016) Ipilimumab-Induced Enteritis without Colitis: A New Challenge. Case Rep Oncol 9:705–713*

157. *Mitchell KA, Kluger H, Sznol M, Hartman DJ (2013) Ipilimumab-induced perforating colitis. J Clin Gastroenterol 47:781–785*

158. *Trullas A, Delgado J, Genazzani A, Mueller-Berghaus J, Migali C, Müller-Egert S, Zander H, Enzmann H, Pignatti F (2021) The EMA assessment of pembrolizumab as monotherapy for the first-line treatment of adult patients with metastatic microsatellite instability-high or mismatch repair deficient colorectal cancer. ESMO Open 6:100145*

159. *Lee HJ, Kim HS, Park NH, Chung HH, Kim JW, Song YS (2013) Feasibility of Oxaliplatin, Leucovorin, and 5-Fluorouracil (FOLFOX-4) Chemotherapy in Heavily Pretreated Patients with Recurrent Epithelial Ovarian Cancer. Cancer Res Treat 45:40–47*

160. *Falcone A, Salvatore L, Boni L, et al (2015) Continuation or reintroduction of bevacizumab beyond progression to first-line therapy in metastatic colorectal cancer: Final results of the randomized BEBYP trial. Annals of Oncology 26:724–730*

161. *Rhodes W, Declue RW, Accortt NA, Jin R, Sandschafer D, Wertz D, Patel K (2021) Real-world use of bevacizumab-awwb, a bevacizumab biosimilar, in US patients with metastatic colorectal cancer. Future Oncology 17:5119–5127*

162. *Tie Y, Ma X, Zhu C, Mao Y, Shen K, Wei X, Chen Y, Zheng H (2017) Safety and efficacy of nivolumab in the treatment of cancers: A meta-analysis of 27 prospective clinical trials. Int J Cancer 140:948–958*

163. *Wrobel P, Ahmed S (2019) Current status of immunotherapy in metastatic colorectal cancer. Int J Colorectal Dis 34:13–25*

164. *Barber FD (2019) Adverse Events of Oncologic Immunotherapy and Their Management. Asia Pac J Oncol Nurs 6:212–226*

165. *Vietor NO, George BJ (2012) Oxaliplatin-induced hepatocellular injury and ototoxicity: A review of the literature and report of unusual side effects of a commonly used chemotherapeutic agent. Journal of Oncology Pharmacy Practice 18:355–359*

166. *Cassidy J, Misset J-L (2002) Oxaliplatin-related side effects: Characteristics and management. Semin Oncol 29:asonc02905p0011*

167. *Giusti RM, Shastri KA, Cohen MH, Keegan P, Pazdur R (2007) FDA Drug Approval Summary: Panitumumab (Vectibix^{TM}). Oncologist 12:577–583*

168. *Gemmete JJ, Mukherji SK (2011) Panitumumab (Vectibix): Fig 1. American Journal of Neuroradiology 32:1002–1003*

169. *Wookey V, Grothey A (2021) Update on the role of pembrolizumab in patients with unresectable or metastatic colorectal cancer. Therap Adv Gastroenterol 14:175628482110244*

170. *O'Neil BH, Wallmark JM, Lorente D, et al (2017) Safety and antitumor activity of the anti–PD-1 antibody pembrolizumab in patients with advanced colorectal carcinoma. PLoS One 12:e0189848*

171. *Muro K, Salinardi T, Singh AR, Macarulla T (2020) Safety of Aflibercept in Metastatic Colorectal Cancer: A Literature Review and Expert Perspective on Clinical and Real-World Data. Cancers (Basel) 12:844*

172. *Saleh M, Cassier PA, Eberst L, et al (2020) Phase I Study of Ramucirumab Plus Merestinib in Previously Treated Metastatic Colorectal Cancer: Safety, Preliminary Efficacy, and Pharmacokinetic Findings. Oncologist 25:e1628–e1639*

173. *Grothey A, Cutsem E Van, Sobrero A, et al (2013) Regorafenib monotherapy for previously treated metastatic colorectal cancer (CORRECT): an international, multicentre, randomised, placebo-controlled, phase 3 trial. The Lancet 381:303–312*

174. *McLellan B, Ciardiello F, Lacouture ME, Segaert S, Van Cutsem E (2015) Regorafenib-associated hand–foot skin reaction: practical advice on diagnosis, prevention, and management. Annals of Oncology 26:2017–2026*

175. *Crona DJ, Keisler MD, Walko CM (2013) Regorafenib: A Novel Multitargeted Tyrosine Kinase Inhibitor for Colorectal Cancer and Gastrointestinal Stromal Tumors. Annals of Pharmacotherapy 47:1685–1696*

176. *Ettrich TJ, Seufferlein T (2018) Regorafenib. pp 45–56*

177. *Ahn D, Walden D, Bekaii-Saab T (2022) Tucatinib: an investigational novel therapeutic agent for the treatment of HER-2 colorectal cancer. Expert Opin Investig Drugs 31:437–441*

178. *Strickler JH, Zemla T, Ou F-S, et al (2019) Trastuzumab and tucatinib for the treatment of HER2 amplified metastatic colorectal cancer (mCRC): Initial results from the MOUNTAINEER trial. Annals of Oncology 30:v200*

179. *Kulukian A, Lee P, Taylor J, Rosler R, de Vries P, Watson D, Forero-Torres A, Peterson S (2020) Preclinical Activity of HER2-Selective Tyrosine Kinase Inhibitor Tucatinib as a Single Agent or in Combination with Trastuzumab or Docetaxel in Solid Tumor Models. Mol Cancer Ther 19:976–987*

180. *Debela DT, Muzazu SG, Heraro KD, Ndalama MT, Mesele BW, Haile DC, Kitui SK, Manyazewal T (2021) New approaches and procedures for cancer treatment: Current perspectives. SAGE Open Med 9:20503121211034370*

181. *Yin S-Y, Wei W-C, Jian F-Y, Yang N-S (2013) Therapeutic applications of herbal medicines for cancer patients. Evid Based Complement Alternat Med 2013:302426*

182. *Naeem A, Hu P, Yang M, Zhang J, Liu Y, Zhu W, Zheng Q (2022) Natural Products as Anticancer Agents: Current Status and Future Perspectives. Molecules 27:8367*

183. *Taylor WF, Moghadam SE, Moridi Farimani M, N. Ebrahimi S, Tabefam M, Jabbarzadeh E (2019) A multi-targeting natural compound with growth inhibitory and anti-angiogenic properties re-sensitizes chemotherapy resistant cancer. PLoS One 14:e0218125*

184. *Ratovitski EA (2017) Anticancer Natural Compounds as Epigenetic Modulators of Gene Expression. Curr Genomics 18:175–205*

185. *G MS, Swetha M, Keerthana CK, Rayginia TP, Anto RJ (2021) Cancer Chemoprevention: A Strategic Approach Using Phytochemicals. Front Pharmacol 12:809308*

186. *Costea T, Hudiță A, Ciolac O-A, Gălățeanu B, Ginghină O, Costache M, Ganea C, Mocanu M-M (2018) Chemoprevention of Colorectal Cancer by Dietary Compounds. Int J Mol Sci. https://doi.org/10.3390/ijms19123787*

187. *Asma ST, Acaroz U, Imre K, et al (2022) Natural Products/Bioactive Compounds as a Source of Anticancer Drugs. Cancers (Basel). https://doi.org/10.3390/cancers14246203*

188. *Khalifa SAM, Elias N, Farag MA, et al (2019) Marine Natural Products: A Source of Novel Anticancer Drugs. Mar Drugs. https://doi.org/10.3390/md17090491*

189. *Ullah R, Rehman NU, Jamshidi-Adegani F, Bari A (2022) Editorial: Medicinal Plants and Marine-Derived Natural Products as Cancer Chemopreventive Agents. Front Pharmacol. https://doi.org/10.3389/fphar.2022.900275*

190. *Talib WH, Alsayed AR, Barakat M, Abu-Taha MI, Mahmod AI (2021) Targeting Drug Chemo-Resistance in Cancer Using Natural Products. Biomedicines. https://doi.org/10.3390/biomedicines9101353*

191. *Tian Y, Lei Y, Wang Y, Lai J, Wang J, Xia F (2023) Mechanism of multidrug resistance to chemotherapy mediated by P-glycoprotein (Review). Int J Oncol. https://doi.org/10.3892/ijo.2023.5567*

192. *Huo J-L, Fu W-J, Liu Z-H, Lu N, Jia X-Q, Liu Z-S (2022) Research advance of natural products in tumor immunotherapy. Front Immunol 13:972345*

193. *Nigam M, Mishra AP, Deb VK, Dimri DB, Tiwari V, Bungau SG, Bungau AF, Radu A-F (2023) Evaluation of the association of chronic inflammation and cancer: Insights and implications. Biomedicine & Pharmacotherapy 164:115015*

194. *Cragg GM, Newman DJ (2013) Natural products: A continuing source of novel drug leads. Biochimica et Biophysica Acta (BBA) - General Subjects 1830:3670–3695*

195. *Dias DA, Urban S, Roessner U (2012) A Historical Overview of Natural Products in Drug Discovery. Metabolites 2:303–336*

196. *Gagare S, Patil P, Jain A (2024) Natural product-inspired strategies towards the discovery of novel bioactive molecules. Futur J Pharm Sci 10:55*

197. *Farooqi AA, Qureshi MZ, Khalid S, Attar R, Martinelli C, Sabitaliyevich UY, Nurmurzayevich SB, Taverna S, Poltronieri P, Xu B (2019) Regulation of Cell Signaling Pathways by Berberine in Different Cancers: Searching for Missing Pieces of an Incomplete Jig-Saw Puzzle for an Effective Cancer Therapy. Cancers (Basel) 11:478*

198. *Montecucco A, Zanetta F, Biamonti G (2015) Molecular mechanisms of etoposide. EXCLI J 14:95–108*

199. *Dhyani P, Quispe C, Sharma E, et al (2022) Anticancer potential of alkaloids: a key emphasis to colchicine, vinblastine, vincristine, vindesine, vinorelbine and vincamine. Cancer Cell Int 22:206*

200. *Jin J-O, Chauhan PS, Arukha AP, Chavda V, Dubey A, Yadav D (2021) The Therapeutic Potential of the Anticancer Activity of Fucoidan: Current Advances and Hurdles. Mar Drugs. https://doi.org/10.3390/md19050265*

201. *Choudhari AS, Mandave PC, Deshpande M, Ranjekar P, Prakash O (2019) Phytochemicals in Cancer Treatment: From Preclinical Studies to Clinical Practice. Front Pharmacol 10:1614*

202. *Radhakrishnan EK, Bava S V, Narayanan SS, Nath LR, Thulasidasan AKT, Soniya EV, Anto RJ (2014) [6]-Gingerol induces caspase-dependent apoptosis and prevents PMA-induced proliferation in colon cancer cells by inhibiting MAPK/AP-1 signaling. PLoS One 9:e104401*

203. *Doi H, Matsui T, Dijkstra JM, Ogasawara A, Higashimoto Y, Imamura S, Ohye T, Takematsu H, Katsuda I, Akiyama H (2021) Andrographolide, isolated from Andrographis paniculata, induces apoptosis in monocytic leukemia and multiple myeloma cells via augmentation of reactive oxygen species production. F1000Res 10:542*

204. *Song M, Nishihara R, Cao Y, et al (2016) Marine ω-3 Polyunsaturated Fatty Acid Intake and Risk of Colorectal Cancer Characterized by Tumor-Infiltrating T Cells. JAMA Oncol 2:1197*

205. *Lucaciu RL, Hangan AC, Sevastre B, Oprean LS (2022) Metallo-Drugs in Cancer Therapy: Past, Present and Future. Molecules. https://doi.org/10.3390/molecules27196485*

206. *Bayat Mokhtari R, Homayouni TS, Baluch N, Morgatskaya E, Kumar S, Das B, Yeger H (2017) Combination therapy in combating cancer. Oncotarget 8:38022–38043*

207. *Stielow M, Witczyńska A, Kubryń N, Fijałkowski Ł, Nowaczyk J, Nowaczyk A (2023) The Bioavailability of Drugs—The Current State of Knowledge. Molecules 28:8038*

208. *Dadwal A, Baldi A, Kumar Narang R (2018) Nanoparticles as carriers for drug delivery in cancer. Artif Cells Nanomed Biotechnol 46:295–305*

209. *Elumalai K, Srinivasan S, Shanmugam A (2024) Review of the efficacy of nanoparticle-based drug delivery systems for cancer treatment. Biomedical Technology 5:109–122*

210. *Wu D, Si M, Xue H-Y, Wong H-L (2017) Nanomedicine applications in the treatment of breast cancer: current state of the art. Int J Nanomedicine 12:5879–5892*

211. *Manzari-Tavakoli A, Babajani A, Tavakoli MM, Safaeinejad F, Jafari A (2024) Integrating natural compounds and nanoparticle-based drug delivery systems: A novel strategy for enhanced efficacy and selectivity in cancer therapy. Cancer Med 13:e7010*

212. *Dang Y, Guan J (2020) Nanoparticle-based drug delivery systems for cancer therapy. Smart Mater Med 1:10–19*

213. *Ezike TC, Okpala US, Onoja UL, et al (2023) Advances in drug delivery systems, challenges and future directions. Heliyon 9:e17488*

214. *Patra JK, Das G, Fraceto LF, et al (2018) Nano based drug delivery systems: Recent developments and future prospects. J Nanobiotechnology. https://doi.org/10.1186/S12951-018-0392-8*

215. *Gurunathan S, Kang M-H, Qasim M, Kim J-H (2018) Nanoparticle-Mediated Combination Therapy: Two-in-One Approach for Cancer. Int J Mol Sci 19:3264*

216. *Zhang RX, Wong HL, Xue HY, Eoh JY, Wu XY (2016) Nanomedicine of synergistic drug combinations for cancer therapy – Strategies and perspectives. Journal of Controlled Release 240:489–503*

217. *Raju GSR, Pavitra E, Varaprasad GL, Bandaru SS, Nagaraju GP, Farran B, Huh YS, Han Y-K (2022) Nanoparticles mediated tumor microenvironment modulation: current advances and applications. J Nanobiotechnology 20:274*

218. *Leowattana W, Leowattana P, Leowattana T (2023) Systemic treatment for metastatic colorectal cancer. World J Gastroenterol 29:1569–1588*

219. *Basak D, Arrighi S, Darwiche Y, Deb S (2021) Comparison of Anticancer Drug Toxicities: Paradigm Shift in Adverse Effect Profile. Life (Basel). https://doi.org/10.3390/life12010048*

220. *Song M-K, Park M-Y, Sung M-K (2013) 5-Fluorouracil-induced changes of intestinal integrity biomarkers in BALB/c mice. J Cancer Prev 18:322–9*

221. *Chang C-T, Ho T-Y, Lin H, Liang J-A, Huang H-C, Li C-C, Lo H-Y, Wu S-L, Huang Y-F, Hsiang C-Y (2012) 5-Fluorouracil induced intestinal mucositis via nuclear factor-κB activation by transcriptomic analysis and in vivo bioluminescence imaging. PLoS One 7:e31808*

222. *McQuade RM, Stojanovska V, Donald EL, Rahman AA, Campelj DG, Abalo R, Rybalka E, Bornstein JC, Nurgali K (2017) Irinotecan-Induced Gastrointestinal Dysfunction Is Associated with Enteric Neuropathy, but Increased Numbers of Cholinergic Myenteric Neurons. Front Physiol 8:391*

223. *de Man FM, Goey AKL, van Schaik RHN, Mathijssen RHJ, Bins S (2018) Individualization of Irinotecan Treatment: A Review of Pharmacokinetics, Pharmacodynamics, and Pharmacogenetics. Clin Pharmacokinet 57:1229*

224. *Muco E, Patail H, Shaik A, McMahon S (2022) Capecitabine-Associated Coronary Vasospasm and Cardiac Arrest. Cureus 14:e28184*

225. *Fontanella C, Aita M, Cinausero M, Aprile G, Baldin MG, Dusi V, Lestuzzi C, Fasola G, Puglisi F (2014) Capecitabine-induced cardiotoxicity: more evidence or clinical approaches to protect the patients' heart? Onco Targets Ther 7:1783–91*

226. *Saif MW, Reardon J (2005) Management of oxaliplatin-induced peripheral neuropathy. Ther Clin Risk Manag 1:249–58*

227. *Rahman AA, Masango P, Stavely R, Bertrand P, Page A, Nurgali K (2023) Oxaliplatin-Induced Damage to the Gastric Innervation: Role in Nausea and Vomiting. Biomolecules. https://doi.org/10.3390/biom13020276*

228. *Unseld M, Fischöder S, Jachs M, et al (2020) Different Toxicity Profiles Predict Third Line Treatment Efficacy in Metastatic Colorectal Cancer Patients. J Clin Med. https://doi.org/10.3390/jcm9061772*

229. *De Wit M, Boers-Doets CB, Saettini A, Vermeersch K, de Juan CR, Ouwerkerk J, Raynard S-S, Bazin A, Cremolini C (2014) Prevention and management of adverse events related to regorafenib. Support Care Cancer 22:837–46*

230. *Rais T, Riaz R, Siddiqui T, Shakeel A, Khan A, Zafar H (2024) Innovations in colorectal cancer treatment: trifluridine and tipiracil with bevacizumab for improved outcomes – a review. Front Oncol. https://doi.org/10.3389/fonc.2024.1296765*

231. *Van Cutsem E, Hochster H, Shitara K, et al (2022) Pooled safety analysis from phase III studies of trifluridine/tipiracil in patients with metastatic gastric or gastroesophageal junction cancer and metastatic colorectal cancer. ESMO Open 7:100633*

232. *Carlsen L, Schorl C, Huntington K, Hernandez-Borrero L, Jhaveri A, Zhang S, Zhou L, El-Deiry WS (2021) Pan-drug and drug-specific mechanisms of 5-FU, irinotecan (CPT-11), oxaliplatin, and cisplatin identified by comparison of transcriptomic and cytokine responses of colorectal cancer cells. Oncotarget 12:2006–2021*

233. *Tsuboya A, Fujita K, Kubota Y, Ishida H, Taki-Takemoto I, Kamei D, Iwai S, Sasaki Y (2019) Coadministration of cytotoxic chemotherapeutic agents with irinotecan is a risk factor for irinotecan-induced cholinergic syndrome in Japanese patients with cancer. Int J Clin Oncol 24:222–230*

234. *De Lisa M, Ballatore Z, Marcantognini G, Pierantoni C, Antognoli S, Pistelli M, Pagliacci A, Berardi R (2020) Irinotecan-Induced Transient Dysarthria: Case Series and Updated Literature Review. Oncol Ther 8:147–160*

235. *Fujii H, Hirata T, Mura T, Okada Y, Ito T, Ozaki S, Tashiro H, Mizunoe T, Kohno H, Nakano K (2017) Risk factors and prophylaxis of irinotecan induced*

cholinergic syndrome in sight of supportive care. Journal of Clinical Oncology 35:216–216

236. *Uchiyama K, Saito Y, Takekuma Y, Yuki S, Sugawara M (2021) Alleviation of Abdominal Pain due to Irinotecan-Induced Cholinergic Syndrome Using Loperamide: A Case Report. Case Rep Oncol 14:806–811*

237. *Zhang L, Watson LT, Heath LS (2011) A Network of SCOP Hidden Markov Models and Its Analysis. BMC Bioinformatics 12:1–11*

238. *Venkitachalam S, Revoredo L, Varadan V, Fecteau RE, Ravi L, Lutterbaugh J, Markowitz SD, Willis JE, Gerken TA, Guda K (2016) Biochemical and functional characterization of glycosylation-associated mutational landscapes in colon cancer. Sci Rep 6:23642*

239. *Yang H, Zhu J, Wang G, Liu H, Zhou Y, Qian J (2020) STK35 Is Ubiquitinated by NEDD4L and Promotes Glycolysis and Inhibits Apoptosis Through Regulating the AKT Signaling Pathway, Influencing Chemoresistance of Colorectal Cancer. Front Cell Dev Biol. https://doi.org/10.3389/fcell.2020.582695*

240. *Xie S, Xia L, Song Y, Liu H, Wang Z, Zhu X (2021) Insights Into the Biological Role of NEDD4L E3 Ubiquitin Ligase in Human Cancers. Front Oncol. https://doi.org/10.3389/fonc.2021.774648*

241. *Yoshimura A, Nishinakamura H, Matsumura Y, Hanada T (2005) Negative regulation of cytokine signaling and immune responses by SOCS proteins. Arthritis Res Ther 7:100*

242. *Oblak A, Jerala R (2011) Toll-Like Receptor 4 Activation in Cancer Progression and Therapy. Clin Dev Immunol 2011:1–12*

243. *Patergnani S, Marchi S, Rimessi A, Bonora M, Giorgi C, Mehta KD, Pinton P (2013) PRKCB/protein kinase C, beta and the mitochondrial axis as key regulators of autophagy. Autophagy 9:1367–1385*

244. *Tochhawng L, Deng S, Pugalenthi G, et al (2016) Gelsolin-Cu/ZnSOD interaction alters intracellular reactive oxygen species levels to promote cancer cell invasion. Oncotarget 7:52832–52848*

245. *Zhuo J, Tan EH, Yan B, et al (2012) Gelsolin Induces Colorectal Tumor Cell Invasion via Modulation of the Urokinase-Type Plasminogen Activator Cascade. PLoS One 7:e43594*

246. *CHEN Q, GUO X, MA W (2024) Opportunities and challenges of CD47-targeted therapy in cancer immunotherapy. Oncol Res 32:49–60*

247. *Catalán R, Orozco-Morales M, Hernández-Pedro NY, Guijosa A, Colín-González AL, Ávila-Moreno F, Arrieta O (2020) CD47-SIRP α Axis as a Biomarker and Therapeutic Target in Cancer: Current Perspectives and Future Challenges in Nonsmall Cell Lung Cancer. J Immunol Res 2020:1–8*

248. *Lugano R, Ramachandran M, Dimberg A (2020) Tumor angiogenesis: causes, consequences, challenges and opportunities. Cellular and Molecular Life Sciences 77:1745–1770*

249. *Qi F, Li A, Inagaki Y, Kokudo N, Tamura S, Nakata M, Tang W (2011) Antitumor activity of extracts and compounds from the skin of the toad Bufo bufo gargarizans Cantor. Int Immunopharmacol 11:342–349*

250. *Han Q, Ma Y, Wang H, Dai Y, Chen C, Liu Y, Jing L, Sun X (2018) Resibufogenin suppresses colorectal cancer growth and metastasis through RIP3-mediated necroptosis. J Transl Med 16:1–13*

251. *Yang T, Jiang YX, Wu Y, Lu D, Huang R, Wang LL, Wang SQ, Guan YY, Zhang H, Luan X (2021) Resibufogenin Suppresses Triple-Negative Breast Cancer Angiogenesis by Blocking VEGFR2-Mediated Signaling Pathway. Front Pharmacol. https://doi.org/10.3389/FPHAR.2021.682735*

252. *Yang T, Shi R, Chang L, et al (2015) Huachansu suppresses human bladder cancer cell growth through the Fas/Fasl and TNF-α/TNFR1 pathway in vitro and in vivo. Journal of Experimental and Clinical Cancer Research 34:1–10*

253. *Zhou G, Zhu Z, Li L, Ding J (2019) Resibufogenin inhibits ovarian clear cell carcinoma (OCCC) growth in vivo, and migration of OCCC cells in vitro, by down-regulating the PI3K/AKT and actin cytoskeleton signaling pathways. Am J Transl Res 11:6290*

254. *Zhang X, Yao Z, Xue Z, Wang S, Liu X, Hu Y, Zhang Y, Wang J, Li X, Chen A (2022) Resibufogenin Targets the ATP1A1 Signaling Cascade to Induce G2/M Phase Arrest and Inhibit Invasion in Glioma. Front Pharmacol 13:855626*

255. *Liu L, Liu Y, Liu X, Zhang N, Mao G, Zeng Q, Yin M, Song D, Deng H (2018) Resibufogenin suppresses transforming growth factor-β-activated kinase 1-mediated nuclear factor-κB activity through protein kinase C-dependent inhibition of glycogen synthase kinase 3. Cancer Sci 109:3611*

256. *Rajput A, Kasar A, Thorat S, Kulkarni M (2021) Borneol: A Plant-Sourced Terpene with a Variety of Promising Pharmacological Effects. Nat Prod J. https://doi.org/10.2174/2210315512666211221115143*

257. *Su J, Lai H, Chen J, Li L, Wong YS, Chen T, Li X (2013) Natural Borneol, a Monoterpenoid Compound, Potentiates Selenocystine-Induced Apoptosis in*

Human Hepatocellular Carcinoma Cells by Enhancement of Cellular Uptake and Activation of ROS-Mediated DNA Damage. PLoS One 8:63502

258. *Li Y, Ren M, Wang J, Ma R, Chen H, Xie Q, Li H, Li J, Wang J (2021) Progress in Borneol Intervention for Ischemic Stroke: A Systematic Review. Front Pharmacol 12:606682*

259. *Li J, Xie Q, Ma R, et al (2021) Recent Progress on the Synergistic Antitumor Effect of a Borneol-Modified Nanocarrier Drug Delivery System. Front Med (Lausanne) 8:750170*

260. *Bansod S, Chilvery S, Saifi MA, Das TJ, Tag H, Godugu C (2021) Borneol protects against cerulein-induced oxidative stress and inflammation in acute pancreatitis mice model. Environ Toxicol 36:530–539*

261. *Zhang R, Mi SQ, Wang NS (2013) Effect of borneol on cytochrome P450 3A enzyme and midazolam pharmacokinetics in rats. Eur J Drug Metab Pharmacokinet 38:159–169*

262. *Sherkheli MA, Schreiner B, Haq R, Werner M, Hatt H (2015) Borneol inhibits TRPA1, a proinflammatory and noxious pain-sensing cation channel. Pak J Pharm Sci 28:1357–1363*

263. *Jiang J, Shen Y, Li J, Lin Y, ... CL-EJ of, 2015 undefined (+)-Borneol alleviates mechanical hyperalgesia in models of chronic inflammatory and neuropathic pain in mice. Elsevier*

264. *Luz MS, Gadelha DDA, Andrade KJS, Travassos RA, Ribeiro JD, Carvalho-Galvão A, Cruz JC, Balarini CM, Braga VA, França-Falcão MS (2022) Borneol reduces sympathetic vasomotor hyperactivity and restores depressed baroreflex sensitivity in rats with renovascular hypertension. Hypertens Res 45:802–813*

265. *Wang S, Zhang D, Hu J, et al (2017) A clinical and mechanistic study of topical borneol-induced analgesia. EMBO Mol Med 9:802*

266. *Liu M, Li Y, development SY-S cells and, 2014 undefined (2014) Curculigoside improves osteogenesis of human amniotic fluid-derived stem cells. liebertpub.comM Liu, Y Li, ST YangStem cells and development, 2014•liebertpub.com 23:146–154*

267. *Wang J, Wang C, Bu G (2018) Curcumin inhibits the growth of liver cancer stem cells through the phosphatidylinositol 3-kinase/protein kinase B/mammalian target of rapamycin signaling pathway. Exp Ther Med 15:3650*

268. *Binion DG, Otterson MF, Rafiee P (2008) Curcumin inhibits VEGF-mediated angiogenesis in human intestinal microvascular endothelial cells through COX-2 and MAPK inhibition. Gut 57:1509*

269. *Tan S, Xu J, Lai A, Cui R, ... RB-M, 2019 undefined Curculigoside exerts significant anti-arthritic effects in vivo and in vitro via regulation of the JAK/STAT/NF-κB signaling pathway. spandidos-publications.comS Tan, J Xu, A Lai, R Cui, R Bai, S Li, W Liang, G Zhang, S Jiang, S Liu, M Zheng, W WangMolecular Medicine Reports, 2019•spandidos-publications.com*

270. *Guo H, Zheng L, Guo Y, Han L, Yu J, Lai F (2022) Curculigoside Represses the Proliferation and Metastasis of Osteosarcoma via the JAK/STAT and NF-κB Signaling Pathways. Biol Pharm Bull 45:1466–1475*

271. *Liu M, Liu S, Zhang Q, et al (2021) Curculigoside attenuates oxidative stress and osteoclastogenesis via modulating Nrf2/NF-κB signaling pathway in RAW264.7 cells. J Ethnopharmacol 275:114129*

272. *Yan CP, Chen L, Deng CG, Chen Q, Jiang K, Yi YY, Li YL (2020) Beta-ecdysterone promotes in vitro proliferation and osteogenic differentiation of MC3T3-E1 cells. Chinese Journal of Tissue Engineering Research 24:4605–4612*

273. *Xu T, Niu C, Zhang X, Dong M (2018) β-Ecdysterone protects SH-SY5Y cells against β-amyloid-induced apoptosis via c-Jun N-terminal kinase-and Akt-associated complementary pathways. Laboratory Investigation 98:489–499*

274. *Zhang X, Xu X, Xu T, Research SQ-DD, 2014 undefined (2014) β-Ecdysterone Suppresses Interleukin-1β-Induced Apoptosis and Inflammation in Rat Chondrocytes via Inhibition of NF-κB Signaling Pathway. Wiley Online LibraryX Zhang, X Xu, T Xu, S QinDrug Development Research, 2014•Wiley Online Library 75:195–201*

275. *Fares J, Fares MY, Khachfe HH, Salhab HA, Fares Y (2020) Molecular principles of metastasis: a hallmark of cancer revisited. Signal Transduct Target Ther. https://doi.org/10.1038/s41392-020-0134-x*

276. *Li F, Jiang T, Li Q, Ling X (2017) Camptothecin (CPT) and its derivatives are known to target topoisomerase I (Top1) as their mechanism of action: did we miss something in CPT analogue molecular targets for treating human disease such as cancer? Am J Cancer Res 7:2350*

277. *Thomas A, Pommier Y (2019) Targeting topoisomerase I in the era of precision medicine. Clinical Cancer Research 25:6581–6589*

278. *Stahley MR, Stivers JT (2010) Mechanism and Specificity of DNA Strand Exchange Catalyzed by Vaccinia DNA Topoisomerase Type i. Biochemistry 49:2786–2795*

279. *Kciuk M, Marciniak B, Kontek R (2020) Irinotecan—Still an Important Player in Cancer Chemotherapy: A Comprehensive Overview. Int J Mol Sci 21:1–21*

280. *Richardson G, Dobish R (2007) Chemotherapy induced diarrhea. http://dx.doi.org/101177/1078155207077335 13:181–198*

281. *Wu C, Zhang Y, Yang D, Zhang J, Ma J, Cheng D, Chen J, Deng L (2019) Novel SN38 derivative-based liposome as anticancer prodrug: an in vitro and in vivo study. Int J Nanomedicine 14:75*

282. *Browning KN, Travagli RA (2014) Central Nervous System Control of Gastrointestinal Motility and Secretion and Modulation of Gastrointestinal Functions. Compr Physiol 4:1339*

283. *Long JZ, Cravatt BF (2011) The Metabolic Serine Hydrolases and Their Functions in Mammalian Physiology and Disease. Chem Rev 111:6022*

284. *Colletier JP, Fournier D, Greenblatt HM, Stojan J, Sussman JL, Zaccai G, Silman I, Weik M (2006) Structural insights into substrate traffic and inhibition in acetylcholinesterase. EMBO J 25:2746–2756*

285. *Johnson G, Moore SW (2005) The Peripheral Anionic Site of Acetylcholinesterase: Structure, Functions and Potential Role in Rational Drug Design. Curr Pharm Des 12:217–225*

286. *Das B, Majumder D (2022) A molecular docking-based comparative assessment of various anticholinergic drugs as antidotes to different nerve agent poisoning. https://doi.org/101080/073911022202225904 1–12*

287. *Kümler I, Sørensen PG, Palshof J, Høgdall E, Skovrider-Ruminski W, Theile S, Fullerton A, Nielsen PG, Jensen BV, Nielsen DL (2019) Oral administration of irinotecan in patients with solid tumors: an open-label, phase I, dose escalating study evaluating safety, tolerability and pharmacokinetics. Cancer Chemother Pharmacol 83:169*

288. *Dodds HM, Rivory LP (1999) The mechanism for the inhibition of acetylcholinesterases by irinotecan (CPT-11). Mol Pharmacol 56:1346–1353*

289. *Lee KJ (2015) Pharmacologic Agents for Chronic Diarrhea. Intest Res 13:306*

290. *Guo X han, Ni J, Xue J lun, Wang X (2017) Phyllanthus emblica Linn. fruit extract potentiates the anticancer efficacy of mitomycin C and cisplatin and reduces their genotoxicity to normal cells in vitro. J Zhejiang Univ Sci B 18:1031*

291. *Baburam S, Ramasamy S, Shanmugam G, Mathanmohun M (2022) Quorum Sensing Inhibitory Potential and Molecular Docking Studies of Phyllanthus*

emblica Phytochemicals Against Pseudomonas aeruginosa. Appl Biochem Biotechnol 194:434–444

292. *Singamaneni V, Dokuparthi SK, Banerjee N, Kumar A, Chakrabarti T (2019) Phytochemical Investigation and Antimutagenic Potential of Ethanolic Extracts of Emblica officinalis, Terminalia chebula and Terminalia bellirica. Nat Prod J 10:488–494*

293. *Wang HMD, Fu L, Cheng CC, et al (2019) Inhibition of LPS-Induced Oxidative Damages and Potential Anti-Inflammatory Effects of Phyllanthus emblica Extract via Down-Regulating NF-κB, COX-2, and iNOS in RAW 264.7 Cells. Antioxidants 2019, Vol 8, Page 270 8:270*

294. *Fatema Pria F, Islam MS (2019) Firuz Fatema Pria, Mohammad Sayful Islam. Phyllanthus emblica Linn. (Amla)-A Natural Gift to Humans: An Overview. Journal of Diseases and Medicinal Plants 5:1–9*

295. *Musial C, Kuban-Jankowska A, Gorska-Ponikowska M (2020) Beneficial Properties of Green Tea Catechins. Int J Mol Sci. https://doi.org/10.3390/ijms21051744*

296. *Singh BN, Shankar S, Srivastava RK (2011) Green tea catechin, epigallocatechin-3-gallate (EGCG): mechanisms, perspectives and clinical applications. Biochem Pharmacol 82:1807–21*

297. *Ferrari E, Bettuzzi S, Naponelli V (2022) The Potential of Epigallocatechin Gallate (EGCG) in Targeting Autophagy for Cancer Treatment: A Narrative Review. Int J Mol Sci. https://doi.org/10.3390/ijms23116075*

298. *Della Via FI, Shiraishi RN, Santos I, Ferro KP, Salazar-Terreros MJ, Franchi Junior GC, Rego EM, Saad STO, Torello CO (2021) (−)-Epigallocatechin-3-gallate induces apoptosis and differentiation in leukaemia by targeting reactive oxygen species and PIN1. Sci Rep 11:9103*

299. *Kashyap D, Tuli HS, Yerer MB, Sharma A, Sak K, Srivastava S, Pandey A, Garg VK, Sethi G, Bishayee A (2021) Natural product-based nanoformulations for cancer therapy: Opportunities and challenges. Semin Cancer Biol 69:5–23*

300. *Manzari-Tavakoli A, Babajani A, Tavakoli MM, Safaeinejad F, Jafari A (2024) Integrating natural compounds and nanoparticle-based drug delivery systems: A novel strategy for enhanced efficacy and selectivity in cancer therapy. Cancer Med. https://doi.org/10.1002/cam4.7010*

301. *Ghazal H, Waqar A, Yaseen F, Shahid M, Sultana M, Tariq M, Bashir MK, Tahseen H, Raza T, Ahmad F (2024) Role of nanoparticles in enhancing chemotherapy efficacy for cancer treatment. Next Materials 2:100128*

302. *Patra JK, Das G, Fraceto LF, et al (2018) Nano based drug delivery systems: recent developments and future prospects. Journal of Nanobiotechnology 2018 16:1 16:1–33*

303. *Maurya A, Singh AK, Mishra G, Kumari K, Rai A, Sharma B, Kulkarni GT, Awasthi R (2019) Strategic use of nanotechnology in drug targeting and its consequences on human health: A focused review. Interv Med Appl Sci 11:38–54*

304. *Chehelgerdi M, Chehelgerdi M, Allela OQB, et al (2023) Progressing nanotechnology to improve targeted cancer treatment: overcoming hurdles in its clinical implementation. Mol Cancer 22:169*

305. *Li Z, Zhao T, Li J, Yu Q, Feng Y, Xie Y, Sun P (2022) Nanomedicine Based on Natural Products: Improving Clinical Application Potential. J Nanomater. https://doi.org/10.1155/2022/3066613*

306. *Martínez-Ballesta Mc, Gil-Izquierdo Á, García-Viguera C, Domínguez-Perles R (2018) Nanoparticles and Controlled Delivery for Bioactive Compounds: Outlining Challenges for New "Smart-Foods" for Health. Foods 7:72*

307. *Liang T, Feng Z, Zhang X, Li T, Yang T, Yu L (2023) Research progress of calcium carbonate nanomaterials in cancer therapy: challenge and opportunity. Front Bioeng Biotechnol. https://doi.org/10.3389/FBIOE.2023.1266888*

308. *Xiao Y, Li Z, Bianco A, Ma B (2023) Recent Advances in Calcium-Based Anticancer Nanomaterials Exploiting Calcium Overload to Trigger Cell Apoptosis. Adv Funct Mater. https://doi.org/10.1002/ADFM.202209291*

309. *Ma DD, Yang WX (2016) Engineered nanoparticles induce cell apoptosis: potential for cancer therapy. Oncotarget 7:40882*

310. *Bai S, Lan Y, Fu S, Cheng H, Lu Z, Liu G (2022) Connecting Calcium-Based Nanomaterials and Cancer: From Diagnosis to Therapy. Nanomicro Lett. https://doi.org/10.1007/S40820-022-00894-6*

311. *Volodkin D (2014) CaCO3 templated micro-beads and -capsules for bioapplications. Adv Colloid Interface Sci 207:306–324*

312. *Liendo F, Arduino M, Deorsola FA, Bensaid S (2022) Factors controlling and influencing polymorphism, morphology and size of calcium carbonate synthesized through the carbonation route: A review. Powder Technol 398:117050*

313. *Ševčík R, Šašek P, Viani A (2018) Physical and nanomechanical properties of the synthetic anhydrous crystalline CaCO3 polymorphs: vaterite, aragonite and calcite. J Mater Sci 53:4022–4033*

314. *Trushina DB, Borodina TN, Belyakov S, Antipina MN (2022) Calcium carbonate vaterite particles for drug delivery: Advances and challenges. Mater Today Adv 14:100214*

315. *Muhammad Mailafiya M, Abubakar K, Danmaigoro A, Musa Chiroma S, Bin Abdul Rahim E, Aris Mohd Moklas M, Abu Bakar Zakaria Z (2019) Cockle Shell-Derived Calcium Carbonate (Aragonite) Nanoparticles: A Dynamite to Nanomedicine. Applied Sciences 9:2897*

316. *Fadia P, Tyagi S, Bhagat S, Nair A, Panchal P, Dave H, Dang S, Singh S (2021) Calcium carbonate nano- and microparticles: synthesis methods and biological applications. 3 Biotech 11:457*

317. *Bahrom H, Goncharenko AA, Fatkhutdinova LI, et al (2019) Controllable Synthesis of Calcium Carbonate with Different Geometry: Comprehensive Analysis of Particle Formation, Cellular Uptake, and Biocompatibility. ACS Sustain Chem Eng 7:19142–19156*

318. *Holder CF, Schaak RE (2019) Tutorial on Powder X-ray Diffraction for Characterizing Nanoscale Materials. ACS Nano 13:7359–7365*

319. *Rodriguez-Blanco JD, Shaw S, Benning LG (2011) The kinetics and mechanisms of amorphous calcium carbonate (ACC) crystallization to calcite, viavaterite. Nanoscale 3:265–271*

320. *Langevin D, Raspaud E, Mariot S, et al (2018) Towards reproducible measurement of nanoparticle size using dynamic light scattering: Important controls and considerations. NanoImpact 10:161–167*